

**DESIGN AND CHARACTERIZATION OF ELECTROSPUN NANOFIBERS
FABRICATED FROM BIODEGRADABLE POLYMERS**



NANTAPRAPA TUANCHAROENSRI

**A Thesis Submitted to the Graduate School of Naresuan University
in Partial Fulfillment of the Requirements
for the Master of Science Degree in Industrial Chemistry**

July 2016


Copyright 2016 by Naresuan University


Thesis entitled "Design and characterization of electrospun nanofibers fabricated from biodegradable polymers"


by Miss Nantaprapa Tuancharoensri

has been approved by the Graduate School as partial fulfillment of the requirements for the Master of Science Degree in Industrial Chemistry of Naresuan University


Oral Defense Committee


..... Chair
(Professor Supawan Tantayanon, Ph.D.)


..... Advisor
(Assistant Professor Sukunya Ross, Ph.D.)


..... Co – Advisor
(Gareth Ross, Ph.D.)


..... Internal Examiner
(Sararat Mahasaranon, Ph.D.)


..... Internal Examiner
(Assistant Professor Supatra Pratumshat, Ph.D.)

Approved



(Panu Putthawong, Ph.D.)

Associate Dean for Administration and Planning
for Dean of the Graduate School

22 JUL 2016

ACKNOWLEDGEMENT

First of all, I would like to express my sincere thanks to my advisor, Assistant Professor Sukunya Ross, Ph.D. and co-advisor Gareth Ross, Ph.D. for all their continuous support, guidance and encouragement during my pleasurable years here to do M.Sc. study since August 2012.

I would like to express my thanks to all the people of our Biopolymer group, my lovely sisters, brothers and M.Sc.'s friends who made my time very enjoyable, for all their hospitality extended to me. Sincere thanks and appreciation are also extended to all committees Professor Supawan Tantayanon, Ph.D., Sararat Mahasaranon, Ph.D. and Assistant Professor Supatra Pratumshat, Ph.D. for your kind suggestions.

A special thanks goes to Department of Chemistry, Faculty of Science and Naresuan University (Phitsanulok, Thailand), for their financial support for the duration of my work.

And finally, many thanks go to all people who helped for experimental analysis during my M.Sc. study, and also to my family for giving me a tremendous amount of support.

Nantaprapa Tuancharoensri

Title DESIGN AND CHARACTERIZATION OF ELECTROSPUN NANOFIBERS FABRICATED FROM BIODEGRADABLE POLYMERS

Author Nantaprapa Tuancharoensri

Advisor Assistant Professor Sukunya Ross, Ph.D.

Co - Advisor Gareth Ross, Ph.D.

Academic Paper Thesis Mater of Science Degree in Industrial Chemistry, Naresuan University, 2016

Keywords Electrospun nanofibers, Poly(lactic acid) (PLA), Tissue engineering scaffolds

ABSTRACT

Electrospinning is a simple method that produces polymer fibers (μm to nm) and materials with a large surface area, high porosity and enhanced specific mechanical performance. It has been widely used to fabricate biomaterials for biomedical applications such as implanted devices, drug delivery media and especially tissue engineering scaffolds. In this work, therefore, electrospinning was chosen to fabricate biocompatible and biodegradable materials that are classified into two approaches. The first approach was to fabricate ternary blends of poly(lactic acid) (PLA), polycaprolactone (PCL) and cellulose acetate butyrate (CAB) into electrospun fibers, then study the effect of PCL molecular weights (PCL1 and PCL2). This approach included the composition selections of PLA/PCL/CAB blends for electrospinning from optical ternary phase diagrams made by the rapid screening method, based on the phase boundaries of optically clear, translucent and opaque regions. Three compositions of PLA/PCL1/CAB and PLA/PCL2/CAB were then chosen; 80/10/10, 50/40/10 and 20/70/10, for fabrication by electrospinning. The second approach, was to fabricate poly(vinyl alcohol) (PVA) and silk sericin (SS) blends, and to fabricate PLA and PVA/SS blends layer by layer. The effect of the PVA and SS concentrations onto the properties of electrospun fibers was also studied. In both approaches, the parameters affecting the electrospinning process were

investigated, such as processing parameters (applied voltage, flow rate, diameter of the tip and distance between the collector and the tip of the syringe) and the viscosity of electrospun solutions. The morphology, functional groups, crystallinity, thermal property and hydrophilicity of all electrospun fibers were determined by scanning electron microscope (SEM), fourier transform infrared spectroscopy (FT-IR), X-ray diffraction (XRD), differential scanning calorimetry (DSC) and contact angle (CA) techniques, respectively. For approach I, the results showed that the non-woven electrospun nanofibers of PLA/PCL1/CAB and PLA/PCL2/CAB blends were successfully fabricated and the optimum conditions were; 10 wt% polymer solution, a flow rate of 0.5 ml/hr, a diameter of tip 0.7 mm and a distance from tip to collector of 10 cm. The average fiber diameters of the fibers were in the micro-nanometer range (1 μ m to 800 nm). All properties of these ternary electrospun fibers depended on the blending ratio of polymer solutions and molecular weight of PCL, in which high loading of PCL (PCL1 and PCL2) and lower molecular weight of PCL (PCL1) promoted beads and microdrops formation in the fibers. This was due to the phase separation (thermodynamically immiscible) between PCL1 and PLA. In contrast, using higher molecular weight PCL (PCL2) enhances the entanglement of polymer chains and causes a decrease in beaded structure and microdrops, as well as a decrease in cold crystallization temperature, which was attributed to the decrease in conformation entropy of the PCL2 chains. In addition, the composition at high loading of PLA blended with PCL2 and CAB gave the best composition with smooth surface fibers and partial miscibility between the polymers chains. For approach II, the optimum conditions for fabrication were a PVA concentration of 10 wt%, a flow rate of 0.015 ml/min, a diameter of tip 0.7 mm and a distance from tip to collector of 15 cm, these conditions yielded fibrous structures with interconnected pores. The electrospun fibers with 7.5 %w/v of PVA and different amounts of SS showed smoother surfaces and lower bead densities than that of 5 %w/v PVA. The concentration of PVA and SS affected the properties of electrospun fibers, in which 7.5 %w/v of PVA and 1.5 and 3.0 %w/v of SS blends gave the best conditions to promote the homogeneity between PVA and SS. For the electrospun fibers fabricated with layers of PLA and PVA/SS, the combinations of PLA and PVA/SS were observed in which PLA fiber diameter was larger than PVA/SS fibers. However, the

crystallinity and functional groups observation were inconclusive. In conclusion, these PLA/PCL/CAB, PVA/SS, and PLA with PVA/SS electrospun fibers will have potential to be used in the field of tissue engineering, such as scaffolds for skin reconstruction.



LIST OF CONTENTS

| Chapter | Page |
|------------------------------------------------------------------------------------------------------------------------|-----------|
| I INTRODUCTION | 1 |
| Introduction..... | 1 |
| Objective | 3 |
| Scope of the research | 4 |
| II LITERATURE REVIEWS | 6 |
| Biodegradable and biocompatible polymers..... | 6 |
| Introduction and background to the miscibility of blends | 18 |
| Electrospinning process | 23 |
| The use of electrospun nanofibers in biomedical applications | 28 |
| III RESEARCH METHODOLOGY | 33 |
| Materials | 33 |
| Instruments..... | 34 |
| Methods for approach I: The electrospinning technique for PLA/PCL/CAB | 34 |
| Methods for approach II: The electrospinning technique for PVA/SS and PLA/(PVA/SS)..... | 43 |
| Characterization | 44 |
| IV RESULTS AND DISCUSSION | 47 |
| Approach I: PLA/PCL/CAB blends..... | 47 |
| Miscibility study between polymer pairs of PLA/PCL, PLA/CAB and PCL/CAB by using the Coleman-Painter approach | 48 |
| Optical ternary phase diagram by rapid screening method..... | 49 |
| Characterization of ternary PLA/PCL/CAB blend films | 51 |
| Non-woven electrospun fibers of PLA/PCL/CAB blend..... | 54 |
| Summary of this section..... | 66 |

LIST OF CONTENTS (CONT.)

| Chapter | Page |
|---------------------------------------------------|------|
| Approach II: PVA/SS and PLA/(PVA/SS) blends | 67 |
| Non-woven electrospun fibers of PVA/SS | 67 |
| Non-woven electrospun fibers of PLA/(PVA/SS)..... | 73 |
| V CONCLUSIONS | 78 |
| Conclusions..... | 78 |
| Future work..... | 80 |
| REFERENCES | 81 |
| BIOGRAPHY | 91 |

LIST OF TABLES

| Table | Page |
|-------------------------------------------------------------------------------------------------------------------------------------|------|
| 1 The molar attraction constants (F) and molar volume (V) of unassociated groups and weakly associated groups | 22 |
| 2 Summary of the upper limit of the critical values of the solubility parameter difference, $(\Delta\chi)^{\circ}\text{Crit}$ | 22 |
| 3 Physical properties of the used solvents | 25 |
| 4 Effects of electrospinning parameters on morphology of fiber | 28 |
| 5 The compositions of two components blends using rapid screening method (PLA/PCL, PLA/CAB and PCL/CAB)..... | 37 |
| 6 The compositions of three components blends using rapid screening method (PLA/PCL/CAB)..... | 38 |
| 7 Compositions of electrospun PVA/SS fibers..... | 43 |
| 8 Miscibility study between polymer pairs by Coleman-Painter approach using the different in value of solubility parameter | 48 |
| 9 Properties of films and fibers of three different compositions of PLA/PCL/CAB blends. | 59 |

LIST OF FIGURES

| Figure | Page |
|----------------------------------------------------------------------------------------------------------------------------------------------|------|
| 1 The classification of biodegradable polyesters..... | 7 |
| 2 Chemical structure of Poly(lactic acid) (PLA) | 8 |
| 3 Stereochemical forms of lactic acids. | 8 |
| 4 Ring opening polymerisation of ϵ -caprolactone to polycaprolactone (PCL)..... | 9 |
| 5 Chemical structure of cellulose acetate butyrate, CAB | 10 |
| 6 Chemical structure of Poly(vinyl alcohol), PVA..... | 10 |
| 7 (A) Water contact angle image and (B) degree of contact angle of PLLA scaffolds with modified chitosan. | 12 |
| 8 SEM image of skin's cell on PLLA scaffold with modified chitosan..... | 13 |
| 9 Present weight loss of nanofibrous scaffolds after degradation for different time in PBS..... | 14 |
| 10 Structure composition of silk [49] | 16 |
| 11 Chemical structure of Sericin (SS) | 17 |
| 12 The free energy of mixing (ΔG_m) of Polymer A and B versus % wt. of polymer B; the miscibility depending on composition..... | 19 |
| 13 Polymer solution phase behavior showing LCST and UCST | 19 |
| 14 Schematic diagram of a general electrospinning setup..... | 24 |
| 15 The compositions of polymer solution that effect to fiber diameter. | 25 |
| 16 The electrical conductivity of the solution. | 26 |
| 17 The composition of CF/DMF solvent that effect to fiber diameter. | 26 |
| 18 SEM image of (A) random and aligned electrospun fibers. (B) Various shapes of scaffolds..... | 27 |
| 19 MTS assay for the cell proliferation on PLLA/PAA/Col I&III scaffolds | 29 |
| 20 MTS assay of cell proliferation on PDLLA/PEG fiber scaffolds..... | 30 |
| 21 Dual spinneret electrospinning apparatus setup. | 31 |

LIST OF FIGURES (CONT.)

| Figure | Page |
|-----------------------------------------------------------------------------------------------------------------------------------------------------------------------------------------------------------------------------------------------------------------|------|
| 22 Release profile of drug of electrospun PLLA nanofiber scaffolds; a. is released lidocaine hydrochloride drug and b. is released mupirocin drug of PLLA scaffolds. | 31 |
| 23 Chemical structures of PLA, PCL and CAB | 36 |
| 24 Shading chart of films classified by percent transmittance. | 36 |
| 25 Ternary phase diagram of three component blends (Ternary plots)..... | 41 |
| 26 Schematic illustration of electrospinning process. | 42 |
| 27 The optical ternary phase diagrams of PLA/PCL/CAB blends with different molecular weight of PCL1 (top) and PCL2 (bottom); all of the points in the diagrams represent the experimental data to classify the phase regions. | 50 |
| 28 FT-IR spectra of ternary blend films of: A. PLA/PCL1/CAB (black line) and B. PLA/PCL2/CAB (gray line), at different compositions..... | 52 |
| 29 XRD patterns of ternary blend films; A. PLA/PCL1/CAB (black line) and B. PLA/PCL2/CAB (gray line) at different compositions..... | 53 |
| 30 SEM images of non-woven electrospun fibers of homopolymers; a. PLA, b. CAB, c. PCL1 and d. PCL2. | 55 |
| 31 SEM images of non-woven ternary blend fibers of PLA/PCL1/CAB (a, b, c) and PLA/PCL2/CAB (d, e, f) at different compositions (80/10/10, 50/40/10, 20/70/10), with magnification of 500x in the main figures and of 5000x in an embedded figures..... | 57 |
| 32 FT-IR spectra of non-woven ternary blend fibers of: A. PLA/PCL1/CAB (black line) and B. PLA/PCL2/CAB (gray line), at different compositions. | 61 |
| 33 XRD patterns of non-woven ternary blend fibers; A. PLA/PCL1/CAB (black line) and B. PLA/PCL2/CAB (gray line) at different compositions. | 62 |

LIST OF FIGURES (CONT)

| Figure | Page |
|-----------------------------------------------------------------------------------------------------------------------------------------------------------------------------------------------|------|
| 34 DSC thermogram of non-woven ternary blend fibers; a. at cooling run and b. at 2nd heat run, of A. PLA/PCL1/CAB (black line) and B. PLA/PCL2/CAB (gray line) at different compositions..... | 65 |
| 35 Degree of water contact angle of non-woven homopolymer fibers (PLA, PCL, CAB) and non-woven ternary blend fibers (PLA/PCL/CAB). | 66 |
| 36 SEM image of electrospun PVA and PVA/SS fibers at different concentrations at magnification of 5000K (big images) and 2000K (small pictures)..... | 68 |
| 37 XRD patterns of electrospun PVA/SS; (a.) EF1 and EF2, and (b.) EF3, EF4 and EF5, together with PVA and SS. | 70 |
| 38 FTIR spectra of electrospun PVA/SS, together with PVA and SS. | 72 |
| 39 SEM image of electrospun PLA, PVA, PLA/PVA, PLA/EF3 and PLA/EF4 fibers at of 5000K (big images) and 1000K (small pictures) | 74 |
| 40 FTIR spectra of electrospun PLA/PVA, PLA/EF3, PLA/EF4 and homopolymer fibers..... | 75 |
| 41 XRD patterns of electrospun PLA/PVA, PLA/EF3, PLA/EF4 and homopolymer fibers..... | 76 |

CHAPTER I

INTRODUCTION

Introduction

The important point of this research was to study and fabricate biodegradable and biocompatible polymers into the form of nanofiber by electrospinning technique for potential use in tissue engineering applications. The work was separated into two approaches. The first approach was the fabrication of non-woven electropun fibers of ternary blends of poly(lactic acid) (PLA), polycaprolactone (PCL) and cellulose acetate butyrate (CAB). The second approach was the fabrication of non-woven electropun fibers of poly(vinyl alcohol) blended with silk sericin (SS) and the fabrication of PVA/SS with PLA. Therefore, this chapters will introduce the formations of these two approaches.

Approach I

PLA and PCL has been widely used for fabrication into electrospun nanofibers and potentially used in the biomedical applications, such as tissue engineering, membranes and drug release, due to their biodegradability, biocompatibility and good mechanical properties [1-5]. The nature of PLA is brittle with high mechanical strength, while PCL is flexible polymer. As known, blending is a good technique that helps to improve several properties. Therefore, many researchers have worked on the PLA/PCL blends to improve mechanical properties of PLA. For example, PLA/PCL, PLA/chitosan were successfully used to fabricate as electrospun nanofibers for biomedical applications. In this work, therefore, PLA and PCL were chosen to blend with a third component to improve the miscibility of the blends, this was cellulose acetate butyrate (CAB). The work started with the study of miscibility prediction between polymers pairs of PLA, PCL and cellulose acetate butyrate (CAB) using the Coleman and Painter approach [6-8]. Then the apparent miscibility of binary and ternary blend of PLA, PCL and CAB was studied using the technique called rapid screening method. In this method, the percent transmittance (%T) of polymer blends were measured and classified into the opaque (immiscible), translucent (apparent partial miscible) and clear (apparent miscible). This was plotted

in the form of ternary phase diagrams of PLA/PCL/CAB. As known from our previous work [6-7], molecular weight of PLA affected the apparent miscibility and optical ternary phase diagram and the phase separation between PLA and PCL were improved by adding CAB with hydrogen bonding to mediate the miscibility. The optically phase regions can be change depending on molecular weight of polymers leading to blends. In this work, therefore, the effect of the molecular weight of PCL onto the optical ternary phase diagram and apparent miscibility was chosen to study. However, the study of the apparent miscibility of ternary blends in each composition from optical ternary phase diagram was a guide to select the compositions for further work in electrospinning nanofibers, which is also an objective of this work.

Electrospinning is a well-known technique for fabrication of micro to nanoscale fibers. The technique contains three major parts; syringe pump, high voltage power supply and collector, which provided high electric force with polymer solutions onto a collector as random fibers [9-10]. The obtained non-woven electrospun fibers have unique properties, such as high surface area, high porous structure and specific mechanical properties [11]. These properties of electrospun fibers are widely used in biomedical applications such as drug delivery, wound dressings, enzyme immobilization and tissue engineering. The tissue engineering for skin is the design and fabrication of fibers in nanometers or micrometers scale that mimic structure and morphology of the natural extracellular matrix (ECM) component of the skin [12] and promote cell binding and cell proliferation [13]. However, electrospinning parameters that effect to the morphology and structure of electrospun fibers and need to be adjusted were solution properties (i.e. concentration of polymer solution, molecular weight, viscosity, surface tension and conductivity), processing conditions (i.e. flow rate of solution, applied voltage, tip-to-collector distance) and ambient conditions (temperature, air velocity and humidity) [14-15]. In this approach, therefore, the study of the fabrication ternary blends of PLA/PCL/CAB using electrospinning was the focus. In addition, the relationships between the miscibility study from the rapid screening method observed by optical ternary phase diagram and the fabrication of electrospun fibers from the same compositions were also investigated.

Approach II

Polyvinyl alcohol (PVA), silk sericin (SS) from silk cocoons and poly(lactic acid) (PLA) were studied in this approach, because they are all biodegradability and biocompatibility. These materials were of interest as they are currently used in biomedical applications such as tissue engineering, drug release, and wound dressing [16-18]. PVA is biodegradable, biocompatible and water soluble synthetic polymer that is non-cytotoxicity. In recent year, PVA has often been added into natural materials to fabricate nanofibers by electrospinning, such as PVA/gelatin, PVA/chitosan and PVA/collagen, which exhibited much better mechanical properties, antibacterial and control drug release [18-20]. SS is a glue-like protein that covers double stands of fibroin of silk cocoon fibers. SS comprises of 18 types of amino acids including up to 32% of essential amino acids, such as serine, glycine, aspartic acid, glutamic acid, threonine and tyrosine. These consist of hydroxyl, carboxyl and amino functional groups, that make sericin enable to dissolve in water and to react with other materials [21-22]. SS has been used in medical applications by incorporating with other biocompatible materials, such as chitosan [23], polyacrylamide [24]. As well as PLA is one of the most frequent to fabricate into the electrospun fibers for use in biomedical applications. It is know that the nature of PLA is hydrophobic, while that both PVA and SS are hydrophilic. In this approach, therefore, the electrospun fibers of PLA were mixed with electrospun fibers of PVA/SS fabricated into a form of layers. As well as, the fabrications of PVA and SS were also observed in order to study the effect of PVA and SS concentrations. However, electrospinning parameters that effect to structure and morphology of fibers were also of need to study. These parameters included polymer concentration, solution of flow rate, applied voltage and tip-to-collector distances.

Objective

The objective of this research work was separated into two parts depending on the technique and the type of materials used to fabricate the nanofibers, termed approach I and II, which are as follows.

Approach I

1. To study the apparent miscibility from optical ternary phase diagrams of PLA/PCL/CAB blends by studying the effect of molecular weights of PCL.
2. To fabricate and characterize the non-woven electrospun nanofibers of PLA/PCL/CAB blends by electrospinning technique, and compositions selected from the ternary phase diagrams obtained from point 1.

Approach II

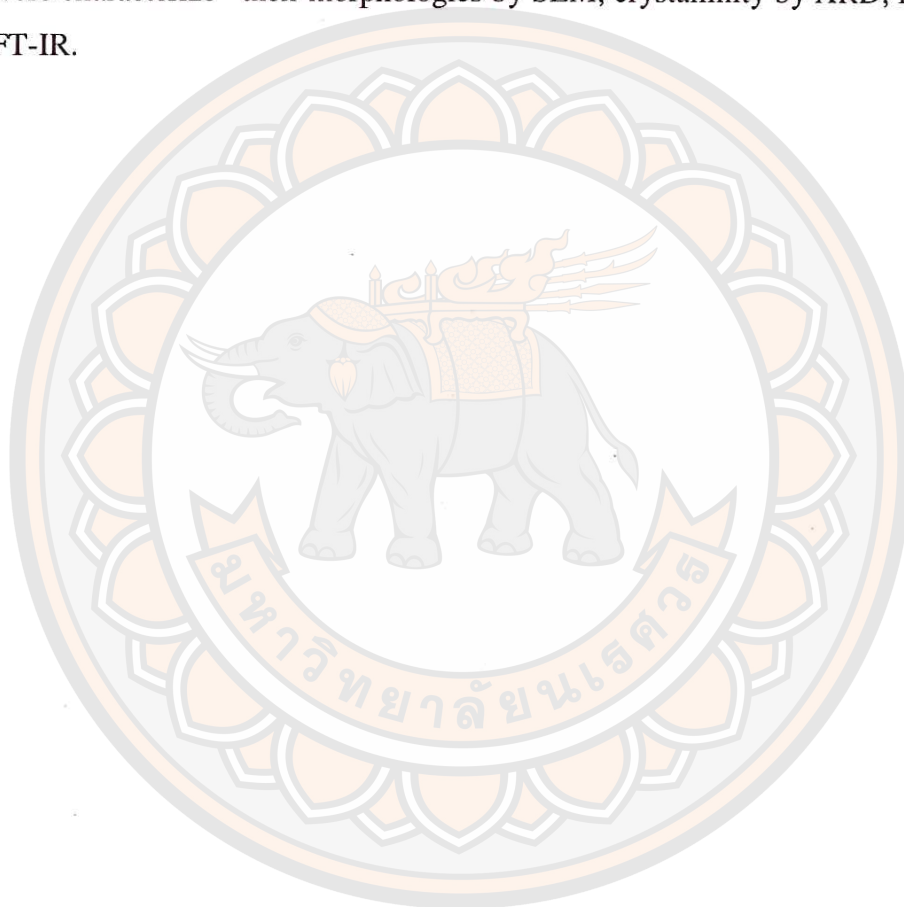
1. To fabricate and characterize the non-woven electrospun nanofibers of PVA and SS by studying the effect of PVA and SS concentrations.
2. To fabricate and characterize the non-woven electrospun nanofibers of PLA and PVA/SS blends, as layer by layer technique.

Scope of the research

The scope of this research work was divided into two approaches, the first is non-woven electrospun fibers of PLA/PCL/CAB blends and the second is non-woven electrospun fibers of PVA/SS and PLA and (PVA/SS) blends.

Approach I: the ternary blends of PLA/PCL/CAB were studied in term of miscibility between polymer pairs by Coleman-Painter approach and practical miscibility study of optical ternary phase diagram obtained from the rapid screening method. Then the selection of compositions was chosen from ternary phase diagram to fabricate into the fibers by electrospinning technique. The processing parameters that affected the electrospinning were studied, such as polymer concentrations, polymer solution flow rate, tip-to-collector distances and applied voltage. The non-woven electrospun fibers of PLA/PCL/CAB blend were characterized their morphology by using scanning electron microscopy (SEM), miscibility by Fourier transform infrared spectrometer (FT-IR), crystallinity by X-ray diffraction (XRD), thermal properties by differential scanning calorimeter (DSC), and hydrophilicity by water contact angle (CA).

Approach II: PVA and SS solutions were fabricated by electrospinning by study the effect of PVA and SS concentrations. Then the suitable compositions of PVA/SS blend were used to fabricate into the form of fibers. The fibers of PLA and PVA/SS were also fabricated into fibers by layer by layer technique. The processing parameters that affected the electrospinning were studied to find the optimized conditions. All non-woven electrospun fibers of PVA/SS and PLA and (PVA/SS) were characterize their morphologies by SEM, crystallinity by XRD, functionality by FT-IR.



CHAPTER II

LITERATURE REVIEWS

This work is concerned to study two different approaches of fabrication of the biodegradable and biocompatible electrospun fibers. The first approach is the fabrication of poly(lactic acid) (PLA), polycaprolactone (PCL) and cellulose acetate butyrate (CAB) blends. This approach contains three parts of; 1. the miscibility study of polymer pairs (PLA/PCL, PLA/CAB and PCL/CAB) by Coleman and Painter approach, 2. the fabrication of ternary PLA/PCL/CAB blend films by the technique called rapid screening method, representing by the optical ternary phase diagrams and 3. the fabrication of ternary PLA/PCL/CAB blend fibers by eletrospinning. The second approach is the fabrication of poly(vinyl alcohol) (PVA) and silk sericin (SS) blends, and PLA with PVA/SS layer by layer fiber mats. Therefore, in this chapter the background theory of biodegradable and biocompatible of PLA, PCL, CAB, PVA and SS will be first discussed. Then the background theory of miscibility, a practical approach to polymer miscibility of Coleman and Painter approach, and the electrospinning technique will be also described embedded with the reviews of the publication works related to this work.

Biodegradable and biocompatible polymers

Biodegradable polymers, which can be both natural and synthetic polymers, are normally degraded via microbial action. However, the word “biodegradable” is described according to ASTM standard D-5488-94d and European norm EN 13432. The “biodegradable” means “capable of undergoing decomposition into carbon dioxide, methane, water, inorganic compounds, and biomass” [25, 26]. ASTM 883-12 (2012) regards a degradable plastic as one that undergoes a significant change in chemical structure under specific environmental conditions. ASTM D 6400-12 (2012) defines a biodegradable plastic as a plastic in which the degradation results from the action of naturally occurring microorganisms such as bacteria, fungi and algae. ASTM sub-committee D20.96 proposal defines degradable plastics as plastic materials

that undergo bond scission in the backbone of the polymer through chemical, biological, and/or physical forces in the environment at a rate which leads to fragmentation or disintegration of the plastics [27, 28].

Biocompatible polymers are the polymers that can be made into devices to reduce the chance of rejection when incorporated into the body. Especially, the family of polyester (poly(lactic acid) and poly(glycolic acid)), play an increasingly important role in biomedical applications (i.e. orthopedics, tissue engineering). These polymers degrade by hydrolysis and enzymatic activity and have a range of mechanical and physical properties that can be designed to suitable in required application [29, 30]. Biocompatibility may be defined as “ability of a biomaterial to perform its desired function with respect to a medical therapy, without eliciting any undesirable local or systemic effects in the recipient or beneficiary of that therapy, but generating the most appropriate beneficial cellular or tissue response to that specific situation, and optimizing the clinically relevant performance of that therapy.” [31]

Polyesters are one of the most important biodegradable plastics being used in industry, due to their potentially hydrolysable ester bonds. They are degraded by cleavage of the ester linkages continues by water hydrolysis, the final products are carbon dioxide and water. The family of polyester can be divided into two major groups, aliphatic and aromatic polyesters, as classified and shown in Figure 1.

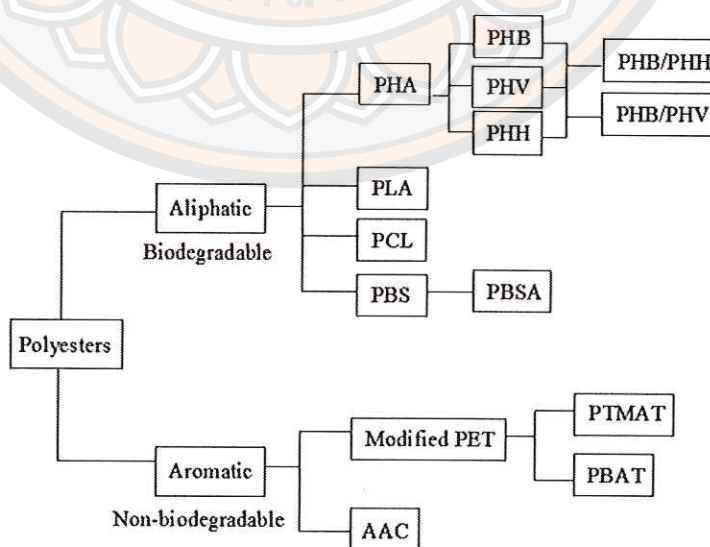


Figure 1 The classification of biodegradable polyesters.

Poly(lactic acid), PLA [32-35]

Poly(lactic acid) (PLA) is a thermoplastic aliphatic polyester derived from renewable resources, such as corn starch, tapioca products, sugarcane, which has been known as a polymer widely used in biomedical fields, including suture, bone fixation material, drug delivery and tissue engineering because PLA is biodegradable and biocompatible in contact with living tissues.

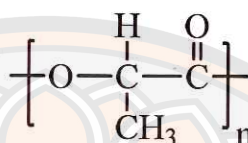


Figure 2 Chemical structure of Poly(lactic acid) (PLA)

PLA complies with the rising worldwide concept of sustainable development and is classified as an environmentally friendly material. In today's world of green chemistry and concern for the environment, PLA has additional drivers that make it unique in the marketplace. The starting material for the final polymer, as long as the basic monomers lactic acid is made by a fermentation process using 100% annually renewable resources such as cassava or corn. The polymer will also rapidly degrade in the environment and the by-products are of very low toxicity, eventually being converted to carbon dioxide and water. PLA complies with the rising worldwide concept of sustainable development and is classified as an environmentally friendly material. PLA can exist in three stereochemical forms: poly(L-lactide) (PLLA), poly(D-lactide) (PDLA), and poly(D, L-lactide) (PDLLA). The most commonly used isomer is the L-isomer and commercial poly(lactic acid) referred to as PLA is the L-isomer.

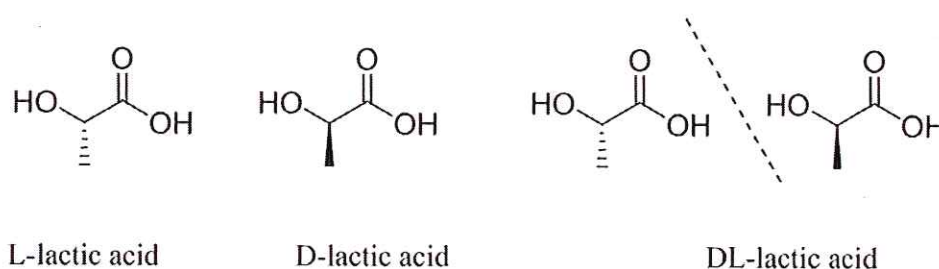


Figure 3 Stereochemical forms of lactic acids.

The properties of PLA depend on the component isomer, processing temperature, annealing time and molecular weight. PLLA is a semi-crystalline polymer, which has a crystallinity of around 37%, crystalline melting temperature (T_m) between 170-180°C, and a glass transition temperature (T_g) between 60-67°C. PLLA can be normally dissolved in halogenated hydrocarbons, such as chloroform, methylene chloride, 1,1,2-trichloroethane, and dichloroacetic acid, but is only partially soluble in ethyl benzene, toluene, acetone, and tetrahydrofuran. PDLLA is an amorphous polymer. It has a T_g in the region of 50-60°C. Since polymers from lactic acids have T_g above body temperature, these matrices are stiff with little elasticity in the body and are somewhat brittle at room temperature.

Polycaprolactone, PCL [32]

PCL is known as a flexible polymer, which is very relatively compatible with other polymers. It degrades predominantly through microbial agents. PCL shows a low T_g at -60°C, which make PCL a rubbery material and exhibits high permeability to low molecular species at body temperature. With the regular structure and low T_m at 60°C, PCL is a crystalline polymer. PCL is obtained by ring opening polymerisation of the 6-membered lactone called ϵ -caprolactone using a catalyst such as stannous octanoate, the reaction as shown in Figure 4.

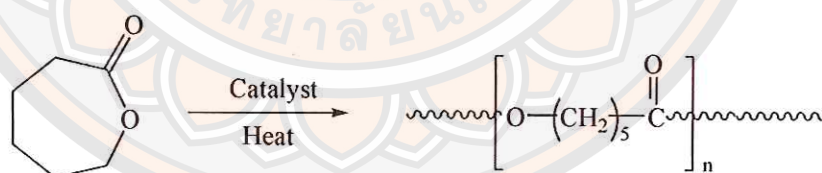


Figure 4 Ring opening polymerisation of ϵ -caprolactone to polycaprolactone (PCL).

Cellulose acetate butyrate, CAB [36, 37]

Cellulose acetate butyrate (CAB) is cellulose ester family, including cellulose acetate (CA), cellulose acetate propionate (CAP) and nitrocellulose. CAB consist ester molecule, butyryl and hydroxyl. Physical, chemical and structural properties can be controlled by chain length, degree of substitution and hydroxyl content depending on the different of requested applications. As CAB butyryl content

increases, solubility, flexibility and compatibility increase. As ester molecular weight increases, solubility and compatibility decrease but while toughness and melt point increase. Hydroxyl content increase, impacts moisture resistance decrease. CAB is wide latitude of solubility, compatibility and performance. Figure 5 shows the chemical structure of CAB.

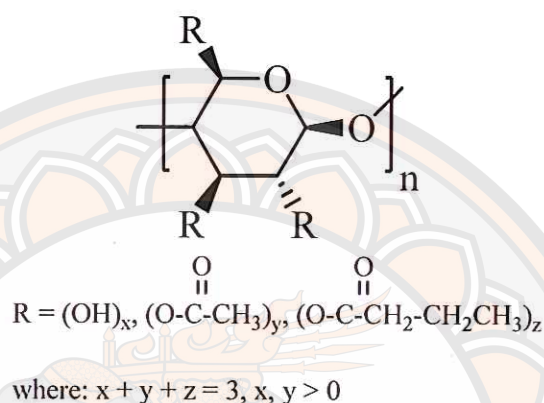


Figure 5 Chemical structure of cellulose acetate butyrate, CAB

Poly (vinyl alcohol), PVA

PVA is a water soluble and biodegradable synthetic polymer. It is a dry solid, and is available in granule and powdered forms. PVA was prepared via the hydrolysis of polyvinyl acetate in ethanol with potassium hydroxide. The most important properties, which affected to the majority of applications, are depending on the degree of polymerization and degree of hydrolysis. In the partially hydrolyzed grades, 86-89 mole% of acetate group is replaced by alcohol group. Likewise, in the fully hydrolyzed grade, 98.5~99.2 mole % of acetate group is replaced by alcohol group. Fully hydrolyzed grade PVA can be easily dissolved in over 90°C water, but it only swells in water at the room temperature. The glass transition temperature of PVA is ~85°C and the melting point is 230°C. Figure 6 shows the chemical structure of PVA.

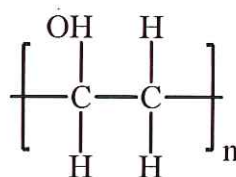


Figure 6 Chemical structure of Poly(vinyl alcohol), PVA

Reviews of the work on biodegradable and biocompatible polymers

Biodegradable polymers are widely used as biomaterials for medical applications [38]. Poly (lactic acid) (PLA) is one of the most widely used biomedical material, due to properties such as easy fabrication, biodegradability, biocompatibility, bioabsorbability and required mechanical performance [39]. There are many works that use PLA for modifying its properties with the different aims of applications. For examples, Dias J.C. et al. [40] studied the influence of morphology, fiber diameter and degree of crystallinity on degradation rate of electrospun PLLA fiber membranes in PBS at 37°C over 20 weeks (similar condition in the body) and found that increasing fiber diameter and degree of crystallinity shows slightly decrease in hydrolytic degradation rate.

Cui, w. et al. [41] have modified hydrophilicity of PLLA electrospun scaffolds by grafting chitosan by aminolysis method and found that it increases the hydrophilicity value on PLLA scaffolds with the increase amounts of the chitosan as shown in figure 7. The chitosan also enhanced the cell adhesion and growth as shown in figure 8.

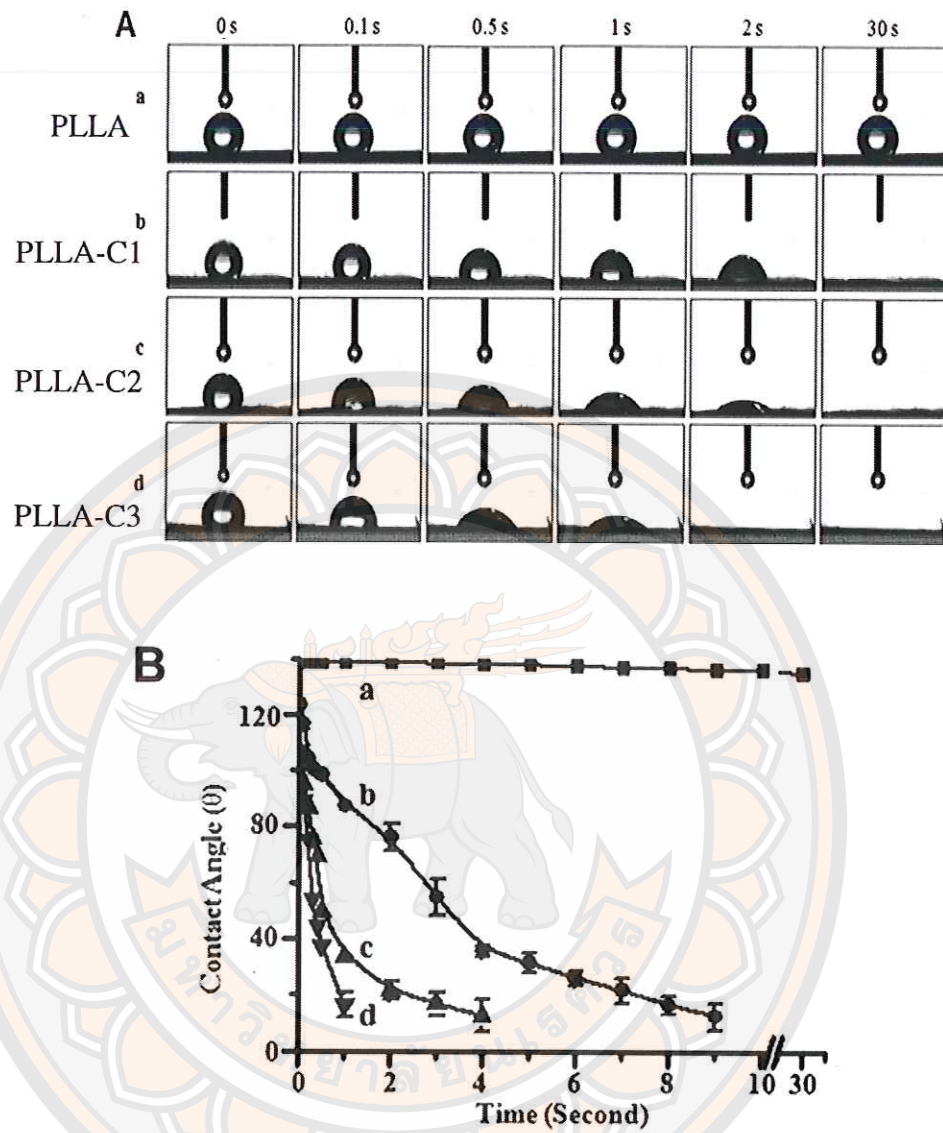


Figure 7 (A) Water contact angle image and (B) degree of contact angle of PLLA scaffolds with modified chitosan.

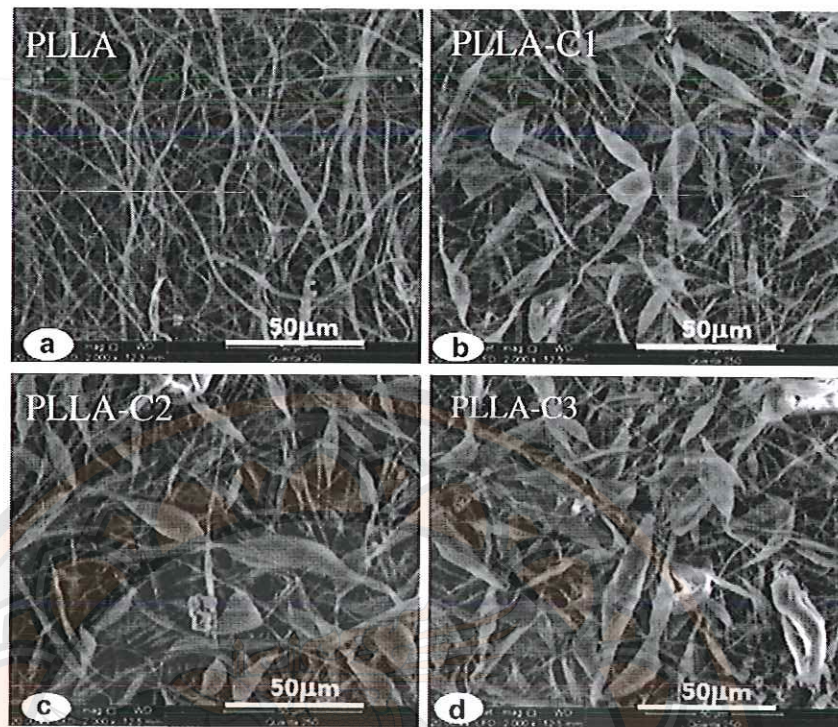


Figure 8 SEM image of skin's cell on PLLA scaffold with modified chitosan.

Kuihua, Z. et. al. [42] prepared silk fibroin and poly (L-lactic acid-co- ϵ -caprolactone) (SF/P(LLA-CL)) blend nanofiber scaffolds by electrospinning process. Degradation behaviors were investigated in PBS solution at 37°C and found that SF assist retarded degradation behaviors (as shown in figure 9) and degradation rate is one of an importance to skin's cell proliferation of electrospun nanofiber scaffolds.

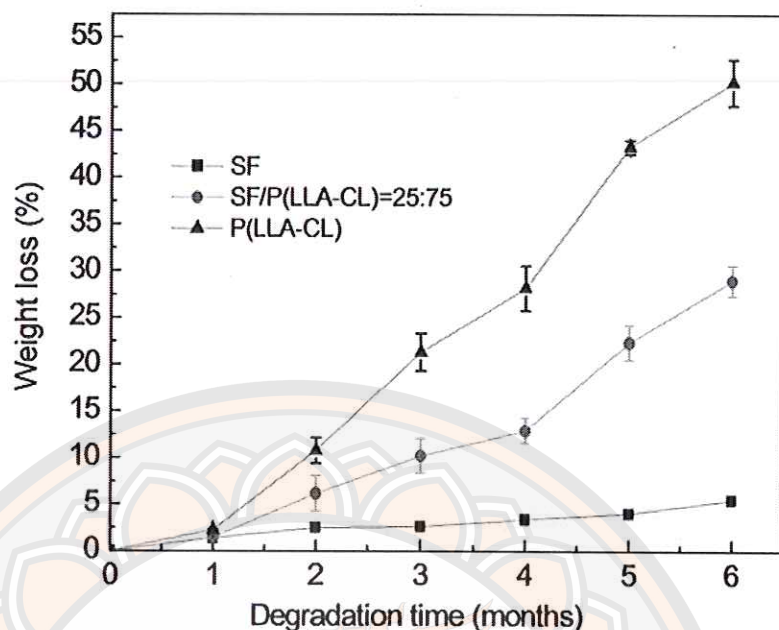


Figure 9 Present weight loss of nanofibrous scaffolds after degradation for different time in PBS.

Lowery, Z. et al. [43] studied the effect of electrospun poly(ϵ -caprolactone) fiber mats such as fiber diameter, pore size and human dermal fibroblasts seeding method and found that faster rate of cell proliferation on scaffold with pore diameters more than 6 μm . The perfusion seeding technique can observed seeded cell on scaffolds more than traditional droplet seeding technique.

There has be interested in biodegradable polymers in order to improve their required properties such as physical, thermal and mechanical properties by blending techniques. For example, Zeng, J.B. et al. [44] have improved PLLA toughness by blending with poly (ester-urethane) (PEU) as flexible polymers. This is due to PLLA has a low impact strength and is a brittle polymer. They found that the elongation at break increased from 7.2% to 320% with increasing PEU contents. Park, J.K. et al. [45] prepare porous polymer blends of PCL with PLLA (PCPL scaffolds) to improve compressive mechanical properties. PCL has much lower mechanical properties with high ductility and found that PCPL scaffolds have increased compressive mechanical strength with increasing PLLA contents.

Another biodegradable and biocompatible used in the medical field is poly(vinyl alcohol) (PVA). The work of Costa, L.M.M. et al. [46] used PVA for preparation of bionanocomposites with pineapple nanofibers and stryphnodendron adstringens bark extract especially for medical applications, by electrospinning technique. They found that PVA nanofibers changed in morphology with pineapple/stryphnodendron adstringens bark extract, giving a bigger fiber diameter and pore size.

Yooyod, M. et al [47] study the conformational structure and crystallinity of silk sericin (SS) from silk cocoon, and then fabricated into the films and three-dimensional (3D) porous polymeric scaffolds by reacting with poly(vinyl alcohol) (PVA) with a new cross-linker (dimethylolurea; DMU). The effect of SS conformational structures, DMU concentrations, and compositions of PVA/SS onto the structure and physical properties were studied. Cell culture study was also an important factor to observe for using scaffolds as a dermal reconstruction. The result show PVA/RT-SS (at room temperature) was chosen for the fabrication of 3D porous scaffolds with 10% DMU. All scaffolds showed good promote for the skin fibroblast cells. Therefore, a novel scaffold based on biomaterials was explored for tissue engineering scaffolds (i.e. skin tissue regeneration).

The literatures shown above are examples of polymers that were modified and studied in different targets and for different applications. However, in this work, the fabrication of biodegradable and biocompatible of polymers, PLA, PCL, CAB, PVA and SS, were used to fabricate into the electrospun fibers with the target to potential used as scaffolds for medical applications.

Silk sericin from silk cocoons

Silk fibers from silk cocoons are naturally occurring material that has been used as an excellent textile material for centuries. The unique mechanical properties of these silk material has attracted attention as a biomedical material owing to its good blood compatibility, low inflammability, excellent compatibility and biodegradability. These properties have prompted extensive studies of the biomedical applications of silk, such as tissue engineering scaffold and wound dressing. Silk fibers consist of a filament core protein, silk fibroin, and a glue-like coating consisting of a family of

sericin. Sericin covers two fibroin strands in a single silk fiber. Silk fibroin and silk sericin have a completely different structure and properties due to composing the different amino acid compositions. Silk fibroin does not dissolve in water due to the hydrophobic amino acids, whereas silk sericin is hydrophilic and more viscous in the solution state. In the field of biomedical applications of silk, both silk sericins and fibroins have been extensive used among the researchers. Figure 10 shows the picture of silk cocoons, demonstrated the silk sericin and fibroin [48].

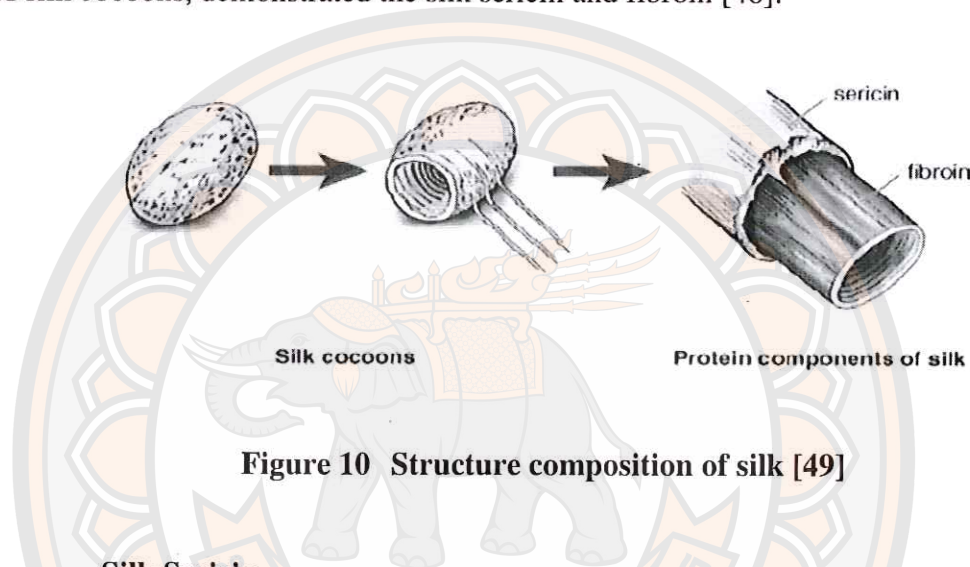


Figure 10 Structure composition of silk [49]

Silk Sericin

As known, silk sericin or silk gum is a natural macromolecular protein that covers the fibroin fibers produced from bombyx Mori silkworm cocoons. It is wasted during the process of degumming of silk cocoons in silk industry. Sericin is the second type of silk protein and contributes about 20-30% of the total cocoon. Silk sericin is a highly hydrophilic macromolecular protein comprising of 18 amino acids including essential amino acids. The major amino acid compositions in sericin, including serine, aspartic acid, glycine and threonine [50]. The total amount of hydroxyl amino acids is 45.8%, polar amino acid 42.3% and nonpolar amino acid residues 12.2% in sericin [51]. It consists of polar side chain made of hydroxyl, carboxyl and amino groups that enable easy crosslinking, copolymerization and blending with other polymers to form improved biodegradable materials [52]. Sericin has a combination of many unique properties such as biodegradability, nontoxicity, antioxidative, antimicrobial activity, UV resistance, and absorbs moisture. Therefore, silk sericin has the potential to be used in many applications such as food, cosmetic,

tissue engineering medical and polymer material. Figure 11 shows the chemical structures of silk sericins and its amino acids.

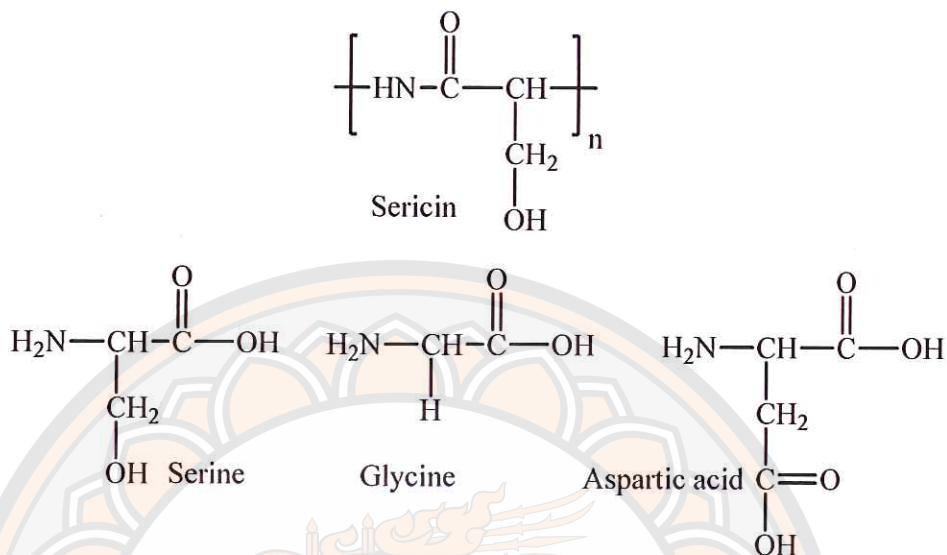


Figure 11 Chemical structure of Sericin (SS)

The literature reviews of the use of SS were discussed here, for example, Hadipour-Goudarzi, E. et al [53] prepared nanofiber mats of chitosan (Cs)/sericin(SS)/PVA composite by using electrospinning. The effect of different spinning conditions (i.e. voltage, spinning distance, and feed rate), volume ratio of chitosan and sericin, morphology, diameter of fiber and chemical structure, were studies. In addition, the effect of AgNO_3 for antibacterial activity was investigated. The optimum conditions used 50:50 v/v of chitosan:sericin, 22 kV, 10 cm spinning distance at 0.25 mL/h to prepare nanofibers with small diameter without beads. The average diameter of nanofibers was 180 nm while AgNO_3 led to smaller nanofibers diameter of 95 nm. AgNO_3 produced an excellent antibacterial activity against *Escherichia coli*. Mandal B.B. et al [54] prepared novel silk sericin/gelatin blend 3-D scaffolds and 2-D films with improves properties. The scaffolds were enhanced mechanical strength and high compressibility. Cytocompatibility of scaffolds was observed by using feline fibroblasts showing normal spreading and proliferation. It has potential use in tissue engineering applications. Dash, B. et al [55] fabricate and characterize the silk gland sericin protein membranes for potential biomedical applications. The membranes show robustness, good mechanical strength and high temperature stability. Cytocompatibility of the membranes was evaluated using feline

fibroblast cells. Morphology of growing cells was observed by confocal microscopy that present the normal spreading and proliferation on the silk sericin membranes.

Introduction and background to the miscibility of blends [32, 56]

There are many objectives for using polymer-blending processes depending on applications and properties of the polymer blends. First, to improve mechanical properties and fracture resistance, such as adding a rubber phase into the rigid polymers. Secondly, to achieve some specific performances, such as transparency, heat distortion, and barrier properties. Two-phase materials can be transparent if the refractive indices are matched close enough or the phases are small enough. Improving the ability of a rigid polymer to function at elevated temperature like heat distortion temperature leading to the formulation of commercially successful products. Thirdly, to reinforce the neat plastics, a variety of reinforcing fillers or polymers are normally used to make polymer blends strong enough for specific required applications. Fourthly, to make elastomeric blends, the mixing of two or more elastomers is subsequently vulcanised in the traditional ways of rubber technology.

The miscibility of polymers is determined by using the Flory Huggins equation and the free energy of mixing (ΔG_m) and is written in equation 1. The polymer blends will be miscible when ΔG_m is negative.

$$\frac{\Delta G_m}{RT} = \frac{\Phi_A}{M_A} \ln \Phi_A + \frac{\Phi_B}{M_B} \ln \Phi_B + \Phi_A \Phi_B \chi + \frac{\Delta G_H}{RT}$$

Eq. 1

The factors that affect the miscibility of polymers blends are usually composition and temperature. There is a range of compositions of polymer blends either miscibility or immiscibility. Figure 12 shows an example of how polymer blends miscibility is affected by composition of another polymer (B). It can be seen that polymer A/B blends will be miscible when polymer B less than 30 %wt and more than 70% wt, while immiscible and showing phase separation when polymer B is between 30-70 % wt.

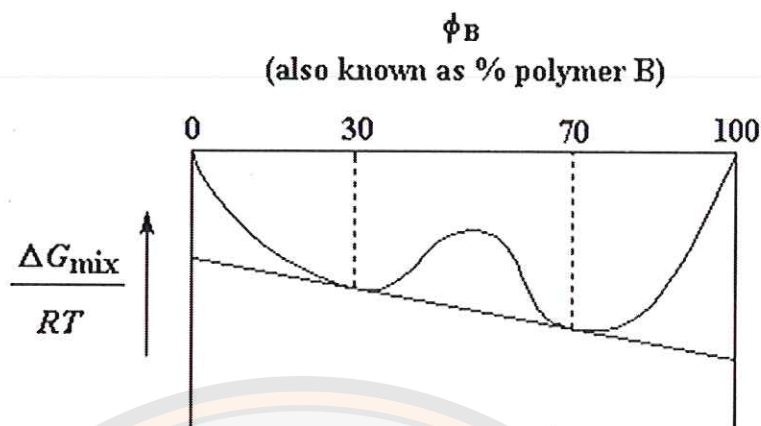


Figure 12 The free energy of mixing (ΔG_m) of Polymer A and B versus % wt. of polymer B; the miscibility depending on composition.

However, the composition ranges for miscibility can be changed by temperature, as shown in figure 13. For some polymer pairs, the components of a mixture are miscible when the temperature below at the critical point. This temperature is called low critical solution temperature (LCST). This means the range of miscibility increases with decreasing temperature. For other polymer pairs, the components of a mixture are miscible when the temperature above the critical point, called upper critical solution temperature (UCST). This means the range of miscibility increases with increasing temperature. The LCST and UCST are depending on pressure, degree of polymerization, polydispersity and branching of polymers.

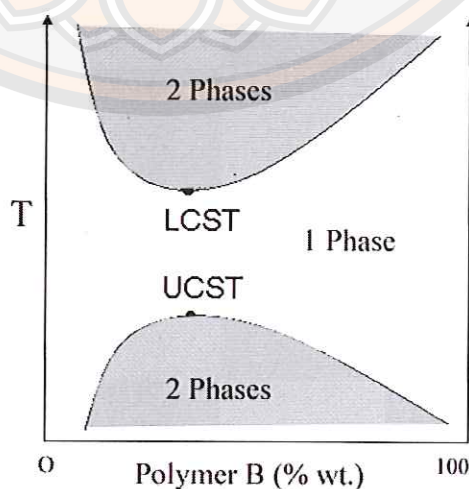


Figure 13 Polymer solution phase behavior showing LCST and UCST

In general, polymer blends have physical and mechanical properties between the neat polymers used to blend. For example, the T_g of polymer blends will depend on the ratio of neat polymers. If two polymers have different T_g , one is low and another one is high, T_g of the blend relatively increases in generally a linear fashion when the composition of polymer having high T_g increases. Sometimes the T_g will be higher than expected because the two polymers entangle more strongly to each other than to themselves to cause lowers chain mobility. The T_g effects other polymer properties, such as mechanical properties, chemical resistance, and heat resistance.

As mentioned in the first paragraph, there are two major methods for polymer blends, solvent blending and melt blending. Solvent blending is dissolving polymers in solvent, and then allowing the solvent to evaporate at the required temperature. This method is normally used in laboratory scale because of the limitation of the price, which is very expensive to evaporate or recapture the solvent in a massive scale. It is also because the solvents themselves are expensive and the evaporating solvents will effect on the environment. Thus, melt blending is regularly used in industries. The polymers used for blending are heated above T_g and mixed together in machines such as extruders, two-roll mills, and internal mixer.

The work is related to the miscibility study of polymer pairs and ternary polymer blends. As mentioned above, the first observation of miscibility between polymer pairs that will be used is the Coleman and Painter Approach. The second observation of miscibility of ternary blend, we used the technique called "rapid screening method". The technique allows us to predict the apparent miscibility by using optical clarity of the blended films. Therefore, in this section, the detail of the Coleman and Painter approach and the rapid screening method will be described.

Coleman and Painter Approach

The miscibility guide by Coleman-Painter (equation shown below) is used.

$$\frac{\Delta G_m}{RT} = \frac{\Phi_A}{M_A} \ln \Phi_A + \frac{\Phi_B}{M_B} \ln \Phi_B + \Phi_A \Phi_B \chi + \frac{\Delta G_H}{RT}$$

Eq.1

Where ΔG_H term is the free energy changes as a result of specific interactions. Φ_A and Φ_B , and M_A and M_B , are the volume fractions and degrees of polymerization of A and B, respectively, while χ is the Flory interaction parameter. The approach uses structural interaction factors, such as H-bonding and polar interaction, as a means of explaining why polymer systems can show the symptoms of miscibility, these will be used to interpret the miscibility behavior of PLA blends, although they are not perfectly matched in thermodynamic terms.

A practical approach to polymer miscibility

The critical values of χ in Eq.1 and the upper limits of the non-hydrogen bonded solubility parameter difference $[(\Delta\delta)^{\circ\text{Crit}}]$ of Coleman and Painter are a practical approach to polymer miscibility used in this work. A summary of the range of values of $(\Delta\delta)^{\circ\text{Crit}}$ is shown in Table 2. The polymer pairs will have the greatest miscibility when the values of the two non-hydrogen bonded solubility parameters ($\Delta\delta$) are very close, and the relative strengths of any specific intermolecular interactions between the polymer pairs are high values.

To estimate the interaction parameters (χ), the solubility parameters (δ) can be calculated by dividing the sum of molar attraction constants (F) by the molar volume of the groups present in the repeat unit of the polymer, as shown in Eq. 2.

$$\delta = \sum \frac{F_i}{V} \quad \text{Eq. 2}$$

The values of F and V of unassociated groups and weakly associated groups, from Coleman, Painter and coworkers, are shown in Table 1.

Table 1 The molar attraction constants (F) and molar volume (V) of unassociated groups and weakly associated groups [32].

| Group | F (cal.cm ³) ^{1/2} | V (cm ³ /mole) | Group | F (cal.cm ³) ^{1/2} | V (cm ³ /mole) |
|-------------------------------|--------------------------------------------|------------------------------|--------------------------|--------------------------------------------|------------------------------|
| <u>Unassociated</u> | | | <u>Unassociated</u> | | |
| -CH ₃ | 218 | 31.8 | -OCO- | 298 | 19.6 |
| -CH ₂ - | 132 | 16.5 | -CO- | 262 | 10.7 |
| >CH- | 23 | 1.9 | -O- | 95 | 5.1 |
| >C< | -97 | -14.8 | >N- | -3 | -5.0 |
| C ₆ H ₃ | 562 | 41.4 | <u>Weakly Associated</u> | | |
| C ₆ H ₄ | 652 | 58.8 | -Cl | 264 | 23.9 |
| C ₆ H ₅ | 735 | 75.5 | -CN | 426 | 23.6 |
| CH ₂ = | 203 | 29.7 | -NH ₂ | 275 | 18.6 |
| -CH= | 113 | 13.7 | >NH | 143 | 8.5 |
| >C= | 18 | -2.4 | | | |

Table 2 Summary of the upper limit of the critical values of the solubility parameter difference, $(\Delta\delta)^{\circ\text{Crit}}$ [32].

| Specific Interactions Involved | Polymer Blend Examples | $(\Delta\delta)^{\circ\text{Crit}}$ (cal.cm ⁻³) ^{1/2} |
|-----------------------------------|------------------------|-------------------------------------------------------------------------------|
| Dispersive Forces Only | PBD-PE | ≤ 0.1 |
| Dipole-Dipole | PMMA-PEO | 0.5 |
| Weak | PVC-BAN | 1.0 |
| Weak to Moderate | PC-Polyesters | 1.5 |
| Moderate | SAN-PMMA | 2.0 |
| Moderate to Strong | Nylon-PEO | 2.5 |
| Strong | PVPh-PVAc | 3.0 |
| Very Strong | PMAA-PEO | ≥ 3.0 |

The polymer miscibility observations in this work are based on the Coleman and Painter miscibility guideline but only by using it as a simple guideline to predict trends in polymer miscibility - because it cannot be directly applied to three-component blends. Therefore, the Coleman-Painter approach will be used as a preliminarily guide to detect apparent or temporary miscibility of the blends, whereas they do not predict that the system obeys the criteria for thermodynamic miscibility.

Ross S. et al [6] studies optically clear regions of ternary blend of poly (L-lactic acid)(PLLA)/polycaprolactone(PCL)/cellulose acetate butyrate(CAB) using a novel rapid screening method. First, the Coleman-Painter approach were used to predict miscibility of PLA, PCL and CAB. It is know that PLA/PCL are immiscible, PLA/CAB are miscible and PCL/CAB may be immiscible or miscible. Rapid screening method provide optical phase diagram of ternary blend films. The optically regions of ternary phase diagram were described by WAXS, demonstrated that different crystalline regions with the molecular weight effects.

Ross S. et al [8] studies novel ternary blends based on poly(L-lactide) (PLLA) together with polycaprolactone (PCL) and thermoplastic polyurethane (TPU) into the films using a solvent meditated technique called the rapid screening method. Miscibility prediction of polymers were investigated by Coleman-Painter approach. The results showed that the different of optical phase boundaries in PLLA/PCL blends were strongly influenced by TPU. The different boundaries depended on the molecular weight of the PLLA and PCL selected.

Ross S. et al [7] studies the effect of stereo-regularity and molecular weight of poly(lactic acid) (PLA) on ternary polymer blend films (PLLA/PCL/CAB and PDLLA/PCL/CAB) was analyzed using optical clarity phase diagram. The results of the ternary blends optical clarity showed the position of the phase boundaries in PLLA/PCL/CAB and PDLLA/PCL/CAB blends are significantly affected by the stereo-regularity and molecular weight of PLA.

Electrospinning process [57-59]

Electrospinning is a unique technique using electrostatic forces to produce fibers from polymer fluid (solutions or melt) through a small nozzle and thus fibers

have a thinner diameter in nanometer to micrometer scale than other spinning processes. The principle of electrospinning process was strong mutual electrical repulsive forces overcome weaker force of surface tension in polymer solutions, the pendant droplet will deform into a conical droplet or called “Taylor cone”. A general electrospinning setup contains three components as shown in Figure 14, high voltage power supply (kV), a syringe pump to inject polymer fluid and a grounded collector. At present, electrospinning processes have been widely used in tissue engineering applications to fabricate two-or-three-dimensional biomaterial nanofiber scaffolds. The morphology and orientation of fabricated fibers can be controlled by processing, solution and ambient parameters such as solution conductivity, polymer concentration, applied voltage, flow rate, tip diameter, spinning design, collector design, collector distance etc.

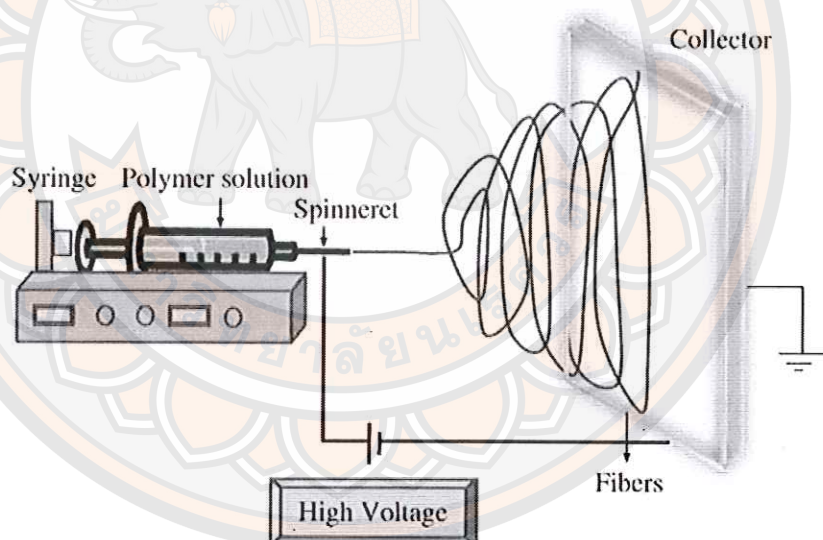


Figure 14 Schematic diagram of a general electrospinning setup

Lu, L. et al. [60] have focused on the preparation of polylactide/poly (ϵ -caprolactone) (PLA/PCL) blend fibers by studying the effect of the compositions of polymer solution and solution conductivity. Blending ratios of PLA/PCL and compositions of mixed solvent (chloroform/dimethylformamide, CF/DMF) effect the morphology of fibers. They found that the average fiber diameter increases from 280 nm to 640 nm when using PLA content of 90 wt%. The result is shown in figure 15.

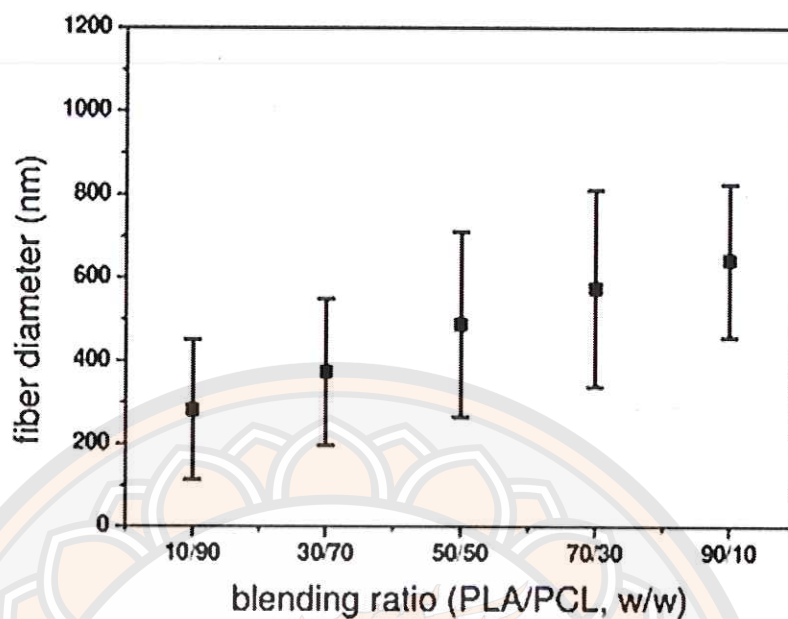


Figure 15 The compositions of polymer solution that effect to fiber diameter.

Chloroform (CF) is good solvent for dissolved PLA and PCL polymers and that have dielectric constant as 4.8. Dimethylformamide (DMF) is poor solvent for dissolved PLA and PCL polymers and that have dielectric constant more than chloroform as 38.3 as shown in table 3.

Table 3 Physical properties of the used solvents

| Solvents | Solubility ^a | bp (°C) | D_m ^b | Dielect ^c |
|----------|-------------------------|---------|--------------------|----------------------|
| CF | Good solvent | 61.6 | - | 4.8 |
| DMF | Poor solvent | 153.0 | 3.9 | 38.9 |

^aFor both PLA and PCL. ^bDipole moment in debyes. ^cDielectric constant at 20°C.

The electrical conductivity of the solution increases with increasing DMF content that decreases the average fiber diameter from 1800 nm to 200 nm and smooth surface fibers as shown in figure 16 and 17.

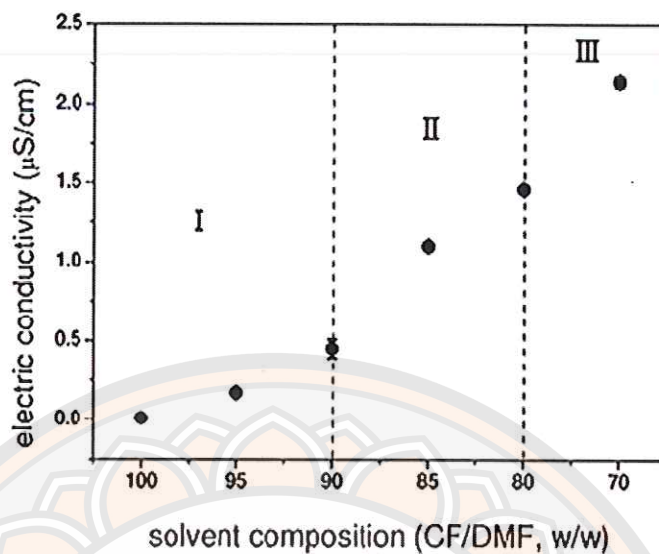


Figure 16 The electrical conductivity of the solution.

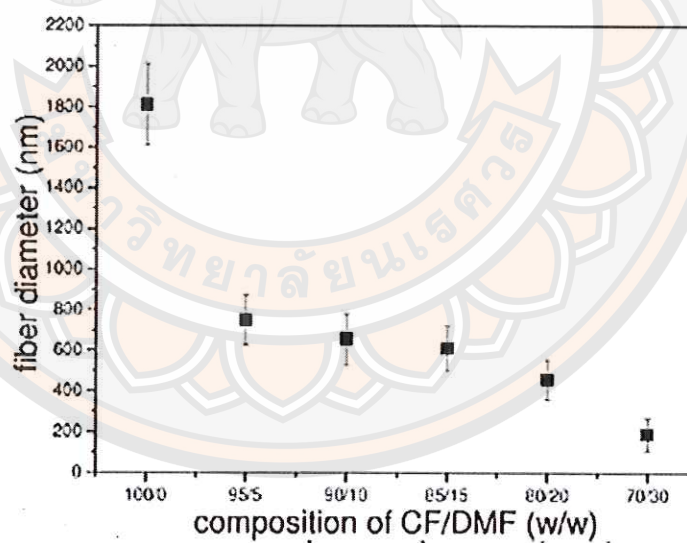
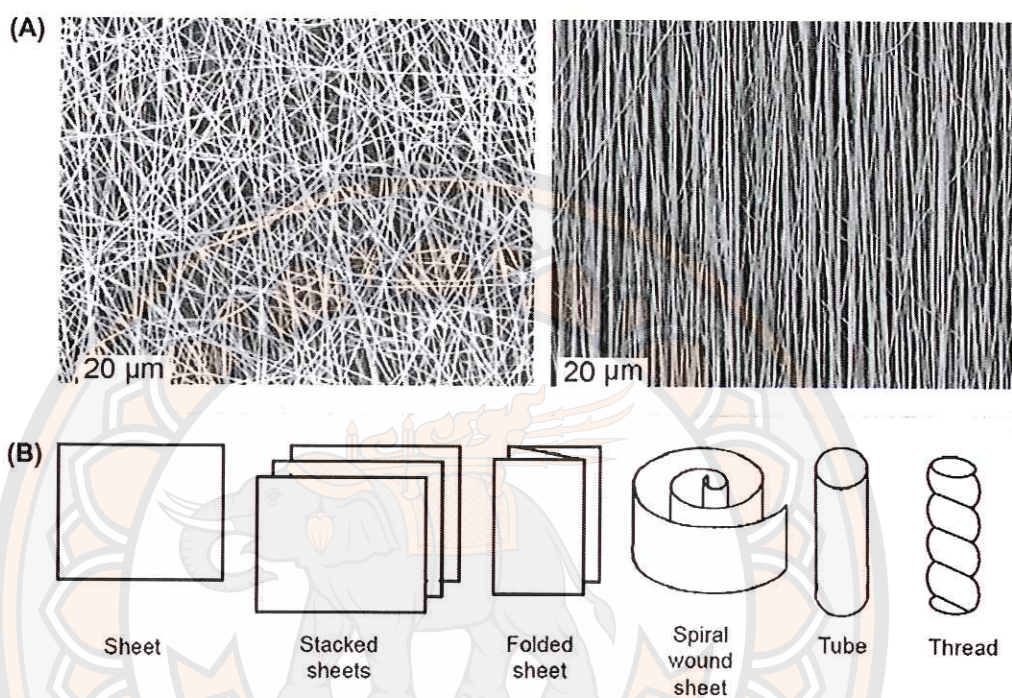


Figure 17 The composition of CF/DMF solvent that effect to fiber diameter.

Meinel, A.J. et al [61] have fabricated nano or micro fibers for drug delivery by using electrospinning technique. Various parameters that effect the morphology of fiber such as solution parameters (e.g., viscosity, conductivity, surface tension), processing parameters (e.g., electric field strength. Flow rate, collector set-up) and

ambient parameters (e.g., temperature, humidity). Example of collector set-up are random and aligned fiber that there can design various form by stacking, folding, winding or twisting of flat electrospun fibers as shown in figure 18.



**Figure 18 SEM image of (A) random and aligned electrospun fibers.
(B) Various shapes of scaffolds.**

Sill, T.J. et al [62] studied the electrospinning parameters that effect to morphology of fibers for drug delivery and tissue engineering applications (i.e., applied voltage, flow rate, distance between capillary and collector, polymer concentration, solution conductivity and solvent volatility) as shown in table 4.

Table 4 Effects of electrospinning parameters on morphology of fiber

| Parameter | Effect on fiber morphology |
|--------------------------------------------|-----------------------------------------------------------------------------------------------------------|
| Applied voltage ↑ | Fiber diameter ↓ initially, then ↑ (not monotonic) |
| Flow rate ↑ | Fiber diameter ↑ (beaded morphologies occur if the flow rate is too high) |
| Distance between capillary and collector ↑ | Fiber diameter ↓ (beaded morphologies occur if the distance between capillary and collector is too short) |
| Polymer concentration (viscosity) ↑ | Fiber diameter ↑ (within optimal range) |
| Solution conductivity ↑ | Fiber diameter ↓ (broad diameter distribution) |
| Solvent volatility ↑ | Fibers exhibit microtexture pores on their surfaces, which increase surface area) |

The use of electrospun nanofibers in biomedical applications

Tissue engineering scaffolds for skin tissue regeneration were continually developed for use in damaged dermal. In recent years, Ravichandran, R. et al. [63] fabricated PLLA/poly-(α , β)-DL-aspartic acid (PAA)/Collagen (Col I&III) nanofiber scaffolds by electrospinning. The results of morphology, contact angle, functionality, and cell proliferation showed that cell proliferation rate significantly increased in PLLA/PAA/Col I&III scaffolds when compared with PLLA and PLLA/PAA scaffolds as shown in figure 19.

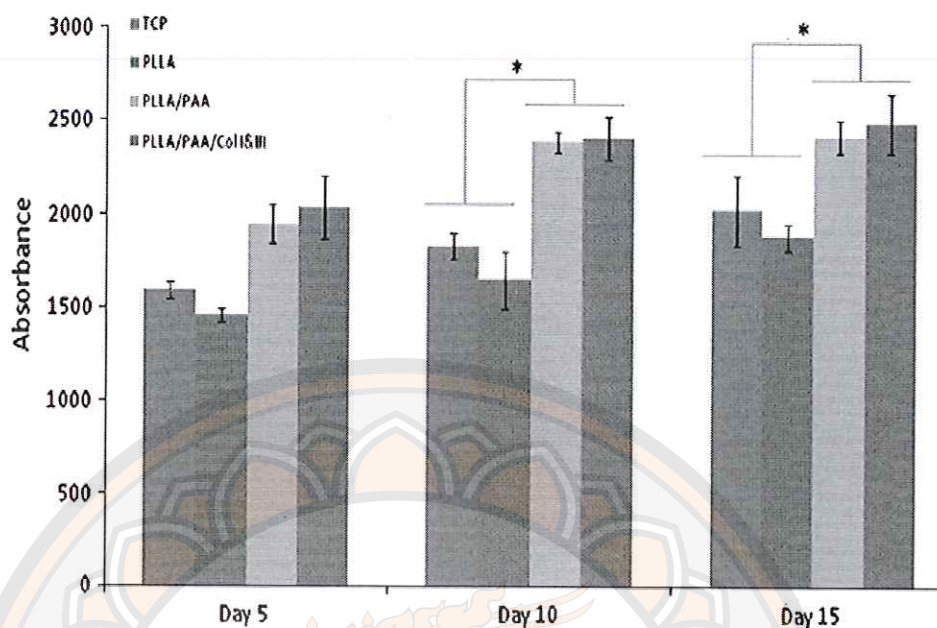


Figure 19 MTS assay for the cell proliferation on PLLA/PAA/Col I&III scaffolds

Cell proliferation on the nanofibers were observed by the colorimetric MTS assay. The reduction of [3-(4,5-dimethylthiazol-2-yl)-5-(3-carboxymethoxyphenyl)-2-(4-sulfophenyl)-2H-tetrazolium] (yellow tetrazolium salt) to form purple formazan crystals by the dehydrogenase enzymes within mitochondria of metabolically active of cells and formazan form shown the absorbance at 492 nm.

Cui, W. et al. [64] fabricated poly(DL-lactic acid) blending with poly(ethylene glycol) (PDLLA/PEG) fiber scaffolds with different PEG contents for optimal tissue engineering scaffolds by electrospinning process. The result demonstrated that 30% PEG was the most balanced properties of middle range hydrophilic surface, a little dimensional shrinkage, adjust biodegradation and enhance cell penetration in fiber mats as shown in figure 20.

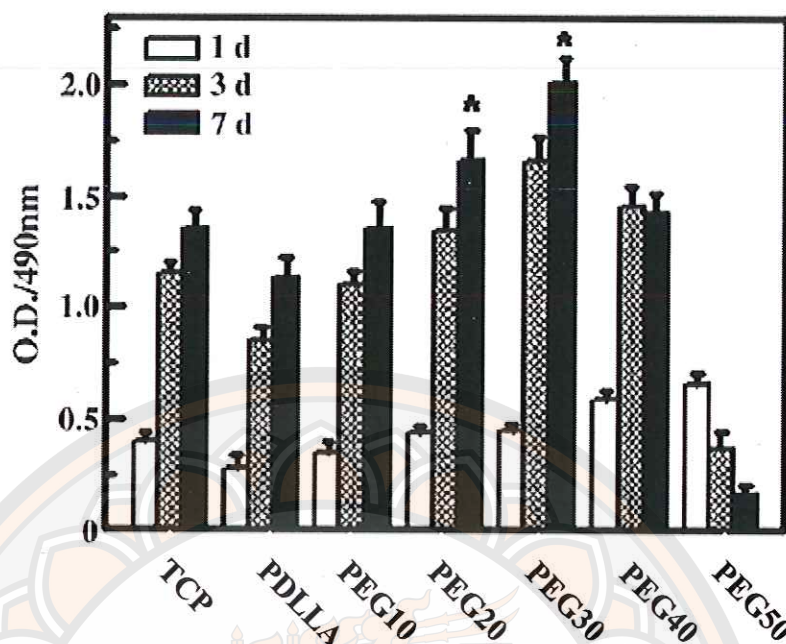


Figure 20 MTS assay of cell proliferation on PDLLA/PEG fiber scaffolds.

Blackwood, K.A. et al. [65] developed the fabrication of electrospun nanofiber scaffold for dermal tissue engineering, to enhance cell growth. Six compositions of scaffold were prepared; 1. PLLA, 2. PLLA/10% oligolactide, 3. PLLA/rhodamine, 4-6. PLGA random multiblock copolymers in lactide/glycolide ratio of 85:15, 75:25 and 50:50 and studied in vitro-in vivo degradation found that the PLLA scaffold was stable even after 12 months, while PLGA (85:15, 75:25) scaffolds degraded 50% after 3-4 months. The in vitro PLGA (85:15, 75:25) supported the Keratinocyte, fibroblast and endothelial cell growth and the extracellular matrix (ECM). Therefore, PLGA (85:15, 75:25) electrospun scaffolds have potential to be used as biodegradable materials for dermal replacement.

In the addition, Thakur R.A. et al. [66] have successfully fabricated electrospun PLLA nanofiber scaffolds with targeted drug release for wound dressing application by using dual spinneret electrospinning into the single scaffold as shown in figure 21.

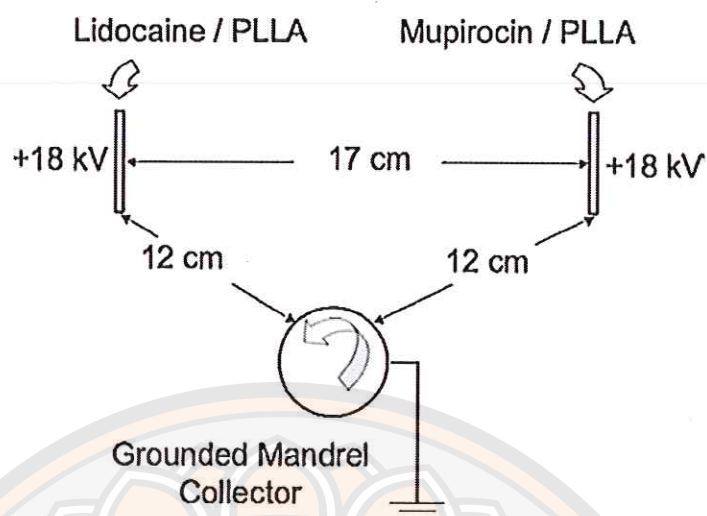


Figure 21 Dual spinneret electrospinning apparatus setup.

They found that deliver therapeutic concentration of drug is useful in wound healing for a 3-plus day therapy of dressing as shown in figure 22.

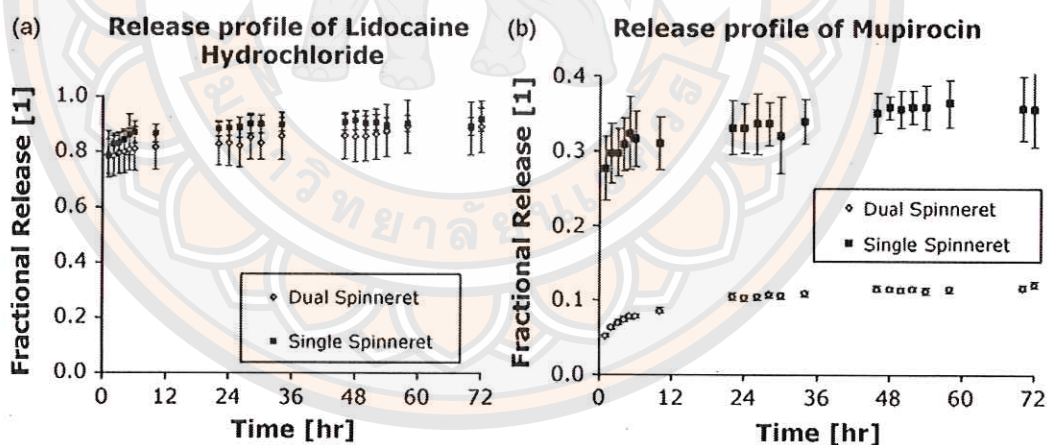
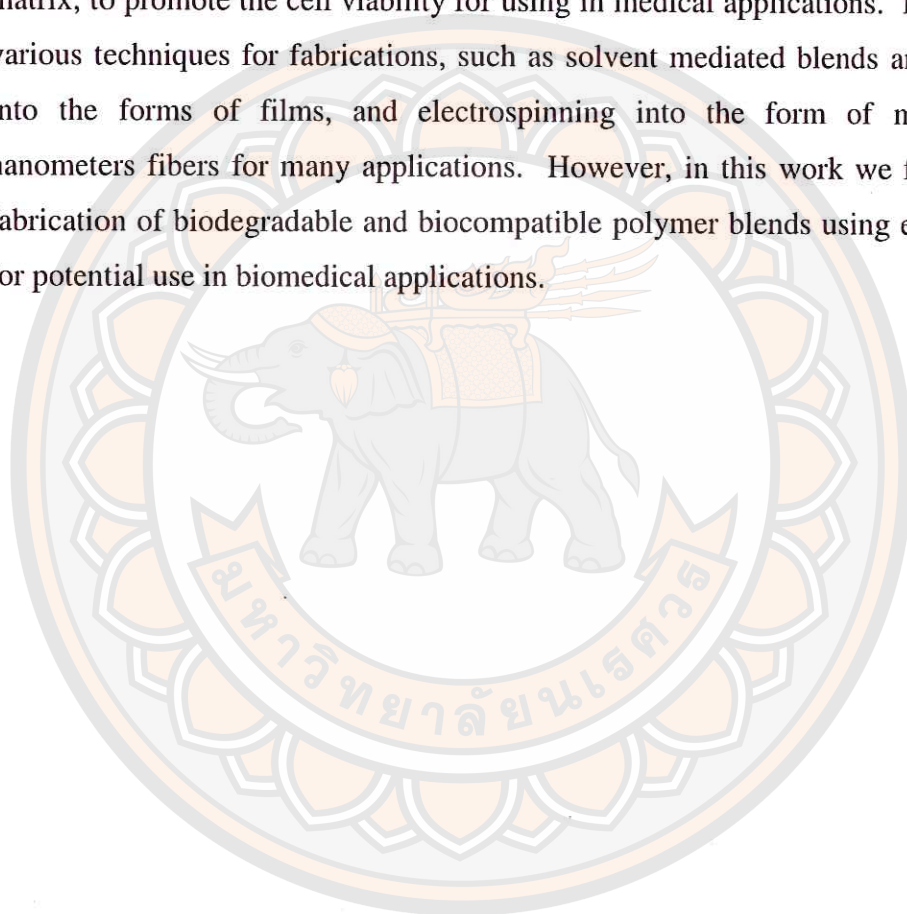


Figure 22 Release profile of drug of electrospun PLLA nanofiber scaffolds;
a. is released lidocaine hydrochloride drug and
b. is released mupirocin drug of PLLA scaffolds.

Summary of the chapter

There are many research works that focused on the use of biodegradable and biocompatible polymers, especially poly(lactic acid) and the alpha-polyesters, as well as the natural non-toxic materials, such as silk fibroin, silk sericins. They have many different objectives to work on these biodegradable and biocompatible polymers and natural non-toxic materials, such as to enhance the mechanical properties of the matrix, to promote the cell viability for using in medical applications. In addition, the various techniques for fabrications, such as solvent mediated blends and melt blends into the forms of films, and electrospinning into the form of micrometers to nanometers fibers for many applications. However, in this work we focused on the fabrication of biodegradable and biocompatible polymer blends using electrospinning for potential use in biomedical applications.



CHAPTER III

RESEARCH METHODOLOGY

This chapter contains the information of materials, instrument and methods used in this work. The work is divided into two approaches depending on the techniques and the types of materials to fabricate the nanofibers. The first approach is the electrospinning technique to fabricate the ternary blends of poly(lactic acid) (PLA), polycaprolactone (PCL) and cellulose acetate butyrate (CAB) into electrospun nanofiber scaffolds. The second approach is the electrospinning technique to fabricate poly(vinyl alcohol) (PVA) and silk sericin (SS), and the combination of PLA and PVA/SS. To be noted that all materials used in this work are biocompatible and biodegradable polymers that can be possible to use for biomedical applications.

Materials

Poly(lactic acid) (PLA)

Poly(lactic acid) (PLA) was supplied by PTT Chemical Co. Ltd, Thailand ($M_n = 58,760, 4032D$).

Polycaprolactone (PCL)

Two different molecular weights of polycaprolactone (PCL); PCL1 ($M_n = 10,000 \text{ g.mol}^{-1}$), PCL2 ($M_n = 42,500 \text{ g.mol}^{-1}$) from Sigma-Aldrich Co. Inc. Gillingham, Dorset, UK, and PCL3 ($M_n = 80,000 \text{ g.mol}^{-1}$) from Shenzhen Esun Industrial Co., Ltd, Guangdong, China, were used.

Cellulose acetate butyrate (CAB)

Cellulose acetate butyrate (CAB) ($M_n = 30,000 \text{ g.mol}^{-1}$, 2 wt% acetyl and 52 wt% butyryl content) was purchased from Sigma-Aldrich, UK.

Solvents

Chloroform (CF) and dimethylformamide (DMF), from RCI Labscan Limited, Bangkok, Thailand, were selected to use as solvents for electrospinning. CF is a good solvent and has dielectric constant at 20°C of 4.8, while DMF is a poor solvent for PLA, PCL and CAB and has dielectric constant at 20°C of 38.3.

Poly(vinyl alcohol) (PVA)

Poly(vinyl alcohol) (PVA) was supplied by Sigma-Aldrich Co. Inc, Singapore ($M_w = 77,000\text{--}82,000 \text{ g.mol}^{-1}$).

Silk cocoons

Silk cocoons (*Bombyx mori*) provided from Tak province in the lower northern region of Thailand.

Instruments

The major instruments used are listed below.

1. Fourier Transform Infrared Spectroscopy (FT-IR, Perkin Elmer Spectrum GX, $4000\text{--}400 \text{ cm}^{-1}$)
2. Scanning Electron Microscopy (SEM, Leo Model 1455VP)
3. X-ray Diffraction Spectroscopy (XRD, Philips Model X'Pert Por)
4. Differential Scanning Calorimetry (DSC, Mettler Model DAC1)
5. Water contact angle (CA, Dataphysics Model OCA20)
6. Microplate reader (Biotek, Model Synergy H1 Hybrid Reader)
7. Precision pump (NE-300, New Era Pump Systems, Inc., USA)
8. High-voltage power supply (maximum voltage 30 kV, Genvolt, General High Voltage Ind. Ltd, UK)

Methods for approach I: The electrospinning technique for PLA/PCL/CAB

In this approach, the electrospinning technique was used to fabricate the ternary blends of poly(lactic acid) (PLA), polycaprolactone (PCL) and cellulose acetate butyrate (CAB) into the form of electrospun nanofibers. The 4:1 weight ratio of chloroform (CF) and dimethylformamide (DMF) was used as a dual solvent to dissolve PLA, PCL and CAB. However, the study of the miscibility of polymer pairs by Coleman & Painter approach was the first study and then the optical ternary phase diagram of PLA/PCL/CAB using the rapid screening method was observed. Finally, the fabrication of PLA/PCL/CAB nanofibers by electrospinning process was performed.

1. Miscibility study of polymer pairs by Coleman & Painter approach

The polymers chosen to fabricate into ternary blend fibers can be first selection from miscibility guide by Coleman and Painter [6-8, 32, 56], which focuses on the importance of the interaction parameter termed χ_r , which is related to the Hildebrand solubility parameter δ (see Eq.1) and V_r defined as reference volume of polymer A and B. Therefore, the Coleman and Painter's term of the critical solubility parameter difference, $(\Delta\delta)^{\text{crit}}$ was estimated. This value assigned to both non-polar and weak, moderate or strong polar interactions estimated from the polymer structures. If the $\Delta\delta$ value of polymer pairs is not more than the $(\Delta\delta)^{\text{crit}}$ value at a certain interaction, the polymer pairs will be miscible together. From the quantitative system proposed by Coleman and Painter, values of δ range from ca 0.1 (cal.cm⁻³)^{1/2} for purely dispersive forces through weak dipolar forces (ca 1.0 (cal.cm⁻³)^{1/2}) to strong polar interactions which can exceed 3.0 (cal.cm⁻³)^{1/2}. The solubility parameter (δ) of individual polymers is calculated from Eq.2.

$$\chi_r = \frac{V_r}{RT} (\delta_A - \delta_B)^2 \quad \text{Eq. 1}$$

$$\delta = \sum \frac{F_i}{V} \quad \text{Eq. 2}$$

Where δ_A and δ_B are solubility parameter of polymer A and B, respectively. F_i is the sum of molar attraction constants and V is the molar volume of repeating units in the polymer (see Table 1). PLA and PCL, the biodegradable and compatible polymers, were known that they are immiscible. In this work, therefore, CAB was selected as the third component due to it contains hydroxyl groups that can promote hydrogen bond interaction between polymer pairs (PLA/CAB and PCL/CAB). The structure of PLA, PCL and CAB show in the figure 23.

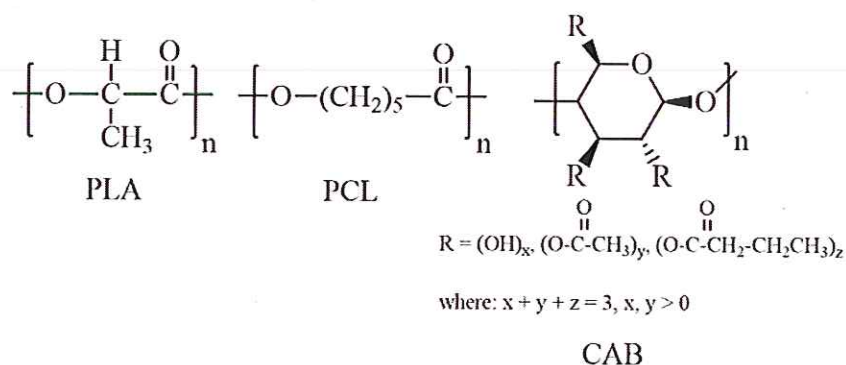


Figure 23 Chemical structures of PLA, PCL and CAB

2. Optical ternary phase diagram of PLA/PCL/CAB using the rapid screening method

Rapid screening method is a new technique developed by S Ross and coworkers to prepare ternary polymer blends [6-8, 32]. This technique uses a combination of a micro-plate reader and 96-well plate to measure either the transmittance or absorbance of the blend films. It is a quick and quantitative method, which can prepare a huge of samples within a short time period. Films are classified by percent transmittances as shown in figure 24. It is clear when %T \geq 76, translucent at %T = 51-75, semi-translucent at %T = 31-50 and opaque at %T = 0-30.

| %T | Clear ≥ 76 | Translucent 51 - 75 | Semi-translucent 31 - 50 | Opaque 0 - 30 |
|----|--------------------|------------------------|-----------------------------|------------------|
|----|--------------------|------------------------|-----------------------------|------------------|

Figure 24 Shading chart of films classified by percent transmittance.

3. Preparation of the blends using rapid screening method

10%w/v of binary (PLA/PCL, PLA/CAB and PCL/CAB) and ternary solution blends were prepared by dissolving in chloroform with various compositions shown in table 5 (for two component blends) and table 6 (for three component blends) into the polypropylene 96-well plate, and the blend solutions were then left to evaporate the solvent within 24 hours before testing their percent transmittance (%T) at wavelength 450 nm by using microplate reader. The optical clarity of ternary

blends will be presented in the form of ternary phase diagram as shown in figure 25 (ternary plots), illustrating ranges in behavior varying from miscible blends giving rise to clear films and to immiscible blends which give opaque films.

Table 5 The compositions of two components blends using rapid screening method (PLA/PCL, PLA/CAB and PCL/CAB).

| Composition of Polymers pairs (wt%) | | | | | | | |
|-------------------------------------|----|--|----|----|--|----|-----|
| A | B | | A | B | | A | B |
| 100 | 0 | | 65 | 35 | | 30 | 70 |
| 95 | 5 | | 60 | 40 | | 25 | 75 |
| 90 | 10 | | 55 | 45 | | 20 | 80 |
| 85 | 15 | | 50 | 50 | | 15 | 85 |
| 80 | 20 | | 45 | 55 | | 10 | 90 |
| 75 | 25 | | 40 | 60 | | 5 | 95 |
| 70 | 30 | | 35 | 65 | | 0 | 100 |

Note: A is the first component and B is the second component of binary blends.

Table 6 The compositions of three components blends using rapid screening method (PLA/PCL/CAB).

| Composition of Polymers (wt%) | | | | | |
|-------------------------------|-----|-----|-----|-----|-----|
| PLA | PCL | CAB | PLA | PCL | CAB |
| 5 | 5 | 90 | 10 | 45 | 45 |
| 5 | 10 | 85 | 10 | 50 | 40 |
| 5 | 15 | 80 | 10 | 55 | 35 |
| 5 | 20 | 75 | 10 | 60 | 30 |
| 5 | 25 | 70 | 10 | 60 | 30 |
| 5 | 30 | 65 | 10 | 65 | 25 |
| 5 | 35 | 60 | 10 | 70 | 20 |
| 5 | 40 | 55 | 10 | 75 | 15 |
| 5 | 45 | 50 | 10 | 80 | 10 |
| 5 | 50 | 45 | 10 | 85 | 5 |
| 5 | 55 | 40 | 15 | 5 | 80 |
| 5 | 60 | 35 | 15 | 10 | 75 |
| 5 | 65 | 30 | 15 | 15 | 70 |
| 5 | 70 | 25 | 15 | 20 | 65 |
| 5 | 75 | 20 | 15 | 25 | 60 |
| 5 | 80 | 15 | 15 | 30 | 55 |
| 5 | 85 | 10 | 15 | 35 | 50 |
| 5 | 90 | 5 | 15 | 40 | 45 |
| 10 | 5 | 85 | 15 | 45 | 40 |
| 10 | 10 | 80 | 15 | 50 | 35 |
| 10 | 15 | 75 | 15 | 55 | 30 |
| 10 | 20 | 70 | 15 | 60 | 25 |
| 10 | 25 | 65 | 15 | 65 | 20 |
| 10 | 30 | 60 | 15 | 70 | 15 |
| 10 | 35 | 55 | 15 | 75 | 10 |
| 10 | 40 | 50 | 15 | 80 | 5 |

Table 6 (cont.)

| Composition of Polymers (wt%) (cont.) | | | | | |
|---------------------------------------|-----|-----|-----|-----|-----|
| PLA | PCL | CAB | PLA | PCL | CAB |
| 20 | 5 | 75 | 25 | 60 | 15 |
| 20 | 10 | 70 | 25 | 65 | 10 |
| 20 | 15 | 65 | 25 | 70 | 5 |
| 20 | 20 | 60 | 30 | 5 | 65 |
| 20 | 25 | 55 | 30 | 10 | 60 |
| 20 | 30 | 50 | 30 | 15 | 55 |
| 20 | 35 | 45 | 30 | 20 | 50 |
| 20 | 40 | 40 | 30 | 25 | 45 |
| 20 | 45 | 35 | 30 | 30 | 40 |
| 20 | 50 | 30 | 30 | 35 | 35 |
| 20 | 55 | 25 | 30 | 40 | 30 |
| 20 | 60 | 20 | 30 | 45 | 25 |
| 20 | 65 | 15 | 30 | 50 | 20 |
| 20 | 70 | 10 | 30 | 55 | 15 |
| 20 | 75 | 5 | 30 | 60 | 10 |
| 25 | 5 | 70 | 30 | 65 | 5 |
| 25 | 10 | 65 | 35 | 5 | 60 |
| 25 | 15 | 60 | 35 | 10 | 55 |
| 25 | 20 | 55 | 35 | 15 | 50 |
| 25 | 25 | 50 | 35 | 20 | 45 |
| 25 | 30 | 45 | 35 | 25 | 40 |
| 25 | 35 | 40 | 35 | 30 | 35 |
| 25 | 40 | 35 | 35 | 35 | 30 |
| 25 | 45 | 30 | 35 | 40 | 25 |
| 25 | 50 | 25 | 35 | 45 | 20 |
| 25 | 55 | 20 | 35 | 50 | 15 |

Table 6 (cont.)

| Composition of Polymers (wt%) (cont.) | | | | | |
|---------------------------------------|-----|-----|-----|-----|-----|
| PLA | PCL | CAB | PLA | PCL | CAB |
| 35 | 55 | 10 | 50 | 25 | 25 |
| 35 | 60 | 5 | 50 | 30 | 20 |
| 40 | 5 | 55 | 50 | 35 | 15 |
| 40 | 10 | 50 | 50 | 40 | 10 |
| 40 | 15 | 45 | 50 | 45 | 5 |
| 40 | 20 | 40 | 55 | 5 | 40 |
| 40 | 25 | 35 | 55 | 10 | 35 |
| 40 | 30 | 30 | 55 | 15 | 30 |
| 40 | 35 | 25 | 55 | 20 | 25 |
| 40 | 40 | 20 | 55 | 25 | 20 |
| 40 | 45 | 15 | 55 | 30 | 15 |
| 40 | 50 | 10 | 55 | 35 | 10 |
| 40 | 55 | 5 | 55 | 40 | 5 |
| 45 | 5 | 50 | 60 | 5 | 35 |
| 45 | 10 | 45 | 60 | 10 | 30 |
| 45 | 15 | 40 | 60 | 15 | 25 |
| 45 | 20 | 35 | 60 | 20 | 20 |
| 45 | 25 | 30 | 60 | 25 | 15 |
| 45 | 30 | 25 | 60 | 30 | 10 |
| 45 | 35 | 20 | 60 | 35 | 5 |
| 45 | 40 | 15 | 65 | 5 | 30 |
| 45 | 45 | 10 | 65 | 10 | 25 |
| 45 | 50 | 5 | 65 | 15 | 20 |
| 50 | 5 | 45 | 65 | 20 | 15 |
| 50 | 10 | 40 | 65 | 25 | 10 |
| 50 | 15 | 35 | 65 | 30 | 5 |
| 50 | 20 | 30 | 70 | 5 | 25 |

Table 6 (cont.)

| Composition of Polymers (wt%) (cont.) | | | | | |
|---------------------------------------|-----|-----|-----|-----|-----|
| PLA | PCL | CAB | PLA | PCL | CAB |
| 70 | 10 | 20 | 75 | 20 | 5 |
| 70 | 15 | 15 | 80 | 5 | 15 |
| 70 | 20 | 10 | 80 | 10 | 10 |
| 70 | 25 | 5 | 80 | 15 | 5 |
| 75 | 5 | 20 | 85 | 5 | 10 |
| 75 | 10 | 15 | 85 | 10 | 5 |
| 75 | 15 | 10 | 90 | 5 | 5 |

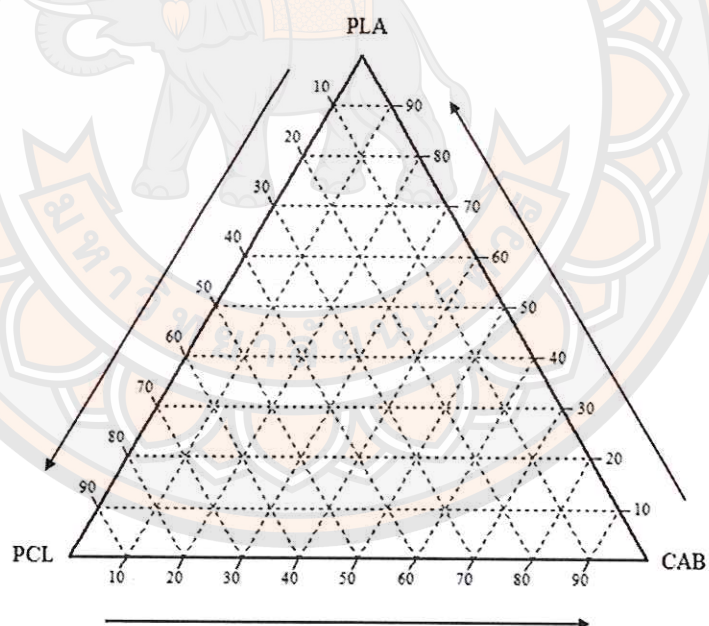


Figure 25 Ternary phase diagram of three component blends (Ternary plots)

Electrospinning technique for PLA/PCL/CAB electrospun nanofibers

The compositions of polymer blends chosen from ternary optical phase diagram will be used to fabricate electrospun nanofibers. The parts of electrospinning instrument are a high-voltage power supply (maximum voltage 30 kV, Genvolt, General High Voltage Ind. Ltd, UK), precision pump (NE-300, New Era Pump Systems, Inc., USA) and a grounded aluminum foil collector. All polymers (10 %w/v) were dissolved in chloroform (CF)/dimethyl formamide (DMF) (4:1 wt) solutions and then polymer blend solution were loaded in a syringe with metal needle with 0.7 mm diameters of tip and then injected at flow rate of 0.50 mL/h. High voltage is applied at 25 kV and the tip-to-collector distance is set at 10 cm. The electrospun nanofiber were collected on an aluminum foil collector and dried at room temperature. The schematic structure of electrospinning set up shows in figure 26.

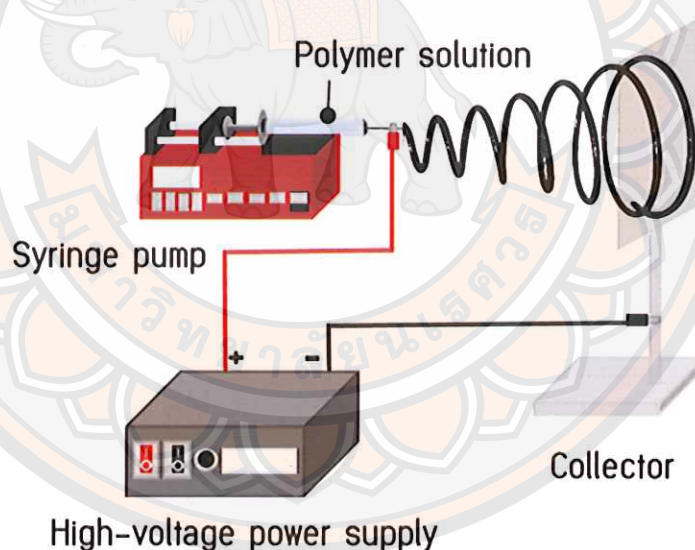


Figure 26 Schematic illustration of electrospinning process.

Methods for approach II: The electrospinning technique for PVA/SS and PLA/(PVA/SS)

In this section, the second approach for electrospinning of poly(vinyl alcohol) (PVA) and silk sericin (SS), and the combination of PLA and PVA/SS (layer by layer technique) was studied. This includes the preparation of silk sericin powders (SS) from degumming process, PVA/SS solution for electrospinning and the electrospun layer by layer technique of PLA and PVA/SS solutions.

Preparation of silk sericine powders from water degumming process)

Silk sericins (SS) were prepared by water degumming process. Silk cocoons were cut into small pieces and weighed for 20 grams and then added 500 mL of DI water, and heated at 100°C for 4 hrs. After that the sericin solution was dried in an oven at 60°C for 12 hrs, and finally the silk sericin powders were achieved.

1. Preparation of poly(vinyl alcohol) with silk sericine solutions (PVA/SS)

10 % w/v of poly (vinyl alcohol) (PVA) solution is dissolved in DI water at 100°C for 4 hrs. 3, 6 and 10 % w/v of sericin solutions were prepared by dissolving sericin powders in DI water at 100°C for 3 hrs to use as stock solutions. Then PVA/SS solutions were prepared at different compositions (grams per 100 mL of DI water) used to electrospin as shown in Table 7.

Table 7 Compositions of electrospun PVA/SS fibers.

| Sample Code | Wt.% in 100 mL of solution | |
|-------------|----------------------------|--------|
| | PVA (g) | SS (g) |
| EF 1 | 5.0 | 1.5 |
| EF 2 | 5.0 | 3.0 |
| EF 3 | 7.5 | 0.75 |
| EF 4 | 7.5 | 1.5 |
| EF 5 | 7.5 | 2.5 |

2. Fabrication of PLA and PVA/SS layer by layer nanofiber by electrospinning process

Poly (lactic acid) (PLA) with concentration of 10% w/v is dissolved in a mixed solvent of chloroform and dimethylformamide (CF/DMF) (4:1 wt). The solution of PVA/SS at the compositions of EF3 and EF4 (see table 7) were also prepared. The electrospun fibers were prepared in the forms of layer by layer technique between PLA and either EF3 or EF4. The first layer is PLA, followed with EF3 or EF4, PLA and finally EF3 or EF4 at the last layer. For PLA electrospun fibers, the PLA solution was injected at flow rates of 0.50 mL/h. High voltage was applied at 25 kV and the tip-to-collector distance is set at 10 cm. In case of PVA/SS (EF3 and EF4), PVA/SS is injected at flow rates of 0.02 mL/min. High voltage was applied at 25 kV and the tip-to-collector distance is set at 15 cm for PVA/SS. The electrospun nanofibers are collected on an aluminum foil collector and dried at room temperature.

Characterization

1. Optical transparency observation by Microplate reader

The Microplate reader (Biotek, Model Synergy H1 Hybrid Reader), which is a UV/Visible plate reader, was used to observe the percent transmittance (%T) of solvent blends. The Microplate reader is a multi-detection microplate reader with dual-mono chromators, dual-mode cuvette ports and top-reading capability. Detection modalities include absorbance (UV-Visible absorbance) and fluorescence intensity (FI). The system has optical performance comparable to a top-of-the-range dedicated spectrophotometer or spectro-fluorometer. The optical system has an integrated dual-mode cuvette port and microplate reading

2. Miscibility by Fourier Transform Infrared Spectroscopy (FT-IR)

In this work, FT-IR (FT-IR, Perkin Elmer Spectrum GX) was used to identify the miscibility of ternary blend nanofibers over a range of 4000-400 cm^{-1} . The first step, a background spectrum was measured to be a relative scale for the absorption intensity. This can be compared to the measurement with the sample in the beam to determine the percent transmittance (%T). In the second step, a solid sample was placed onto the sample compartment and pressed with a diamond plate. The beam emitted from a glowing black-body source passes through an aperture which controls

the amount of energy presented to the sample, enters the interferometer resulting the interferogram signal, and then enters the sample compartment. The beam finally passes to the detector, which is specially designed to measure the special interferogram signal and sent to the computer where the Fourier transformation takes place. The final infrared spectrum is then presented.

3. Morphology by Scanning Electron Microscopy (SEM)

The morphology of electrospun fibers was observed by scanning electron microscopy (SEM, Leo Model 1455VP) at 20 kV in high vacuum. Samples were mounted on metal stubs and gold coating in vacuum chamber. The gold covered sample fibers were placed onto the stage of the SEM machine. An electron beam is produced at the top of microscope by an electron gun. The electron beam passes through the microscope in a vertical direction and moves through electromagnetic fields and lenses, which focus the electron beam down toward the sample fibers. As the electron beam hits the samples, electron and X-rays are ejected from the fibers. In this work, the secondary electrons are collected and converted by detectors into a signal that is sent to a screen producing an SEM image. The average of nanofiber diameters was measured by SEM image at magnification of 5,000x.

4. Crystallinity by X-ray Diffraction Spectroscopy (XRD)

Crystallinity of electrospun fibers were investigated by X-Ray diffraction (XRD, Philips Model X'Pert Por) with a diffraction angle range (2θ) from 5 to 60 degrees ($\text{Cu K}\alpha$, 1.54 Å). The X-ray are generated form cathode ray tube through monochromatic radiation and directed toward the sample fibers. X-ray diffraction pattern have been use to investigate unique "fingerprint" of crystalline structure in the sample.

5. Thermal properties by Differential Scanning Calorimetry (DSC)

Thermal properties were observed by differential Scanning Calorimetry (DSC, Mettler Model DAC1). A sample of approximately 10-15 mg were weighted into aluminum pan. The conditions were used, as shown below. The homopolymers of PLA and CAB were heated from 25 to 200°C (first heat), cooled to 25°C and then heated to 200°C (second heat) at heating and cooling rate of 10°C/min. While, PCL was heated from 25 to 100°C (first heat), cooled to -100°C and then heated to 100°C (second heat) at same heating and cooling rate.

Ternary blend nanofibers were heated from 25 to 200°C (first heat), cooled to -100°C and then heated to 200°C (second heat) at heating and cooling rate of 10°C/min in every run under a nitrogen atmosphere. The onset temperature, crystalline temperature, melting temperature and heat of fusion (ΔH) of samples were recorded.

6. Hydrophilicity by water contact angle (CA)

Hydrophilicity behavior of electrospun fibers was observed by contact angle (CA, Dataphysics Model OCA20) at room temperature. Water was loading in syringe and injecting at 2.000 μL of dosing volume, 0.50 $\mu\text{L/s}$ of dosing rate (slow). Image of water drop were recorded by video camera. The contact angles of samples were observed.



CHAPTER IV

RESULTS AND DISCUSSION

In this chapter, the results and discussion will be separated into two parts, based on the two approaches proposed for electrospinning. The first approach is the ternary blends of poly(lactic acid) (PLA), polycaprolactone (PCL) and cellulose acetate butyrate (CAB) blends. The second approach is the blends of poly(vinyl alcohol) (PVA) and silk sericin (SS), and the fibers of PVA/SS blends and PLA using layer by layer electrospinning technique. For the first approach, the ternary blends of PLA/PCL/CAB were first studied in term of miscibility by using the rapid screening method. Then, the selection of the compositions was made from the ternary phase diagrams, and these were fabricated into fibers by electrospinning technique. For the second approach, PVA/SS blends were fabricated into the fibers and the effect of PVA and sericin concentrations was studied. In addition, layer by layer technique of PVA/SS blends and PLA fibers were also studied. The parameters that effect to electrospin were also studied to find the proper compositions and conditions for fabrication into fibers by electrospinning technique.

Approach I: PLA/PCL/CAB blends

In this section, the miscibility study between polymer pairs of PLA, PCL and CAB was studied first using the Coleman-Painter approach. Then the apparent miscibility of ternary blends was studied using the rapid screening method. Their results are shown in terms of optical clarity using optical ternary phase diagrams. The effect of molecular weight of PCL (PCL1 and PCL2) was studied, in which the molecular weight of PCL1 is less than PCL2.

Miscibility study between polymer pairs of PLA/PCL, PLA/CAB and PCL/CAB by using the Coleman-Painter approach

The miscibility prediction was studied by using the Coleman-Painter approach. The term of critical solubility parameter difference $(\Delta\delta)^{\circ\text{Crit}}$ is used as a tool to predict the miscibility between polymer pairs. The difference of solubility parameter between polymer pairs ($\Delta\delta$) should not more than the $\Delta\delta^{\circ\text{Crit}}$ and then the polymer pairs can be miscible with each other. An estimate of the solubility parameter may be obtained by dividing the sum of the molar attraction constants (F) by the molar volume (V) of the repeat units present in the polymer. However, the $\Delta\delta^{\circ\text{Crit}}$ value depends on the interaction types between polymer pairs.

Table 8 Miscibility study between polymer pairs by Coleman-Painter approach using the different in value of solubility parameter [6-8]

| Polymers | PLA | PCL | CAB |
|-------------------------------------|------------------------|-----------------------------------|-------------|
| $F (\text{cal cm}^3)^{1/2}$ | 598 | 1017 | 1848 |
| $V (\text{cm}^3 \text{mol}^{-1})$ | 49.5 | 98.3 | 154 |
| $\delta (\text{cal cm}^{-3})^{1/2}$ | 12.1 | 10.3 | 12.0 |
| $\Delta\delta$ | Interaction types | $\Delta\delta^{\circ\text{Crit}}$ | Miscibility |
| PLA/PCL | Dispersive forces only | ≤ 0.1 | No |
| | Dipole-Dipole | 0.5 | No |
| | Weak | 1.0 | No |
| | Weak to moderate | 1.5 | No |
| PLA/CAB | Dispersive forces only | ≤ 0.1 | Yes |
| | Dipole-Dipole | 0.5 | Yes |
| | Weak | 1.0 | Yes |
| | Weak to moderate | 1.5 | Yes |
| | Moderate | 2.0 | Yes |
| | Moderate to strong | 2.5 | Yes |
| PCL/CAB | Weak to moderate | 1.5 | No |
| | Moderate | 2.0 | Yes |
| | Moderate to strong | 2.5 | Yes |

Note: $\Delta\delta$ and $\Delta\delta^{\circ\text{Crit}}$ are in unit of $(\text{cal.cm}^{-3})^{1/2}$

Table 8 shows the miscibility prediction of PLA/PCL, PLA/CAB and PCL/CAB, in which if they miscible the term then called “Yes” and immiscible called “No” (depending on the interaction between polymer pairs). PLA/PCL is predicted to be immiscible blend, while PLA/CAB is predicted to be miscible blend. PCL/CAB might be miscible or immiscible blend depending on their interaction types, if weak dipolar forces $[(\Delta\delta)^{\circ\text{crit}} = 1.0 \text{ (cal.cm}^{-3})^{1/2}]$ it is not miscible (No), but if strong polar interactions $[(\Delta\delta)^{\circ\text{crit}} = 3.0 \text{ (cal.cm}^{-3})^{1/2}]$ it is miscible (Yes). It can be seen that PLA is predicted to be more miscible with CAB than with PCL. Interactions between PLA and PCL are classified as weak to moderate, whilst those between PLA and CAB, influenced by a degree of hydrogen bonding, are moderate or moderate to strong. This miscibility prediction suggests the possible miscible pairs of PLA/CAB and PCL/CAB in ternary blend of PLA/PCL/CAB. Therefore, CAB is able to mediate miscibility in the ternary blends.

Optical ternary phase diagram by rapid screening method

From the previous section, PLA, PCL and CAB were chosen to study miscibility of ternary polymer blended with CAB as mediate miscibility between PLA and PCL. In this section, the three polymers were blended into the films and classified into optical ternary phase diagram by the rapid screening method. This method helps to classify the apparent miscibility region of PLA/PCL/CAB blend by studying the effect of molecular weight of PCL. Two different molecular weights of PCL were used, PCL1 ($M_n = 42,500 \text{ g.mol}^{-1}$) and PCL2 ($M_n = 80,000 \text{ g.mol}^{-1}$). While the molecular weight of PLA was controlled ($M_n = 58,760 \text{ g.mol}^{-1}$), which can be classified as high molecular weight PLA. Figure 27 shows the optical ternary phase diagrams of PCL1 and PCL2 blended with PLA and CAB.

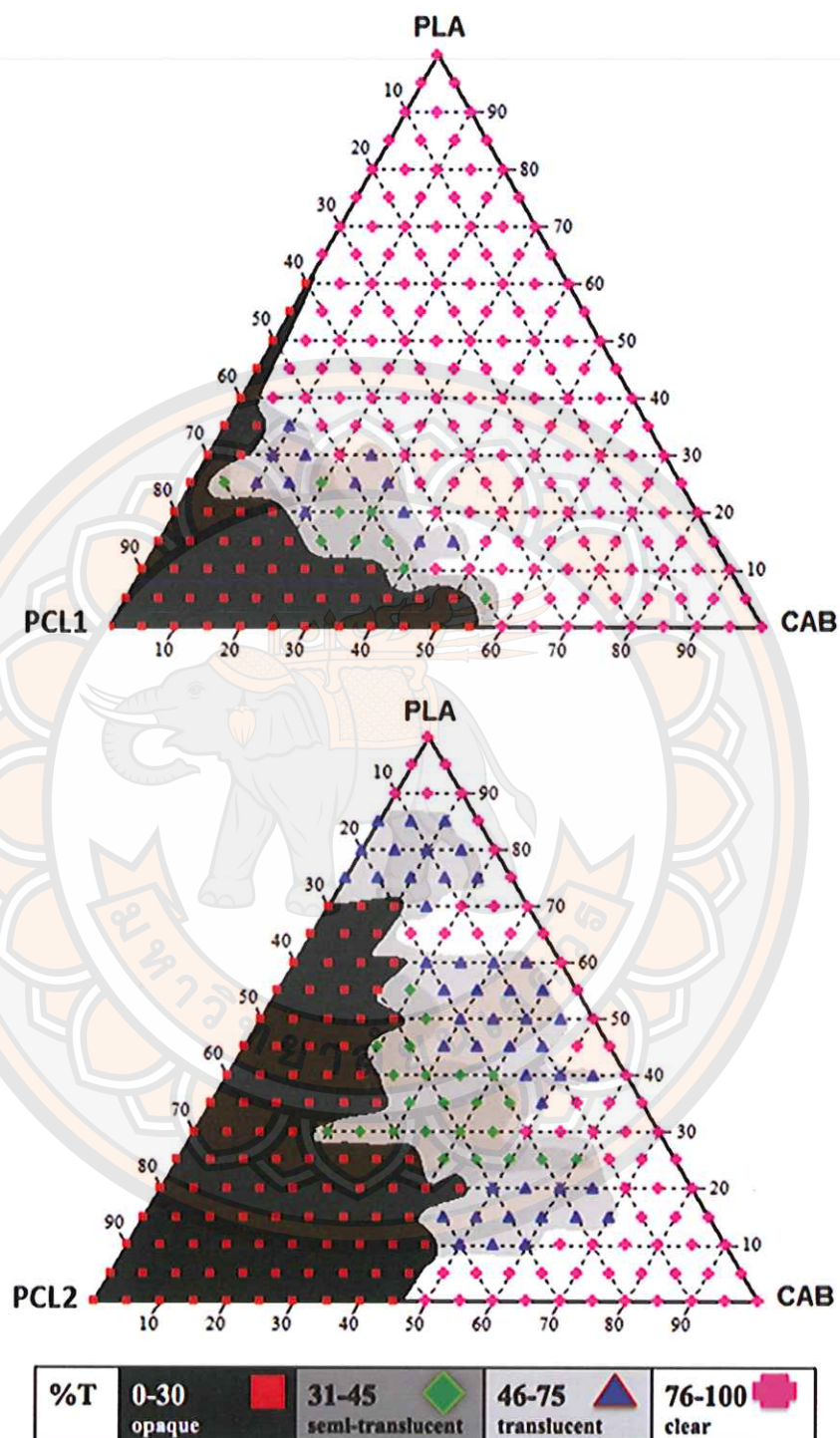


Figure 27 The optical ternary phase diagrams of PLA/PCL/CAB blends with different molecular weight of PCL1 (top) and PCL2 (bottom); all of the points in the diagrams represent the experimental data to classify the phase regions.

From figure 27, the regions of optical ternary phase diagrams of PLA/PCL1/CAB and PLA/PCL2/CAB were different depending on the molecular weight of PCL used. High molecular weight of PCL2 seems to promote the opaque region of PLA/PCL2/CAB blends. This might be because longer chains of PCL2 (zig-zag conformational structure) promote the alignment of carbon-carbon $-(CH_2)_5-$ in the backbone. Whereas PCL1, which also has high molecular weight but lower than PCL2, can be able to intermingle and restrict to the alignment of its backbone, resulting PLA/PCL1/CAB to show higher optically clear region than PLA/PCL2/CAB. Therefore, it can be seen from the ternary phase diagrams that molecular weight of PCL affected to the apparent miscibility between ternary polymers.

The rapid screening method is a technique to produces the films samples by allowing polymer chains to move around (annealing). If they like each other, the polymer blend can mix but if they do not it will result in phase separation. Therefore, all ternary blended films were investigated for their miscibility, crystallinity and thermal properties, as discussed in the next sections.

Characterization of ternary PLA/PCL/CAB blend films

Three different compositions of ternary blend films; 80/10/10, 50/40/10 and 20/70/10 of PLA/PCL/CAB, were selected from optical phase diagrams of PLA/PCL/CAB blends (Fig. 27). These compositions of ternary blend were observed for their miscibility, crystallinity, thermal properties and hydrophilicity, as described in this section.

1. Miscibility observation of ternary blend films by FT-IR

The miscibility or immiscibility of ternary blend fibers can be observed using FTIR technique. Figure 28 shows FT-IR spectra of ternary blend films of A. PLA/PCL1/CAB and B. PLA/PCL2/CAB at different compositions of 20/70/10, 50/40/10 and 80/10/10 together with FT-IR homopolymers of PLA, PCL and CAB, in range of $4000-400\text{ cm}^{-1}$.

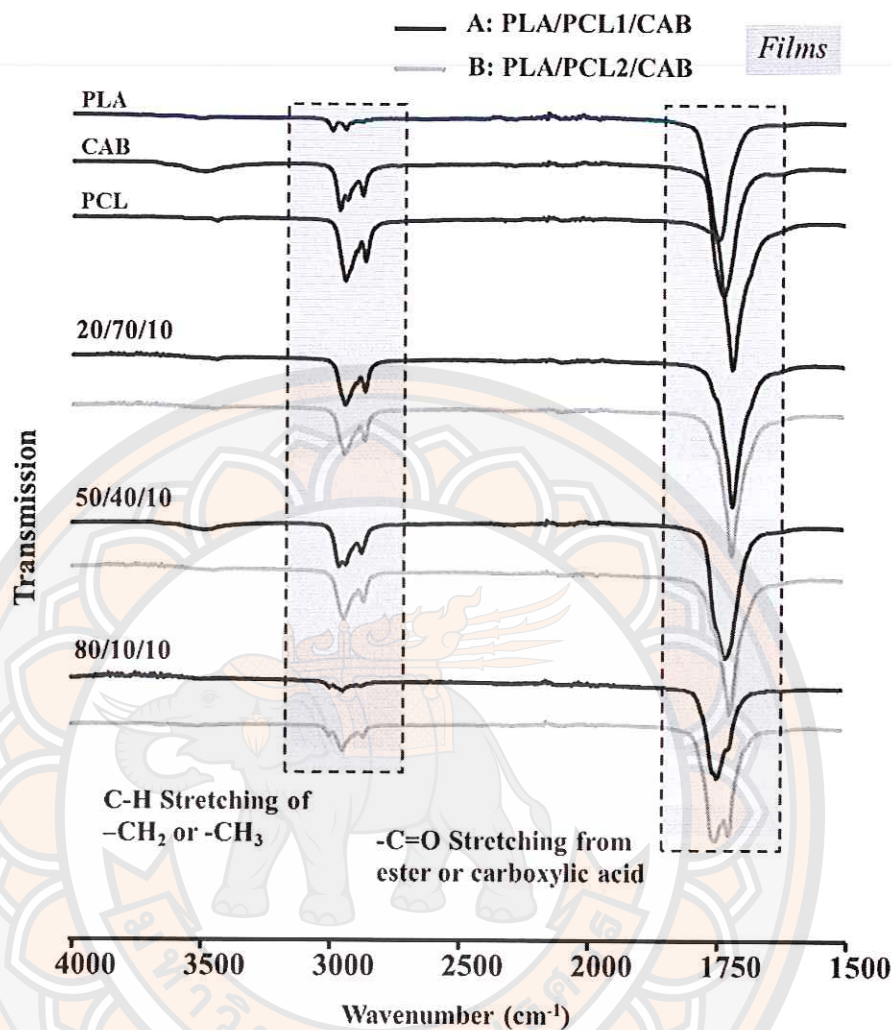


Figure 28 FT-IR spectra of ternary blend films of: A. PLA/PCL1/CAB (black line) and B. PLA/PCL2/CAB (gray line), at different compositions.

From figure 28, two main FT-IR peaks of all samples were C-H stretching of $-\text{CH}_2$ or $-\text{CH}_3$ ($2800\text{--}3200\text{ cm}^{-1}$) and $-\text{C}=\text{O}$ stretching from ester or carboxylic acid (approximately 1750 cm^{-1}). All compositions of PLA/PCL1/CAB and PLA/PCL2/CAB show the spectrum sum of homopolymers, which means all samples are immiscible blends. In addition, all FT-IR spectra (except the composition at 80/10/10) show the sharp peaks of $-\text{C}=\text{O}$ stretching from PCL, which means both PCL1 and PCL2 might be clearly immiscible in these PLA/PCL/CAB blends. However, the carbonyl peak of the samples at 80/10/10 of PLA/PCL2/CAB shows

double peaks, which is different from other samples. This might be caused by some partial miscible between polymer pairs in this ternary blend.

2. Crystallinity observation of ternary blend films by XRD

The crystallinity of ternary blend films can be observed using XRD technique. Figure 29 shows XRD patterns of films of A. PLA/PCL1/CAB and B. PLA/PCL2/CAB at different compositions of 20/70/10, 50/40/10 and 80/10/10 together with XRD patterns of homopolymers of PLA, PCL and CAB.

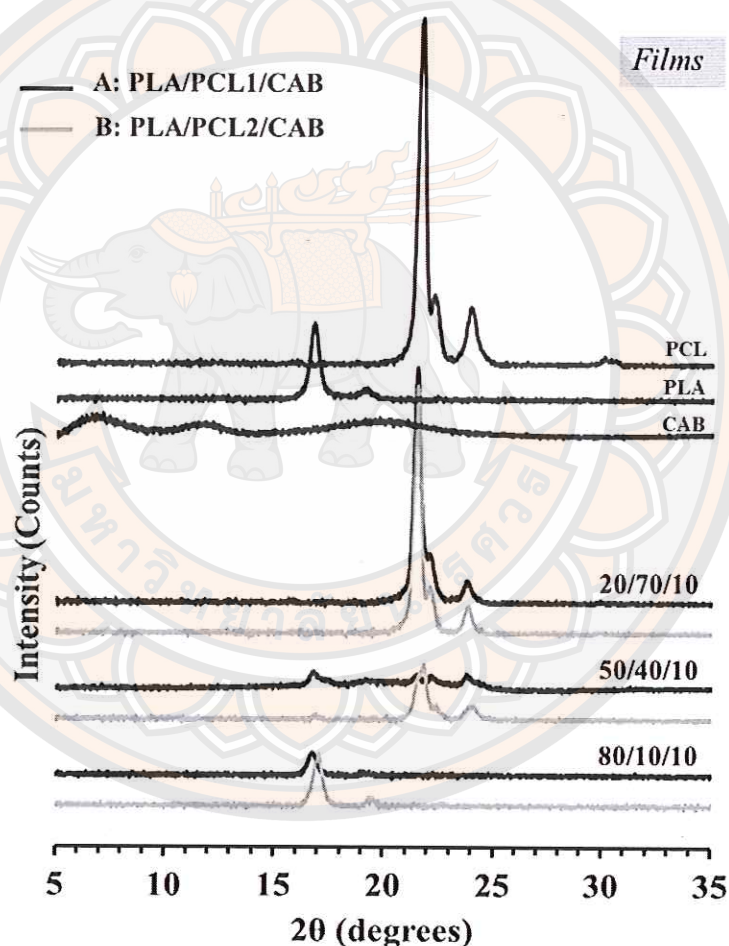


Figure 29 XRD patterns of ternary blend films; A. PLA/PCL1/CAB (black line) and B. PLA/PCL2/CAB (gray line) at different compositions.

From figure 29, it can be seen that PCL film shows two major crystalline peaks at 21.5° and 24.0° , while PLA shows crystalline peaks at 17.0° and 19.5° , and CAB shows broad amorphous peaks. The crystalline peaks of ternary blend films at the same compositions of both PLA/PCL1/CAB and PLA/PCL2/CAB are similar in which higher PCL contents show higher crystalline peak intensity, as seen at the composition of 20/70/10 in both blends. The blends of 50/40/10 and 80/10/10 show small crystalline intensity peaks of PLA and PCL depending on loading of PLA and PCL. However, the crystalline peaks of PCL were disappeared in both blends at the composition of 80/10/10.

3. Summary of characterization of blend films

In this section, the miscibility study between polymer pairs of PLA/PCL, PLA/CAB and PCL/CAB were preliminarily studied. It was observed that PLA/PCL was immiscible blend, while PLA/CAB and PCL/CAB are possible to be miscible blends. Then the ternary blends of PLA/PCL1/CAB and PLA/PCL2/CAB were studied using the rapid screening method and used to select compositions of blends. The compositions of 80/10/10, 50/40/10 and 20/70/10 were chosen to observe the morphology, miscibility and crystallinity. The results indicated that films of higher loading of PCL promoted opaque regions, immiscible blends and high crystallinity in the films. However, three different areas of ternary blends (Fig. 27) of PLA/PCL1/CAB; 80/10/10 (clear), 50/40/10 (clear) and 20/70/10 (opaque), and of PLA/PCL2/CAB; 80/10/10 (translucent), 50/40/10 (opaque) and 20/70/10 (opaque), were chosen for further study to fabricate into the nonwoven nanofibers by solvent electrospinning technique.

Non-woven electrospun fibers of PLA/PCL/CAB blend

In this section, three different compositions selected from the optical ternary phase diagrams of PLA/PCL/CAB blends at 80/10/10, 50/40/10 and 20/70/10 (Fig. 27), were selected to fabricate into the form of fibers by electrospinning technique. This was to observe the effect of molecular weight of PCL (PCL1 and PCL2) and composition of blends on the morphology, miscibility, crystallinity, thermal properties and hydrophobicity of the electrospun fibers. In addition the homopolymers were also fabricated and their properties analyzed. The

electrospinning conditions used to fabricate fibers were an applied voltage of 25 kV, polymer concentrations of 10 %w/v in 4:1 wt of CF/DMF, polymer solution flow rate of 0.50 mL/h and a tip-to-collector distance of 10 cm.

1. Morphology of non-woven of homopolymer fibers

In this section, the morphology of homopolymer fibers were studied (PLA, CAB, PCL1 and PCL2). Figure 30 shows the Scanning Electron Microscopy (SEM) images.

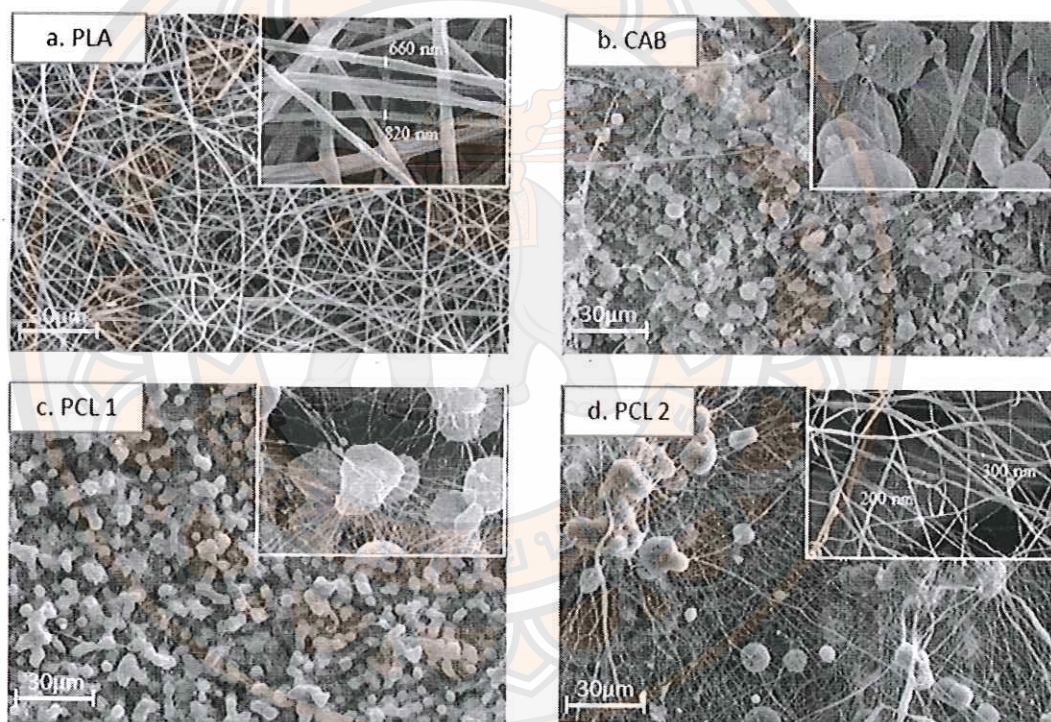


Figure 30 SEM images of non-woven electrospun fibers of homopolymers; a. PLA, b. CAB, c. PCL1 and d. PCL2.

Form figure 30, it can be seen that PLA is successfully fabricated into the nanofibers, and resulted in fibers with diameters ranging from 660-820 nm (Fig. 30a) with a smooth surface, while CAB, PCL1 and PCL2 are possible to form fiber incorporated with beads and microdrops. In general, the electrospun fiber features depend on the electrospinning parameters, such as polymer concentration and

viscosity, solution surface tension, solution conductivity, collector design, applied voltage and polymer molecular weight. In case of the formation of beads and microdrops, it generally caused by using low concentration of polymer solution or low molecular weight, which produce a low degree of entanglement between the polymer chains [67]. However, high molecular weight are not always essential for making electrospun fibers if sufficient intermolecular interaction can provide a substitute for interchain connectivity obtained through chain entanglements [68]. Comparing between PCL1 and PCL2, PCL2 showed a smaller number of beads and microdrops with very fine fiber diameter approximately 200-300 nm. In this case, PCL2 has two times molecular weight higher than PCL1, which can be able to produce higher chain entanglements and intermolecular interactions resulting to form less numbers of beads and provides more interchain connectivity.

2. Morphology of non-woven of ternary blend fibers

The electrospun fibers of non-woven ternary blend nanofibers of PLA/PCL1/CAB and PLA/PCL2/CAB at different compositions (20/70/10, 50/40/10, 80/10/10) were fabricated using 4:1 wt of chloroform (CF)/dimethylformamide (DMF) as the solvent. All polymer solutions had a concentration of 10 %w/v, were injected from the syringe with applied voltage of 25 kV, polymer solution flow rate of 0.50 mL/h and a tip-to-collector distance of 10 cm. Figure 31 shows SEM images of these non-woven ternary blend nanofibers.

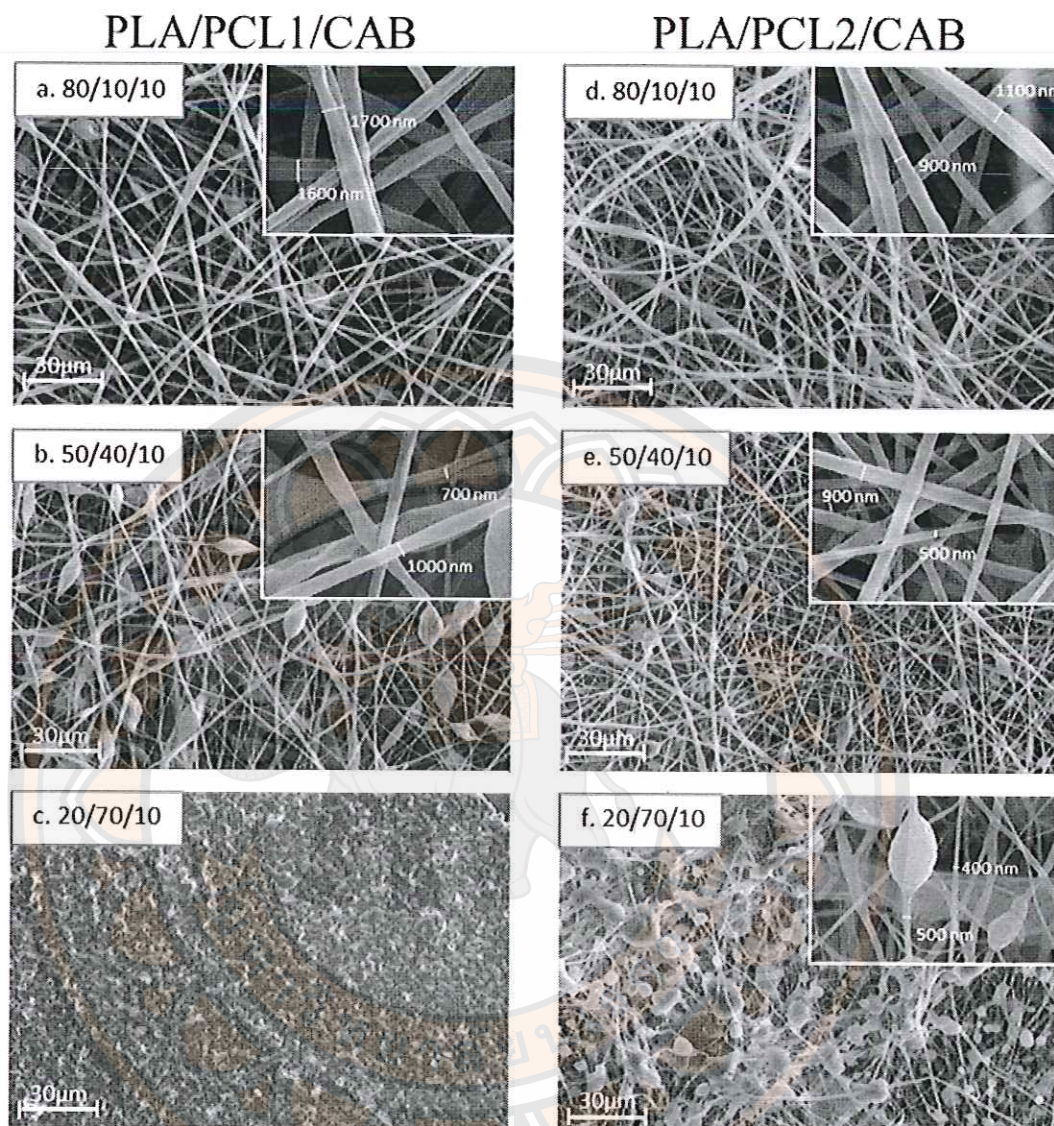


Figure 31 SEM images of non-woven ternary blend fibers of PLA/PCL1/CAB (a, b, c) and PLA/PCL2/CAB (d, e, f) at different compositions (80/10/10, 50/40/10, 20/70/10), with magnification of 500x in the main figures and of 5000x in an embedded figures.

Comparing the fibers fabricated from PLA/PCL1/CAB at different compositions (CAB content was controlled), at 80/10/10 the ternary blend fibers are in diameter the ranges of 1,600 nm – 1,700 nm and has smooth surfaces with small number of beads (Fig. 31a). The fibers with beads are obtained from the 50/40/10 sample and have the diameter in the range of 700 nm – 1,000 nm (Fig. 31b).

However, the blend could not form the fibers for 20/70/10 PLA/PCL1/CAB blend (Fig. 31c). This shows the effect of composition of the ternary blend fibers as higher amount of PCL1 (low loading in PLA) promoted less ability to fabricate into the electrospun nanofibers. With increasing PCL1 content, the amount of beads increases as well as a decrease in average fiber diameter (Fig. 31b). Plus, high PCL1 content was not able to fabricate into the nanofibers (Fig. 31c). Noticeably, using high loading of PLA encourages more formation of the uniform fibers. This is due to the higher chain entanglement of PLA than that of PCL1, resulting in the continuity of the polymer solution jet is easy to form under the elongation of the electric field force to form fibers (Fig. 31a). In opposite way, PCL1 elongated jet is broken easily to form microdrops and beads when using high loading. In addition, the average fiber diameter increases, as PLA content increases due to greater resistance of the PLA viscous solution to stretching and elongation.

In case of using higher molecular weight of PCL (PCL2) for PLA/PCL2/CAB, when using higher amounts of PCL2 it shows the same trend of results as PLA/PCL1/CAB, with higher PCL2 content giving fibers mixed with beads (Fig. 31e), and fibers mixed with both beads and microdrops (Fig. 31f), as well as smaller fiber diameters (Fig. 31e and 31f compared to 31d). However, the nanofibers from PLA/PCL2/CAB have smaller fiber diameters and less bead density than the nanofibers from PLA/PCL1/CAB when compared at the same compositions. In addition, at high PCL2 content (20/70/10 PLA/PCL2/CAB, Fig. 31f) the polymer solution blend can be fabricated into fibers better than that of 20/70/10 PLA/PCL1/CAB (Fig. 31c) but with a higher amount of beads and microdrops.

The results show that the blending compositions of these ternary blends affect to the formation of fibers, as high PLA component favors improvement in the fiber morphology during the electrospinning process, with the same polymer solution concentration, polymer solution flow rate, applied voltage, tip-to-collector distance. Besides the blending compositions of the ternary polymer blends, the molecular weight of PCL also affects the fiber morphology. As higher molecular weight of PCL2 enhances its viscosity and conductivity solutions, resulting in continuity of the fibers formation and possessing less beads.

In this work, therefore, we can be able to use regions of clear, translucent and opaque from the optical ternary phase diagrams of PLA/PCL1/CAB and PLA/PCL2/CAB to fabricate into the nanofibers. Table 9 shows the summary of film properties from the phase regions (Fig. 27) and fiber properties (Fig. 31) of the selected compositions. This is because the electrospinning process is a quench process that does not need the miscible blends but require a good entanglement. However, the miscible or partial miscible blended fibers might require for a good fiber properties, as fibers can lead to toughened mechanical properties.

Table 9 Properties of films and fibers of three different compositions of PLA/PCL/CAB blends.

| Blends | Films opacity from ternary phase diagrams (Fig. 27) | Electrospun fibers from SEM images (Fig. 31) |
|---------------------|-----------------------------------------------------|--------------------------------------------------------|
| PLA/PCL1/CAB | | |
| 80/10/10 | Clear – apparent miscible | Smooth fiber (1600-1700 nm) with small number of beads |
| 50/40/10 | Clear – apparent miscible | Fiber (700-1000 nm) with beads |
| 20/70/10 | Opaque - immiscible | Cannot fabricate into fiber |
| PLA/PCL2/CAB | | |
| 80/10/10 | Translucent – partial miscible | Smooth fiber (900-1100 nm) with no beads |
| 50/40/10 | Opaque – immiscible | Fiber (500-900 nm) with small number of beads |
| 20/70/10 | Opaque - immiscible | Fiber with a large number of beads and microdrops |

2. Miscibility observation of non-woven ternary blend fibers by FT-IR

The electrospun fibers of non-woven ternary blend nanofibers of PLA/PCL1/CAB and PLA/PCL2/CAB at different compositions (20/70/10, 50/40/10, 80/10/10) were also studied their miscibility. The miscibility or immiscibility of ternary blend fibers can be observed using FT-IR technique. If the blends are immiscible the FT-IR spectrum of the blends is simply the spectrum of the two or three homopolymers, while a shift in FT-IR spectrum describes as a miscible blend

[69, 70]. Figure 32 shows FTIR spectra of non-woven homopolymer fibers (PLA, PCL, CAB) and ternary blend fibers of PLA/PCL1/CAB and PLA/PCL2/CAB. FT-IR spectra of PCL1 and PCL2 are identical, therefore, herein showing by PCL to represent both PCL1 and PCL2.

PLA, PCL and CAB homopolymer fibers show their FT-IR absorption bands of sp^3 C-H stretching of $-\text{CH}_2$ or $-\text{CH}_3$ or saturated $-\text{CH}$ at $2700\text{--}2900\text{ cm}^{-1}$, and bands of $-\text{C}=\text{O}$ from ester or carboxylic acid at $1720\text{--}1750\text{ cm}^{-1}$. All these spectra are similar but show a small difference in frequency shifts, in which, for example, $-\text{C}=\text{O}$ peak of PLA shows at 1750 cm^{-1} , while that of CAB and PCL shows at 1740 cm^{-1} and 1720 cm^{-1} , respectively. Almost of all ternary blend fibers at different compositions, both from A. PLA/PCL1/CAB and B. PLA/PCL2/CAB, show simply the spectrum sum of all homopolymers indicating that they are most likely to be immiscible blends. However, the carbonyl stretching vibration region of the blends at high loading of PLA (80/10/10) seems to be shifted from homopolymers, in which carbonyl band of PLA shifted to lower frequency (loose intermolecular packing - freedom movement), PCL shifted to higher frequency (close intermolecular packing - self-aggregation) and CAB cannot be seen. In addition, the peak is broader, especially in PLA/PCL2/CAB blend. This confirms that the blends of PLA/PCL1/CAB and PLA/PCL2/CAB at high loading of PLA show similar behavior in blend miscibility. However, the blend seems to be more miscible when using high molecular weight PCL2. The blends of high loading of PCL (50/40/10 and 20/70/10) are most likely to be immiscible.

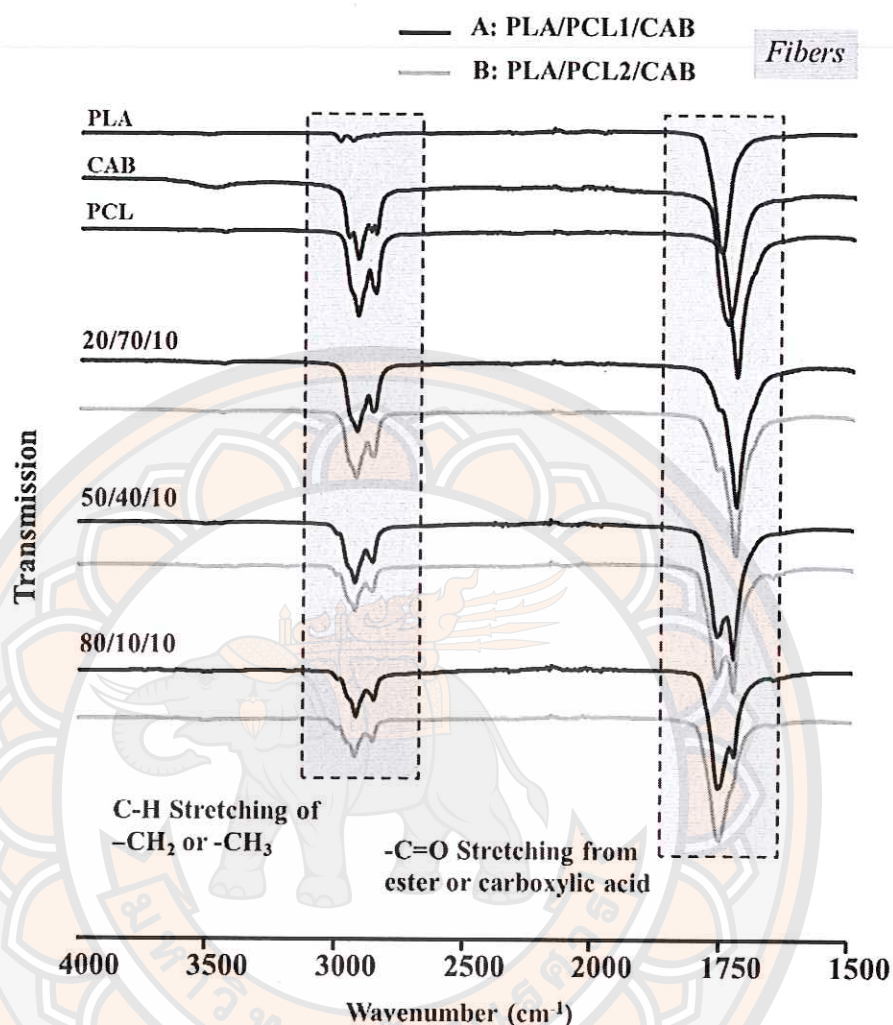


Figure 32 FT-IR spectra of non-woven ternary blend fibers of:
A. PLA/PCL1/CAB (black line) and B. PLA/PCL2/CAB
 (gray line), at different compositions.

4. Crystallinity of non-woven ternary blend nanofibers by XRD

Figure 33 shows the XRD patterns of homopolymer fibers and nonwoven ternary blend nanofibers of A. PLA/PCL1/CAB and B. PLA/PCL2/CAB characterized by X-ray diffraction spectroscopy (XRD) technique, at the same scale of intensity and 2θ . Homopolymer fiber of PCL (represented both PCL1 and PCL2) exhibited two main diffraction peaks of crystalline phase at 2θ values of 21.50° and 24.00° , while that of PLA and CAB has no crystalline peaks observed, only the broad peak of the amorphous phase. The XRD peaks of homopolymer films were also observed and

showed in figure 29. The crystalline phase of PCL film (represented both PCL1 and PCL2) (fig. 29) exhibited at the same 2θ and shows higher intensity than PCL fiber, while PLA film shows at 16.70° and 19.00° with three times smaller intensity than the PCL film. CAB film showed broad peaks of amorphous phase at 5.00 - 6.60° , 9.75 - 14.23° and 15.62 - 55.00° . It can be seen that fibers made from electrospun process revealed less crystalline phase than film casting process in case of PCL, while absence in case of PLA.

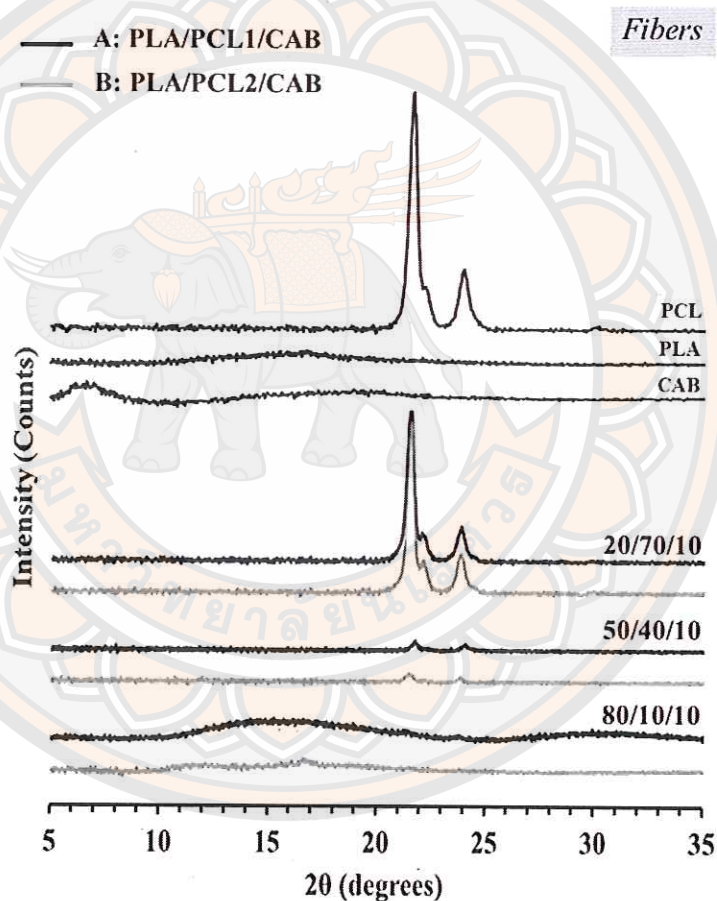


Figure 33 XRD patterns of non-woven ternary blend fibers;
A. PLA/PCL1/CAB (black line) and B. PLA/PCL2/CAB
(gray line) at different compositions.

Figure 33 indicates that the PCL molecular weight and polymer blend composition affect the internal molecular structure in ternary blend electrospun fibers.

Both blends (A. PLA/PCL1/CAB and B. PLA/PCL2/CAB) show similar trends of XRD patterns, however, the peak intensity of PCL2 in PLA/PCL2/CAB blends is smaller than that of PCL1 in PLA/PCL1/CAB blends. This is due to the higher chain entanglement of PCL2, which has higher molecular weight than PCL1, during electrospinning process. In addition, peaks of PCL2 show a small lower number of 2θ , corresponding to higher distance between crystalline structures (d -spacing) than peaks of PCL1, due to the change in crystalline structure caused by recrystallization after electrospinning.

In case of the effect of blend compositions, it is clearly shown that only PCL (PCL1 and PCL2) peaks can be observed, in which high peak intensity shows at high PCL content of 20/70/10 and small intensity peaks at 50/40/10, while none are observed in 80/10/10. The crystalline peaks of PLA disappeared without respect to the polymer blend compositions. This is because PLA chains (helical conformational structure) has a good ability to intermingle in the polymer blend solution with CAB and form high entanglement during the electrospinning process, while PCL seems to recrystallize easy due to its zig-zag conformational structure to promote the chains alignment.

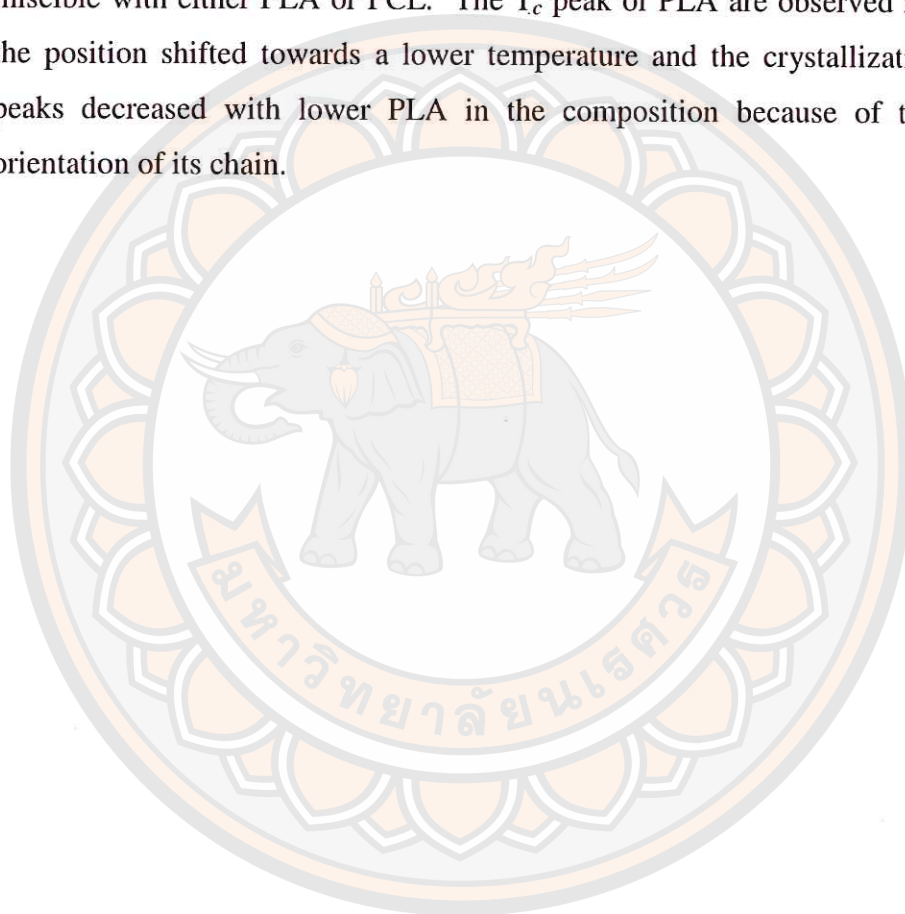
5. Thermal properties of non-woven ternary blend nanofibers by DSC

Thermal properties of non-woven ternary blend nanofibers of PLA/PCL1/CAB and PLA/PCL2/CAB with different compositions were observed, using differential scanning calorimeter (DSC) and shown in figure 34. In this work the cooling run and the second heat run were monitored and shows in figure 34a and 34b, respectively.

Figure 34a demonstrates that the cold crystallization temperature (T_c) of PCL (both PCL1 and PCL2) was dependent on the blend compositions, in which the T_c peak of PCL shifted towards a lower temperature and the crystallization exothermic peaks decreased with a decrease in PCL content. In addition, T_c peak of PCL2 in PLA/PCL2/CAB blends (dash-line) shifted towards a lower temperature than T_c peak of PCL1 in the PLA/PCL1/CAB blends (solid-line). The cold crystallization with decreased T_c of PCL2 (compared to PCL1) was attributed to the decrease of conformation entropy in the PCL2 chains, due to the preferential orientation of its chains. This corresponds to the results seen in the SEM images (figure 31), that PCL2

can be fabricated into better fibers with decreased beaded structure due to higher entanglement or orientation.

Figure 34b shows the second heat run for both blends, it can be seen that the crystalline melting temperature (T_m) of PCL (ca. 55 °C) and that of PLA (ca. 167 °C) do not significantly change in all compositions. CAB melting peak disappears in the ternary blend nanofibers because CAB chains are able to intermingle and be miscible with either PLA or PCL. The T_c peak of PLA are observed in the heat run, the position shifted towards a lower temperature and the crystallization exothermic peaks decreased with lower PLA in the composition because of the preferential orientation of its chain.



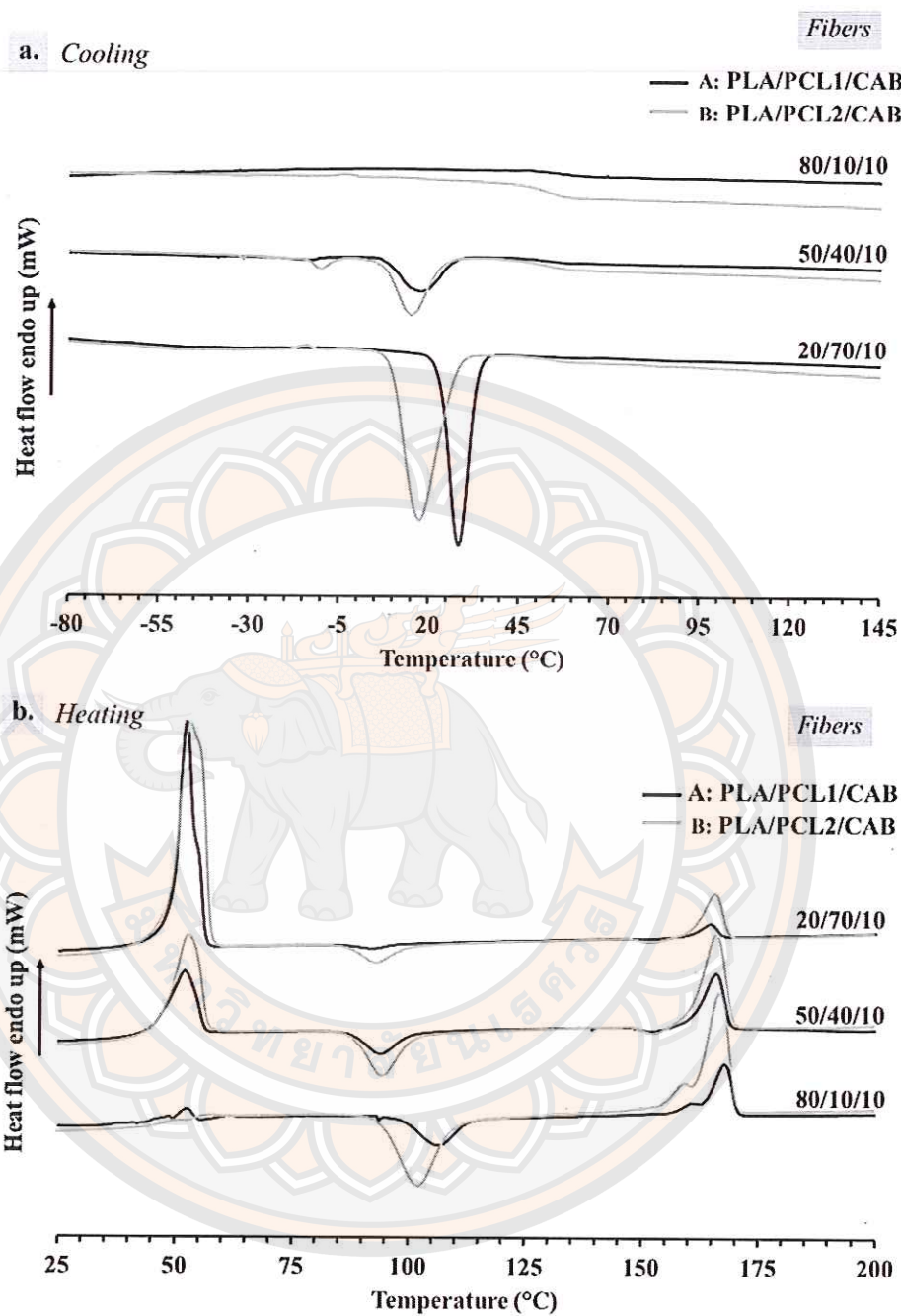


Figure 34 DSC thermogram of non-woven ternary blend fibers;
 a. at cooling run and b. at 2nd heat run, of A. PLA/PCL1/CAB
 (black line) and B. PLA/PCL2/CAB (gray line) at different
 compositions.

6. Hydrophilicity of non-woven electrospun fibers

All ternary blend fibers are hydrophobic, as they show a water contact angle in the range of 130-140 degrees as shown in figure 35, which is a little bit higher than homopolymer fibers and substrate which was polypropylene (95°), while homopolymer fibers of PLA, PCL and CAB have their contact angle of 137° , 97° and 133° , respectively.

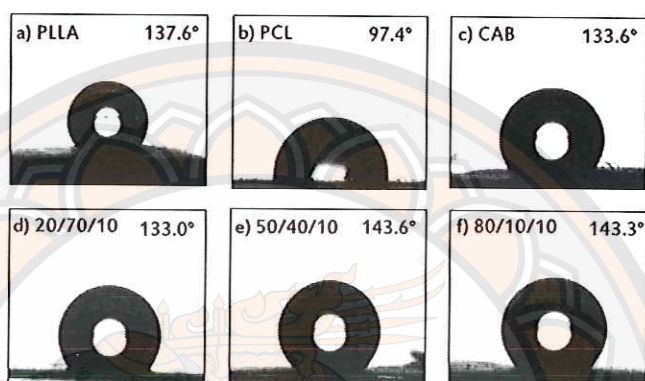


Figure 35 Degree of water contact angle of non-woven homopolymer fibers (PLA, PCL, CAB) and non-woven ternary blend fibers (PLA/PCL/CAB).

Summary of this section

The non-woven electrospun nanofibers of biocompatible and biodegradable PLA/PCL/CAB blend were successfully fabricated, with different blending ratio and molecular weight of PCL. The apparent miscibility of ternary blends from optically ternary phase diagrams was first observed that both clear (apparent miscibility) and opaque (immiscibility) regions are enable to use to be used and fabricated into electrospun nanofibers, depending on blending ratio of PLA and PCL, and molecular weight of PCL. However, in the opaque region at the composition of 20/70/10, the electrospun nanofibers in both PLA/PCL1/CAB and PLA/PCL2/CAB blends show more amounts of beads and microdrops than the compositions at 80/10/10 and 50/40/10, respectively. It can be seen that using high loading of PCL promoted the beads, microdrops and crystallinity of nanofibers due to phase separation (thermodynamically immiscible) between PCL and PLA. In case of using higher molecular weight PCL2, it can enhance the entanglement of polymer chains and then

causes a decrease in beaded structure and microdrops, as well as the decrease of cold crystallization temperature, which attributed to the decrease of conformation entropy in the PCL2 chains. The composition at high loading of PLA blended with PCL2 and CAB was the best composition that gave a smooth surface and partial miscibility between the polymers chains. However, the different properties of nanofibers, i.e. beads containing, crystallinity, thermal properties, porosity, fiber diameter size, etc., can be used in different applications.

Approach II: PVA/SS and PLA/(PVA/SS) blends

This section was separated into two parts of results and discussion. The first part is the fabrication of poly(vinyl alcohol) (PVA) and silk sericin (SS) blends into a non-woven mat electrospun fibers. The second part is the fabrication of PLA (a first layer) and PVA/SS blends (a second layer) into the layer by layer non-woven mat electrospun fibers.

Non-woven electrospun fibers of PVA/SS

From table 7, the compositions of PVA/SS were classified into two groups. The first group is EF1 and EF2, which show the difference in SS concentrations, while PVA concentration was maintained at 5 %w/v. The second group is EF3, EF4 and EF5, which also showed different SS concentrations but this time increased the PVA concentration to 7.5 %w/v. The morphology, crystallinity and functional groups of the samples and differences among each group were the main discussion points in this work.

1. Morphology of PVA/SS electrospun nanofibers

Figure 36 shows the SEM images of PVA/SS electrospun nanofibers, together with PVA, while SS could not form fibers.

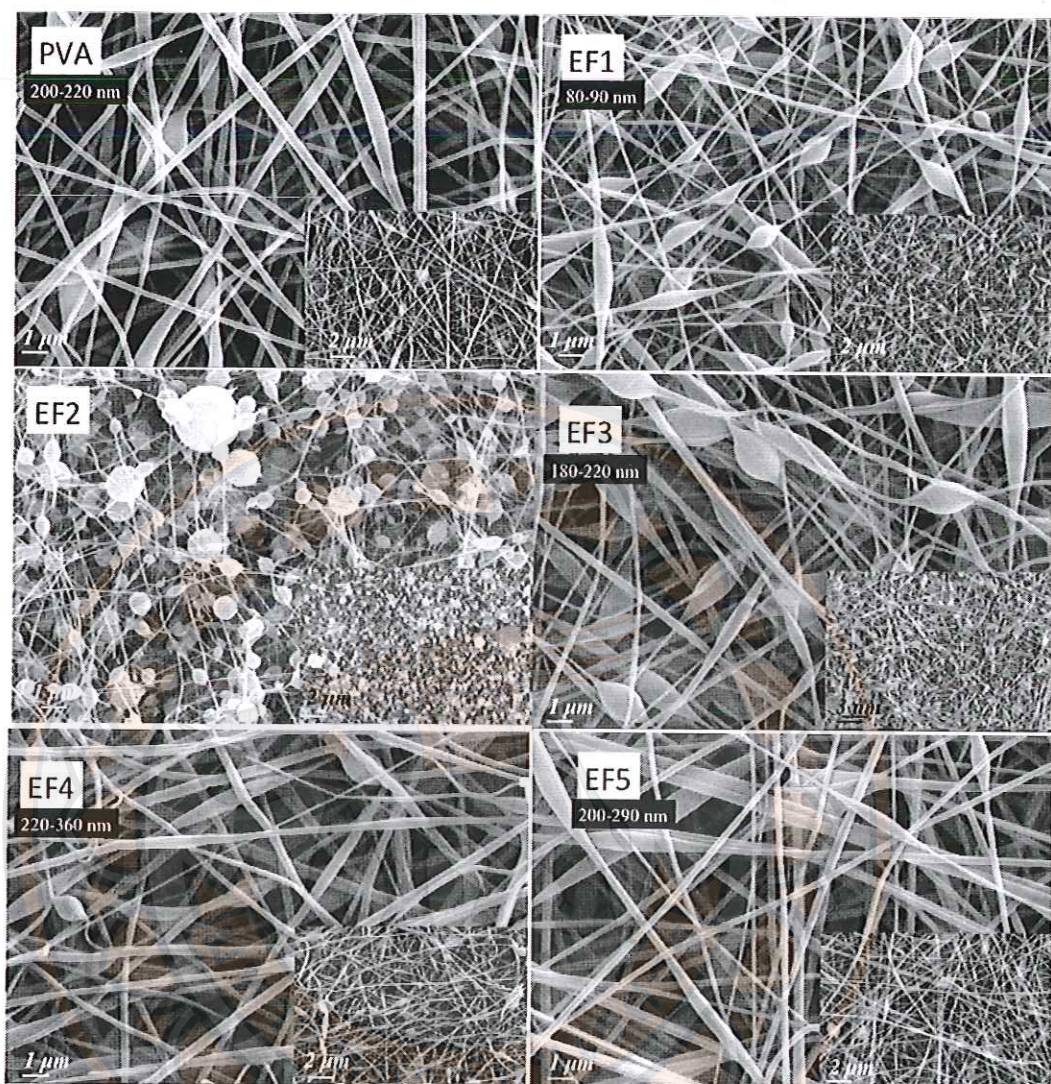


Figure 36 SEM image of electrospun PVA and PVA/SS fibers at different concentrations at magnification of 5000K (big images) and 2000K (small pictures)

PVA fibers were successfully fabricated and had diameters in the range of 200-220 nm, these also contain only a small amount of beads. The formation of these beads is due to the low concentration of PVA and high surface tension. When 1.5 %w/v of SS was added to 5 %w/v PVA of EF1 the beads density in EF1 was promoted with a smaller diameter range (80-90 nm) compared to that of PVA. Adding more SS (3.0 %w/v) into 5 %w/v PVA (EF2) showed a higher density of beads and microdrops. This shows that adding higher SS loading into 5 %w/v PVA promoted the formation

of beads. For EF3, EF4 and EF5, which have higher PVA contents than EF1 and EF2, they formed better fibers in terms of morphology (less beads and no microdrops). However, among them EF4 and EF5 showed similar diameters and has lower bead density than EF3. Therefore, the concentration of PVA and SS solutions play an important role in the fiber formation during the electrospinning process, in which higher PVA and SS concentration showed presented smooth and continuous fibers with less bead formation.

2. Crystallinity observation of PVA/SS electrospun nanofibers by XRD

The crystallinity of PVA/SS nanofibers was observed, as shown in figure 37a and 37b. Homopolymer PVA nanofiber showed a sharp peak of crystalline structure at 19.5° and a broad peak (shoulder peak) at $10-17^\circ$, which has a distance between the crystal (d -spacing) of 4.5 \AA and $8.8-5.2 \text{ \AA}$, respectively. While silk sericin from electrospinning fabrication (no fiber formation) showed a broad peak of amorphous structure at $16-35^\circ$ (d -spacing = $5.5-2.5 \text{ \AA}$).

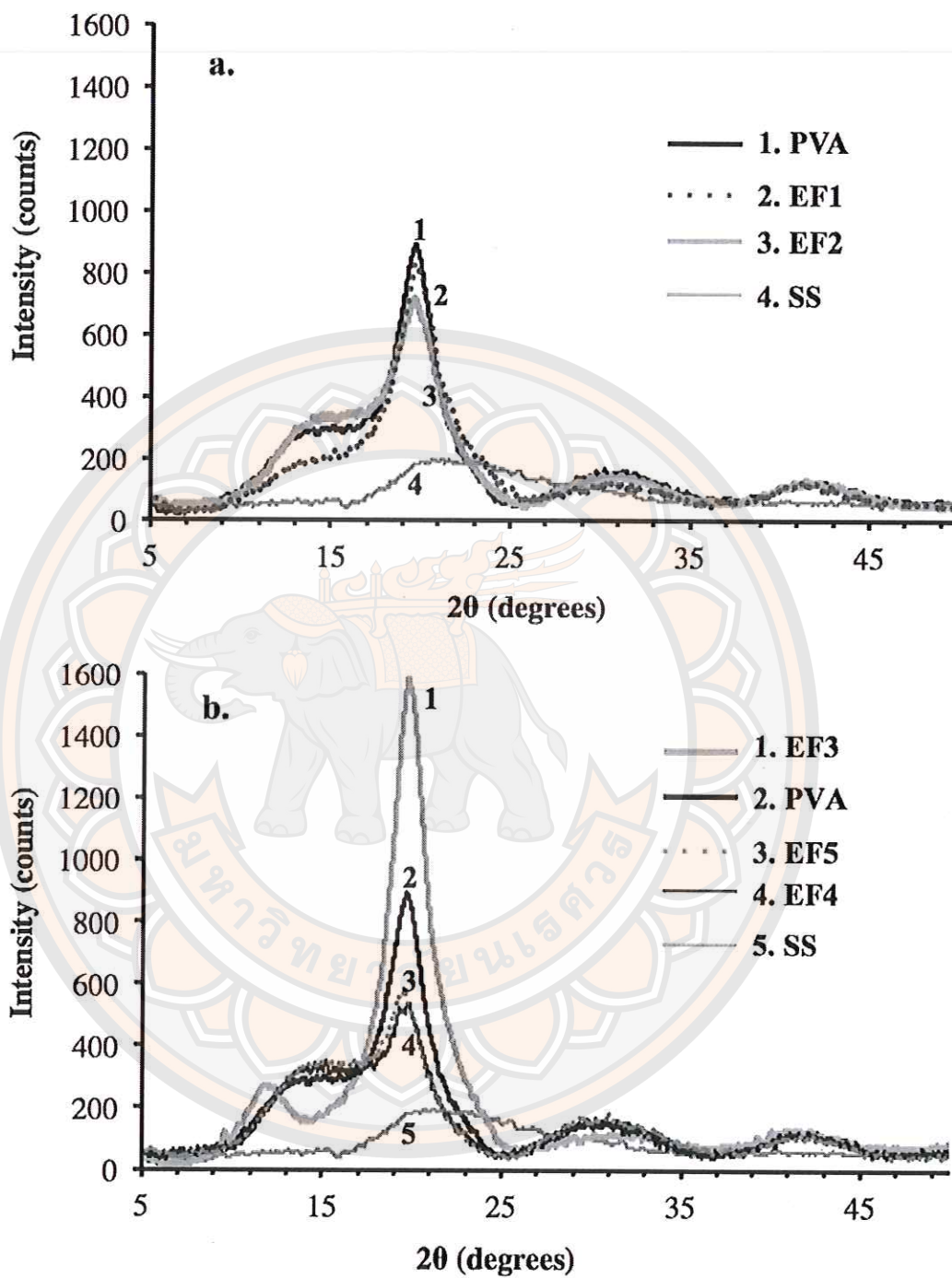


Figure 37 XRD patterns of electrospun PVA/SS; (a.) EF1 and EF2, and (b.) EF3, EF4 and EF5, together with PVA and SS.

From figure 37a, the intensities of crystallinity of EF1 and EF2 are similar to PVA. This means that the addition of SS into the 5 %w/v PVA does not disturb the recrystallization of the PVA chains when they are solidified during the electrospinning process. In figure 37b, the crystalline peaks of PVA in EF3, EF4 and EF5 are significantly different from pure PVA (7.5 5 w/v). As seen, EF3 showed higher intensity of PVA crystalline peak (label number 1) than pure PVA (label number 2). In addition another crystalline peak was observed at 12° (d -spacing = 7.4 Å). This is possibly due to a small amount of SS (0.75 %w/v) can act as a nucleating agent to induce the PVA chains to recrystallize after the electrospinning process. Whereas using higher amounts of SS, for example in EF4 and EF5, can intermingle into the PVA chains and then prohibits the formation of PVA crystallization, as seen the lower crystalline intensity peaks of PVA in EF4 and EF5. However, the XRD peaks of EF4 and EF5 are similar.

3. Functionality observation of PVA/SS electrospun nanofibers by FT-IR

The functional groups of all samples were also investigated by FT-IR and the results are shown in figure 38. The first two peaks of PVA and SS from electrospinning showed their characteristic functional groups, in which PVA has broad hydrogen bonded –OH peak at a high frequency range, sp^3 C-H stretching of –CH₂ or saturated C-H, and –OH bending at 1260-1410 cm⁻¹. Whereas SS has –N-H stretching at high frequency, amide I (-C=O stretching vibrations of amide groups), amide II (-N-H bending) and amide III (in-phase combination of N-H in plane-bending and C-N stretching vibrations).

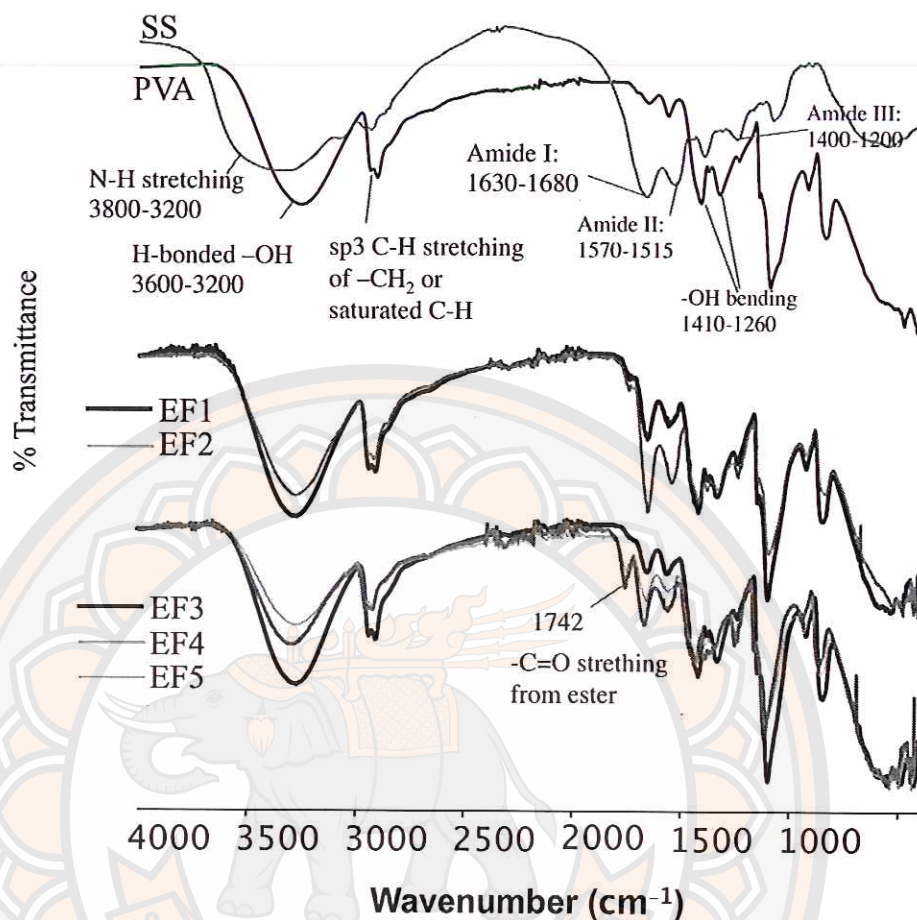


Figure 38 FTIR spectra of electrospun PVA/SS, together with PVA and SS.

All PVA/SS electrospun fibers showed the spectra sum of PVA and SS but at lower intensities in the hydrogen bonded -OH of PVA peaks was observed. The spectra of EF1 and EF2 were similar having hydrogen bonded -OH peak intensities similar to PVA. The spectra of EF3, EF4 and EF5 showed differences in peak intensities of hydrogen bonded -OH , in which EF4 and EF5 are similar and have less intensity than EF3 and PVA, respectively. The peak of carbonyl of an ester group is observed in both EF4 and EF5. This is possibly because of the esterification of the hydroxyl groups of PVA and carboxylic groups of amino acid in SS.

4. Summary of non-woven electrospun PVA/SS fibers

The electrospun fibers of PVA/SS were successful to fabricate in nano-scale ranges. The fiber diameter, morphology and crystallinity were observed to mainly depend on PVA concentration but the SS concentration also had some effect.

From the morphology observations, the electrospun fibers with 7.5 %w/v PVA and different amounts of SS (EF3, EF4 and EF5), showed smoother surfaces and lower bead densities than that of 5 %w/v PVA (EF1 and EF2). From the crystallinity observations, the peak intensities of PVA in EF3, EF4 and EF5 were altered from pure PVA, but not in case of EF1 and EF2. This shows the effect of SS loading, in which small concentration of SS (0.75 %w/v in EF3) acted as a nucleating agent to promote the crystallinity of PVA. In the opposite way, adding higher concentration of SS (1.5 %w/v in EF4 and 2.5 %w/v in EF5) disturbed the recrystallization of PVA after the spinning process due to the SS chains intermingling with the PVA chains, this promotes the homogeneity between PVA and SS. In addition, the carbonyl ester bond can be observed in FT-IR of EF4 and EF5, because of the esterification of hydroxyl group of PVA and carboxylic groups of amino acid in SS. Therefore, EF4 and EF5 are the best electrospun nanofibers in this work that showed good morphology and homogeneity of PVA and SS.

Non-woven electrospun fibers of PLA/(PVA/SS)

In this section, the non-woven electrospun fibers of PLA and that of PVA/SS (EF3 and EF4, see table 7 in chapter 3) were fabricated into the fiber using layer by layer electrospinning technique. The first layer was PLA, the second layer PVA/SS, the third layer PLA and the last layer PVA/SS. The reason for making layer by layer of these electrospun fibers were the limitation of the capability of PLA, PVA and SS to dissolve in the same solvent. As PLA is a hydrophobic polymer that can dissolve in chloroform, while PVA and SS are the hydrophilic polymer that dissolve in water. Therefore, the best technique is to fabricate them by the layer by layer method. Morphology, crystallinity and functionality of these nanofibers were studied and discussed.

1. Morphology of non-woven electrospun fibers of PLA/(PVA/SS)

Figure 39 shows the SEM images of homopolymer (PLA, PVA) fibers and the layer by layer of PLA/PVA, PLA/EF3 and PLA/EF4. PLA fibers had a diameter in the range of 600-800 nm and no beads or microdrops were observed, while PVA fibers were in the range of 200-220 nm and contained some beads. Therefore, it can see that PVA fibers had a smaller diameter than PLA fibers.

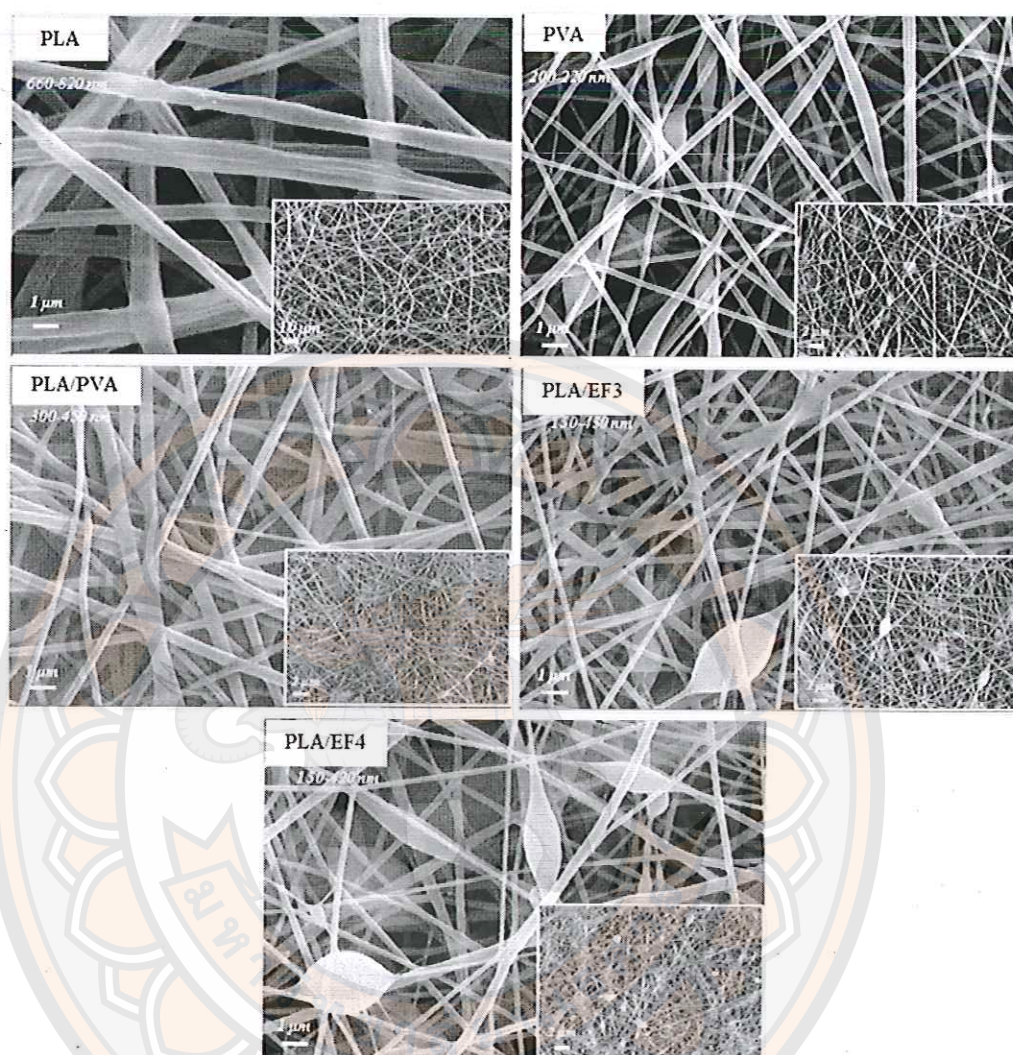


Figure 39 SEM image of electrospun PLA, PVA, PLA/PVA, PLA/EF3 and PLA/EF4 fibers at of 5000K (big images) and 1000K (small pictures)

When PLA fibers were fabricated as the first layer and PVA fibers were the second layer, the mix of PLA fibers and PVA fibers can be observed as seen in Figure 39 (PLA/PVA). However, the PVA fibers layer was seen on top of surface with diameter ranges of pure PVA fibers. For PLA/EF3, which is the layer of PLA fibers on the base and 7.5 %w/v of PVA/0.75 %w/v of SS, its SEM image shows the fiber diameter in range of PVA/SS and the formation of beads can be observed, as EF3 was the last layer of the fabrication not the PLA fibers. The morphology of

electrospun PLA/EF4 shows the same trend of PLA/EF3 but with greater number of beads observed due to the higher content of silk sericin promoting beads.

2. Functionality observation of non-woven electrospun fibers of PLA/(PVA/SS) by FT-IR

FT-IR was used to indicate the components in fibers fabricated from electrospinning technique. Figure 40 shows FT-IR of homopolymer fibers (PLA, PVA and SS), PLA/PVA, EF3, EF4, PLA/EF3 and PLA/EF4. For PLA/PVA, it can be seen that the FT-IR peaks of PLA/PVA shows the spectrum sum of pure PLA and PVA. This indicates both PLA and PVA were contained in this fiber sample. For electrospun fibers of PLA/EF3 and PLA/EF4, they show spectrum sum of only PLA in FT-IR peaks, not any PVA and SS peaks observed. This result is in contrast to the result from SEM (Fig. 39), as the SEM images of PVA/EF3 and PVA/EF4 show the top surface of PVA/SS. This might be due to during the test, as the diamond indenter was pressed through the porous structures of fibers to the PLA fibers in these samples.

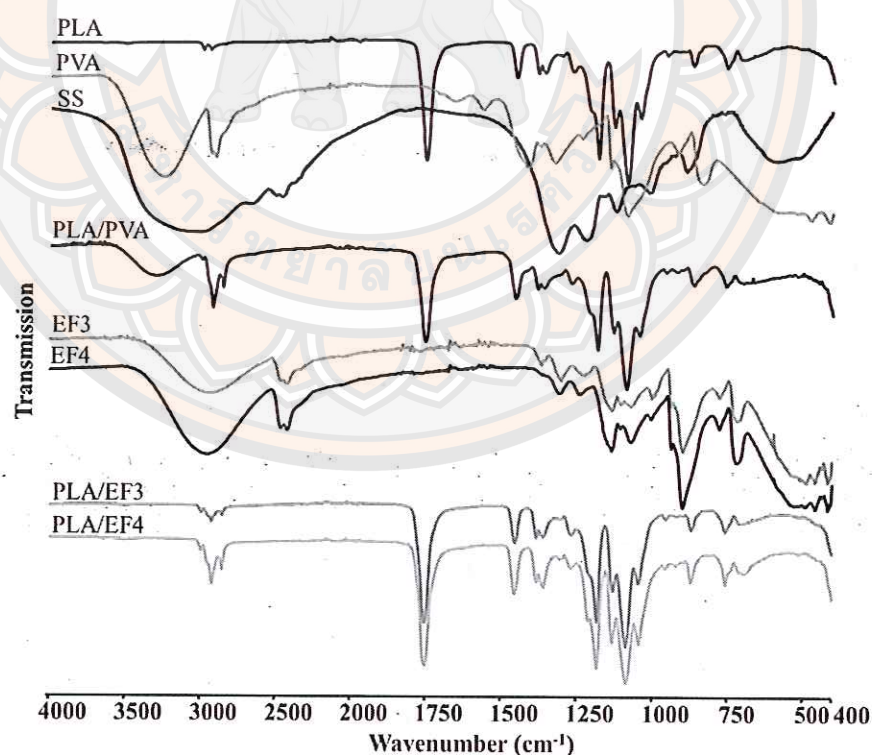


Figure 40 FTIR spectra of electrospun PLA/PVA, PLA/EF3, PLA/EF4 and homopolymer fibers.

3. Crystallinity observation of non-woven electrospun fibers of PLA/(PVA/SS)

XRD was used to assess the crystallinity of polymers composed in fibers fabricated from electrospinning technique. Figure 41 shows XRD of homopolymer fibers (PLA, PVA and SS), PLA/PVA, PLA/EF3 and PLA/EF4. PVA has a crystalline peak at around 15 and 20 degrees, while PLA and SS fibers have broad peaks of amorphous structures. For PLA/PVA and PLA/EF3, peak intensity of PVA can be observed in PLA/PVA at the same degree of pure PVA, while that of PLA/EF3 shifted to the lower value. The XRD result of PLA/EF4 fibers shows a sharp peak of PLA, which should not be the peak of PLA fiber but PLA that has solidified in the fibers. These results do not show a good trend and therefore, a repeat of the experiments are required in future work.

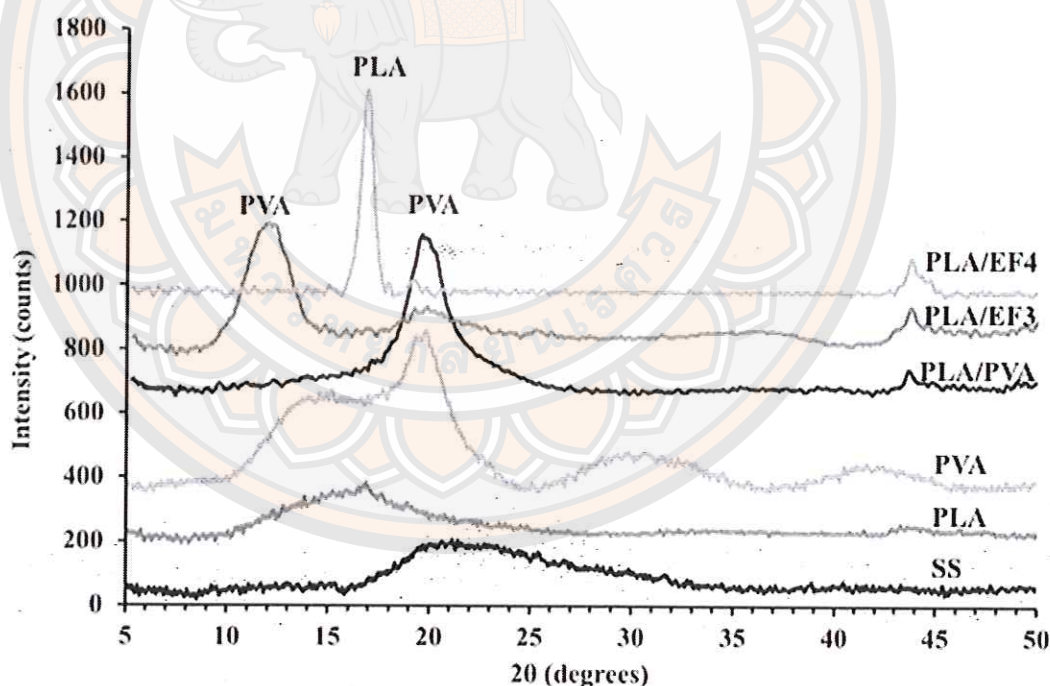
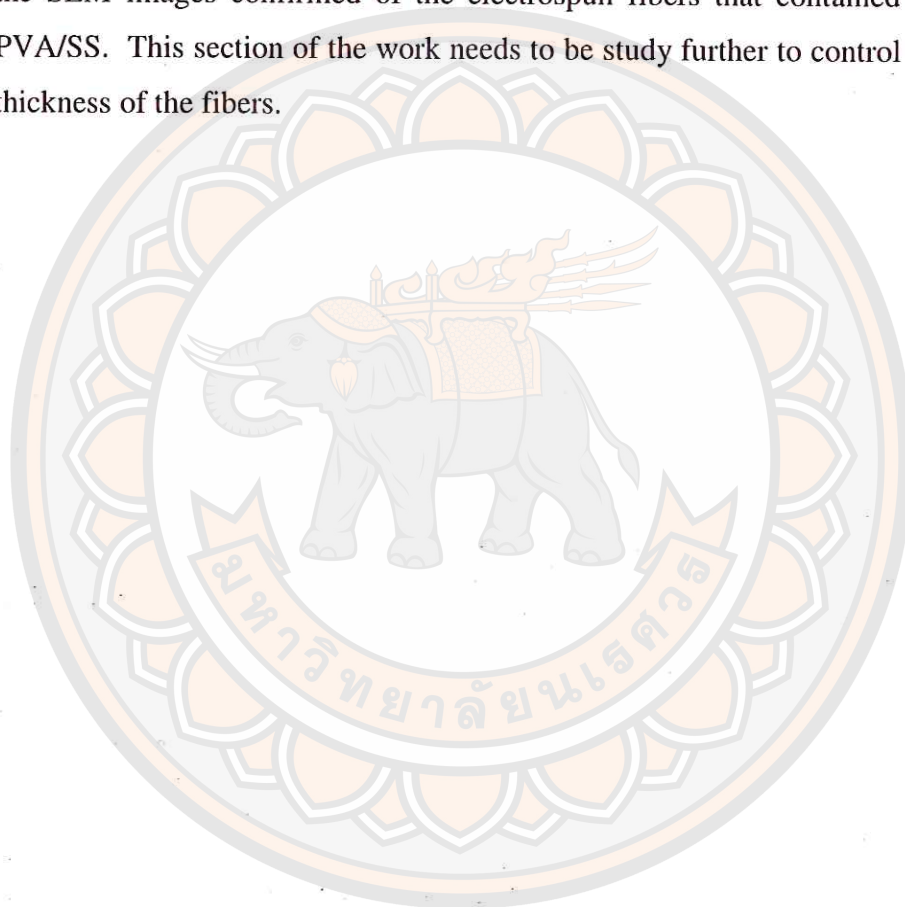


Figure 41 XRD patterns of electrospun PLA/PVA, PLA/EF3, PLA/EF4 and homopolymer fibers

4. Summary of the section

This section contains to study the layer by layer electrospun fibers of hydrophobic polymer (PLA) and hydrophilic polymers (PVA and SS). The work did not show a trend in characteristics, such as functionality and crystallinity. This might be due to the technique of electrospun of layer by layer as well as the porous structures that effect to the capability of the techniques (FT-IR, XRD) required to test. However, the SEM images confirmed of the electrospun fibers that contained both PLA and PVA/SS. This section of the work needs to be study further to control the surface and thickness of the fibers.



CHAPTER V

CONCLUSIONS

Conclusions

This work was concerned with the fabrication of biodegradable and biocompatible materials into fibers by a simple technique called “electrospinning”. This technique produces fibers that have small diameters from micrometers to nanometers containing high surface area and porous structure that can be used in many areas, such as drug delivery, membrane, and especially in tissue engineering applications. Therefore, poly(lactic acid) (PLA), polycaprolactone (PCL), cellulose acetate butyrate (CAB), which are biodegradable and biocompatible polymers, were chosen to fabricate into ternary blend electrospun nanofibers in the approach I. The Coleman-Painter approach of miscibility prediction was used to select the polymers used in this work. This approach studied the effect of molecular weight of PCL and ternary PLA/PCL/CAB blend compositions onto the properties of the formed fibers, such as morphology, crystallinity, functional groups and thermal properties. Poly(vinyl alcohol) and silk sericin (from degumming process of silk cocoons) were also fabricated into electrospun nanofibers in approach II. In addition, these PLA and PVA/SS fibers were fabricated via a layer by layer electrospinning method in this approach. It can be seen that all materials used in this work were biodegradable and biocompatible materials, which will benefit the nanofibers for use in medical applications.

For approach I, first, a novel method named the rapid screening method was employed to assess the apparent miscibility in PLA/PCL1/CAB and PLA/PCL2/CAB ternary solvent blends, and the results are presented in optical ternary phase diagrams. It was observed that using high molecular weight and high compositions of PCL2 promoted the opaque region of PLA/PCL2/CAB blends due to the alignment (zig-zag conformational structure) of carbon-carbon $-(CH_2)_5$ in the backbone. Whereas PCL1, which also has high molecular weight but lower than PCL2, was able to intermingle and restrict to the alignment of its backbone, resulting PLA/PCL1/CAB to

show higher optically clear region than PLA/PCL2/CAB. Therefore, it can be seen from the ternary phase diagrams that the molecular weight of PCL affected the apparent miscibility between ternary polymers. In addition, using high loading of PCL (20/70/10 PLA/PCL/CAB) in both blends produced less apparent miscibility between the polymers. CAB, which has a hydroxyl group (-OH) in its molecular structure, can promote hydrogen bonding interactions with PLA and PCL to enhance the blend miscibility, however, an only small loading of CAB (10 parts in 100 parts of all polymer solutions) was used. Secondly, the compositions from different regions (opaque, translucent and clear) of both PLA/PCL1/CAB and PLA/PCL2/CAB were chosen to fabricate into electrospun nanofibers and the parameters for electrospinning studied along with morphology, crystallinity, and functionality of the nanofibers. It was observed that the processing parameters of electrospinning; concentration of solution (10%w/v), flow rate (0.05 mL/h), applied voltage (25 kV), diameter of tip (0.7 mm) and distance between the end of tip and collector (10 cm), were the most suitable parameters for fabrication. In addition, they also affected the morphology of the electrospun fibers. For the homopolymers it was the neat CAB solution was observed to be the most difficult to fabricate into the fibers due to its low molecular weight. While higher loading of PCL produced the fibers that contained beads. The average fiber diameters of ternary blends of PLA/PCL/CAB are in micro to nanometers ranges (1.6 μm to 340 nm). In this approach, we observed the relationship between the ternary blend films (produced by the rapid screening method) and the ternary blend fibers (produced by electrospinning). We were able to use regions of clear, translucent or opaque from the optical ternary phase diagrams of PLA/PCL1/CAB and PLA/PCL2/CAB to fabricate into the nanofiber forms. However, the clear or translucent blended fibers containing higher molecular weight of PCL2 provided more desirable properties.

For approach II, poly(vinyl alcohol) (PVA)/sericin (SS) nanofibers and PVA/SS together with PLA were fabricated into layer by layer fibers by electrospinning, in which different concentrations of PVA and SS solutions were utilized. The parameters that affected the electrospinning were also observed to find the optimized conditions, such as flow rate (0.02 mL/min), tip-to-collector distance (15 cm) and applied voltage (25 kV). The electrospun fibers of PVA/SS were

successfully fabricated in nanoscale ranges. The fiber diameter, morphology and crystallinity were observed to depend on both PVA and SS concentrations. The fibers fabricated in all compositions had approximate diameter in the range of 100-400 nanometers. High degree of crystallinity in the fibers was observed when 0.75 %w/v of SS added in 7.5 %w/v of PVA, with SS thought to act as a nucleating agent. Whereas, adding higher concentrations of SS (1.5 and 2.5 %w/v) showed the best fiber compositions with smooth fiber surfaces and low bead density. In addition, lower FT-IR peak intensities of hydrogen bonded -OH of PVA and an appearance of carbonyl of ester bonds were observed in these PVA/SS electrospun nanofibers, due to the interaction between hydroxyl groups of PVA and carboxylic groups of SS. For the electrospun layer by layer of fibers PLA and PVA/SS, the result did not show a good trend of characterizations, such as functionality and crystallinity, in which the FT-IR peaks of these fibers demonstrated only PLA but the crystalline peaks showed clearly both PLA and PVA are clearly visible in these samples. This might be due to the technique of the layer by layer electrospun fibers, as well as the porous structures that effect to the capability of the measurement techniques (FT-IR, XRD) used during testing. However, the SEM images confirmed the electrospun fibers contained both PLA and PVA/SS.

Therefore, electrospun micro to nanofiber ranges of ternary blends of PLA/PCL/CAB, PVA/SS and PLA/(PVA/SS) have potential to be used as scaffolds in biomedical applications like tissue engineering but further analysis is still required.

Future work

Study the cell toxicity of these electrospun fiber scaffolds. Design better fabrication technique for the hydrophobic polymer and hydrophilic polymers. Study the degradation profile of PLA/PCL/CAB and PVA/SS electrospun nanofibers and loading of the drug should be tested.



REFERENCES

REFERENCES

- [1] Oh, S. H., Park, I. K., Kim, J. M., & Lee, J. H. (2007). In vitro and in vivo characteristics of PCL scaffolds with pore size gradient fabricated by a centrifugation method. *Biomaterials*, 28, 1664-1671.
- [2] Kim, S. S., Park, M. S., Jeon, O., Choi, C. Y., & Kim, B. S. (2006). Poly(lactide-co-glycolide)/hydroxyapatite composite scaffolds for bone tissue engineering. *Biomaterials*, 27, 1399-1409.
- [3] Wei, G., & Ma, P. X. (2004). Structure and properties of nano-hydroxyapatite/polymer composite scaffolds for bone tissue engineering. *Biomaterials*, 25, 4749-4757.
- [4] Kang, Y., Yin, G., Yuan, Q., Yao, Y., Huang, Z., Liao, B., Liao, L., & Wang, H. (2008). Preparation of poly(L-lactic acid)/beta-tricalcium phosphate scaffold for bone tissue engineering without organic solvent. *Materials Letters*, 62, 2029-2032.
- [5] Joseph, L., Neha D., & Gregory C.R. (2010). Effect of fiber diameter, pore size and seeding method on growth of human dermal fibroblasts in electrospun poly (ϵ -caprolactone) fibrous mats. *Biomaterials*, 31, 491-504.
- [6] Ross, S., Topham, P. D., & Tighe, B. J. (2014). Identification of optically clear regions of ternary polymer blends using a novel rapid screening method. *Polymer International*, 63, 44-51.
- [7] Ross, S., Mahasaranon, S., & Ross, G. M. (2015). Ternary polymer blends based on poly(lactic acid): Effect of stereo-regularity and molecular weight. *Journal of Applied Polymer Science*, 132(14), 41780(1-8).
- [8] Ross, S., Mahasaranon, S., & Ross, G. M. (2015). Optical clarity, crystallinity and morphology of ternary blended films of poly (L-lactide)/polycaprolactone/thermoplastic polyurethane: effect of molecular weight. *Macromolecular Symposia*, 354, 76-83.

- [9] Wutticharoenmongkol, P., Pavasant, P., & Supaphol, P. (2007). Osteoblastic phenotype expression of MC3T3-E1 cultured on electrospun polycaprolactone fiber mats filled with hydroxyapatite nanoparticles. *Biomacromolecules*, 8, 2602-2610.
- [10] Tungprapa, S., Jangchud, I., & Supaphol, P. (2007). Release characteristics of four model drugs from drug-loaded electrospun cellulose acetate fiber mats. *Polymer*, 48, 5030-5041.
- [11] Cheng, M., Chen, P., Lan, C., & Sun, Y. (2011). Structure, mechanical properties and degradable behaviors of the eletrospun fibrous blend of PHBHHx/PDLLA. *Polymer*, 52, 1391-1401.
- [12] Langer, R. & Vacanti, J. P. (1993). Tissue engineering. *Science*, 260, 920-926.
- [13] Stevens, U., & George, J. H. (2005). Exploring and Engineering the Cell Surface Interface. *Science*, 310, 1135-1138.
- [14] Inai, R., Kotaki, M., & Ramakrishna, S. (2005). Structure and properties of eletrospun PLLA single nanofibers. *Nanotechnology*, 16, 208-213.
- [15] Thompson, C. J., Chase, G. G., Yarin, A. L., & Reneker, D. H. (2007). Effects of parameters on nanofiber diameter determined from electrospinning model. *Polymer*, 48, 6913-6922.
- [16] Wenguo, C., Yue, Z., & Jiang, C. (2010). Electrospun nanofibrous materials for tissue engineering and drug delivery. *Science and Technology of Advanced Material*, 11, 014108.
- [17] Pham, Q. P., Sharma, U., & Mikos, A. g. (2006). Electrospinning of polymeric nanofibers for tissue engineering applications: a review. *Tissue Engineering*, 12, 1197-1211.
- [18] Ignatova, M., Starbova, K., Markova, N., Manolova, N., & Rashkov, I. (2006). Electrospun nano-fiber mats with antibacterial properties from quaternised chitosan and poly(vinyl alcohol). *Carbohydrate Research*, 341, 2098-2107.
- [19] Yang, D., Li, Y., & Nie, J. (2007). Preparation of gelatin/PVA nanofibers and their potential application in controlled release of drugs. *Carbohydrate Polymers*, 69, 538-543.

- [20] Zhang, X., Tang, K., & Zheng X. (2016). Electrospinning and Crosslinking of COL/PVA Nanofiber-microsphere Containing Salicylic Acid for Drug Delivery. *Journal of Bionic Engineering*, 13, 143–149
- [21] Zhang, Y. Q. (2002). Application of natural silk protein sericin in biomaterials, *Biotechnology Advances*, 20, 91-100.
- [22] Ho, M.P., Wang, H., Lau, K., Lee, J., & Hui, D. (2012). Interfacial bonding and degumming effects on silk fibre/polymer biocomposites, *Composites B*, 43, 2801-2812.
- [23] Zhao, R., Li, X., & Sun, B. (2014). Electrospun chitosan/sericin composite nanofibers with antibacterial property as potential wound dressings. *International Journal of Biological Macromolecules*, 68, 92-97.
- [24] Kundu, B., & Kundu, S. C. (2012). Silk sericin/polyacrylamide in situ forming hydrogels for dermal reconstruction. *Biomaterials*, 33, 7456-7467.
- [25] Averous, L., & Pollet, E. (2012). Environmental Silicate Nano-Biocomposites. *Green Energy and Technology*, DOI: 10.1007/978-1-4471-4108-2_2.
- [26] Steinbuchel, A. (2003). Biopolymers, *general aspects and special applications*, 10, Wiley-VCH, Weinheim.
- [27] Jessy, R.S., & Ibrahim, M.H. (2014). Biodegradability and biocompatibility of polymers with emphasis on bone scaffolding: a brief review. *International Journal of Scientific and Research Publications*, 4, 2250-3153.
- [28] Chandra, R., & Rustgi, R. (1998). Biodegradable Polymers. *Progress in Polymer Science*, 23, 1273-1335.
- [29] Celerino de Moraes Porto. (2012). Polymer biocompatibility. *Licensee InTech*, <http://creativecommons.org/licenses/by/3.0>.
- [30] Quansah, J.K. (2004). Synthetic polymers for biocompatible biomaterials. *Materials literature seminar*, Retrieved from www.chemistry.illinois.edu/research/materials/seminar_abstract_/2004_2005/Quansah.

- [31] Williams, D. F. (2008). On the mechanisms of biocompatibility. *Biomaterials*, 29, 2941-2953.
- [32] Juikham, S. (2011). *Design and characterization of novel blends of poly(lactic acid)*. (Unpublished doctoral dissertation). Aston University, UK.
- [33] Albertsson, A. C. (2002). *Degradable Aliphatic Polyesters*. Advances in Polymer Science, Springer-Verlag Berlin heidelberg New York: Berlin. 179.
- [34] Amass, W., Amass, A., & Tighe, B. J. (1998). A review of biodegradable polymers: Uses, current developments in the synthesis and characterization of biodegradable polyesters, blends of biodegradable polymers and recent advances in biodegradation studies. *Polymer International*, 47, 89-144.
- [35] Savioli, M.L., Jardini A.L., & Maciel R.F. (2014). Synthesis and Characterizations of Poly (Lactic Acid) by Ring-Opening Polymerization for Biomedical Applications. *Chemical Engineering Transactions*, 38, 331-336.
- [36] Edgar, k.J., Bruchanan, C.M., Debenham, J.S., Rundquist, P.A., Seler, B.D., Shelton, M.C., & Tindall, D. (2001). Advances in cellulose ester performance and application. *Progress in Polymer Science*, 26, 1605-1688.
- [37] Yuan, J., Dunn, D., Clipse, N.M., & Newton, R.J. (2008). Permeability study on cellulose acetate butyrate coating film. *Drug Delivery Technology*, 8, 46-51.
- [38] Williams, D.F. (2009). On the nature of biomaterials. *Biomaterials*, 30, 5897-5909.
- [39] Luckachan, G., & Pillai, C. (2011). Biodegradable polymers – a review on recent trends and emerging perspectives. *Journal of Polymers and Environment*, 19, 637-676.

- [40] Dias, J.C., Ribeiro, C., Sencendas, V., & Botelho, G. (2012). Influence of fiber diameter and crystallinity on the stability of electrospun poly (L-lactic acid) membranes to hydrolytic degradation. *Polymer Testing*, 31, 770-776.
- [41] Cui, W., Cheng, L. Li, H., Zhou, Y., Zhang, Y., & Chang, J. (2012). Preparation of hydrophilic poly(L-lactide) electrospun fibrous scaffolds modified with chitosan for enhanced cell biocompatibility. *Polymer*, 53, 2298-2305.
- [42] Kuihua, Z., Anlin, Y., & El-Newehy, M. (2011). Degradation of electrospun SF/P(LLA-CL) blended nanofibrous scaffolds in vitro. *Polymer Degradation and stability*, 96, 2266-2275.
- [43] Lowery, J.L., Datta, N., & Rutledge, G.C. (2010). Effect of fiber diameter, pore size and seeding method on growth of human dermal fibroblasts in electrospun poly (ϵ -caprolactone) fibrous mats. *Biomaterials*, 31, 491-504.
- [44] Zeng, J.B., Li, Y.D., He, Y.S., Li, S.L., & Wang, Y.Z. (2011). Improving Flexibility of Poly(L-lactic acid) by Blending with Poly(L-lactic acid) Based Poly(ester-urethane): Morphology, Mechanical Properties, and Crystallization Behaviors. *Industrials & Engineering Chemistry Research*, 50, 6124-6131.
- [45] Park, J.E., & Todo, M. (2011). Compressive mechanical properties and deformation behavior of porous polymer blends of poly (ϵ -caprolactone) and poly(L-lactic acid). *Journal of materials Science*, 46, 7850-7857.
- [46] Costa, L.M.M., Olyverira, G.M., Cherian, B.M., Leao, A.L., Souza, S.F., & Ferreira, M. (2013). Bionanocomposites from electrospun PVA/pineapple nanofibers/ Stryphnodendron adstringens bark extract for medical applications. *Industrial Crops and products*, 41, 198-202.
- [47] Yooyod, M., Limpeanchob, N., Suphrom, N., Mahasaranon, S., Ross, G.M., & Ross, S. (2016). Investigation of silk sericin conformational structure for fabrication into porous scaffolds with poly(vinyl alcohol) for skin tissue reconstruction. *European Polymer Journal*, 81, 43-52.

- [48] Ko, J.S., Yoon, K.H., Ki, C.S., Kim, H.J., Bae, D.G., & Lee K.H. (2013). Effect of degumming condition on the solution properties and electrospinnability of regenerated silk solution. *International Journal of Biological Macromolecules*, 55, 161–168.
- [49] Sobajo, C., Behzad, F., Yuan, X.F., & Bayat, A. (2008). Silk a Potential Medium for Tissue Engineering. *Eplasty*, 8, 47, Retrieved from <http://www.ncbi.nlm.nih.gov/pubmed/18997857>.
- [50] Mondal, M., Trivedy, & K., Kumar N.S. (2007). The silk proteins, sericin and fibroin in silkworm, *Bombyx mori* Linn a review. *Caspian Journal of Environmental Sciences*, 5, 63-76.
- [51] Pushpa, A., Vishnu, G., & Reddy, T. (2013). Preparation of nano silk sericin based hydrogels from silk industry waste. *Journal of Environmental Research And Development*, 8, 243-253.
- [52] Rajput, S.K., Kumar M., & Singh. (2015). Sericin-A Unique Biomaterial. *Journal of Polymer and Textile Engineering*, 3, 29-35.
- [53] Hadipour-Goudarzi, E., Montazar, M., Latifi, M., & Aghaji, A.A.G. (2014). Electrospinning of chitosan/sericin/PVA nanofibers incorporated within situ synthesis of nano silver. *Carbohydrate Polymers*, 113, 231-239.
- [54] Mandal, B.B., Priya A.S., & Kundu, S.C. (2009). Novel silk sericin/gelatin 3-D scaffolds and 2-D films: Fabrication and characterization for potential tissue engineering applications. *Acta Biomaterialia*, 5, 3007–3020.
- [55] Dash, B., Mandal, B.B., & Kundu, S.C. (2009). Silk gland sericin protein membranes: Fabrication and characterization for potential biotechnological applications. *Journal of Biotechnology*, 144, 321–329.
- [56] Coleman, M. M., Graf, J. F., & Painter, P. C. (1991). *In Specific Interactions and the Miscibility of Polymer Blends*. Pennsylvania: Technomic Lancaster.
- [57] Bhardwaj, N., & Kunda, S. (2010). Electrospinning: A fascinating fiber fabrication technique. *Biotechnology Advances*, 28, 325-347.

- [58] Raghavan, P., Lim, D.H., Ahn, J.H., Nah, C., Sherrington, D.C., Ryu, H.S., & Ahn, H.J. (2012). Electrospun polymer nanofibers: The booming cutting edge technology. *Reactive & Functional Polymers*, 72, 915–930.
- [59] Shi, X., Zhou, W., Ma, D., Ma, Q., Bridges, D., Ma, Y., & Hu, A. (2015). Electrospinning of Nanofibers and Their Applications for Energy Devices. *Journal of Nanomaterials*, Retrieved from <http://dx.doi.org/10.1155/2015/140716>.
- [60] Lu, L., Wu, D., Zhang, M., & Zhou, W. (2012). Fabrication of Polylactide/Poly(ϵ -caprolactone) Blend Fibers by Electrospinning: Morphology and Orientation. *Industrials & Engineering Chemistry Research*, 51, 3682-3691.
- [61] Meinel, A.J., Germershaus, O., Luhmann, T., Merkle, H.P., & Meinel, L. (2012). Electrospun matrices for localized drug delivery: Current technologies and selected biomedical applications. *European Journal of Pharmaceutics and Biopharmaceutics*, 81, 1–13.
- [62] Sill, T.J., & Recum, H.A. (2008). Electrospinning: Applications in drug delivery and tissue engineering. *Biomaterials*, 29, 1989-2006.
- [63] Ravichandran, R., Venugopal, J.R., Sundarrajan, S., Mukherjee, S., Sridhar, R., & Ramakrishna, S. (2012). Composite poly-L-lactic acid/poly-(α , β)-DL-aspartic acid (PAA)/Collagen nanofibrous scaffolds for dermal tissue regeneration. *Materials Science & Engineering C*, 32, 1443-1451.
- [64] Cui, W., Zhu, X., Yang, Y., Li, X., & Jin, Yan. (2009). Evaluation of electrospun fibrous scaffolds of poly (DL-lactic acid) and poly (ethylene glycol) for skin tissue engineering. *Materials Science & Engineering C*, 29, 1869-1876.
- [65] Blackwood, K.A., McKean, R., Canton, I., ..., & MacNeil, S. (2008). Development of biodegradable electrospun scaffolds for dermal replacement. *Biomaterials*, 29, 3091-3104.

- [66] Thakur, R.A., Florek, C.A., Kohn, J., & Michniak, B.B. (2008). Electrospun nanofibrous polymeric scaffold with targeted drug release profiles for potential application as wound dressing. *International Journal of Pharmaceutics*, 364, 87-93.
- [67] Eda, G., & Shivkumar, S. (2007). Bead-to-fiber transition in electrospun polystyrene. *Journal of Applied Polymer Science*, 106, 475-487.
- [68] Li, Z., & Wang, C. (2013). One-Dimensional nanostructures electrospinning technique and unique nanofibers. *SpringerBriefs in Materials*. DOI: 10.1007/978-3-642-36427-3_2.
- [69] Zia, K. M., Barikani, M., Zuber, M., Bhatti I. A., & Bhatti H. N. (2008). Morphological Studies of Polyurethane Elastomers Extended with $\alpha\omega$ Alkane Diols. *Iranian Polymer Journal*, 17, 61-72.
- [70] Krikorian, V., & Pochan, D. (2003). Poly (L-Lactic Acid)/Layered Silicate Nanocomposite: Fabrication, Characterization, and Properties. *Chemistry of Materials*, 15, 4317-4324.
- [71] Agarwal, S., Wendorff, J. H., & Greiner, A. (2008). Use of electrospun technique for biomedical applications. *Polymer*, 49, 5603-5621.
- [72] Wang, L., Topham, P. D., Mykhaylyk O. O., Yu, H., Ryan, A. J., Fairclough, J. P. A., & Bras, W. (2015). Self-Assembly-Driven Electrospinning: The transition from fibers to intact beaded morphologies. *Macromolecular Rapid Communications*, 2015, 36, 1437-1443.